Equilibrium Modeling of Coal and Biomass Gasification

by

Gregory Charles Vaughan

A thesis submitted to the Graduate Faculty of
Auburn University
in partial fulfillment of the
requirements for the Degree of
Master of Science

Auburn, Alabama
August 1, 2015

Keywords: coal, biomass, gasification, modeling

Approved by

Mario R. Eden, Department Chair and McMillan Professor of Chemical Engineering
Christopher B. Roberts, Dean of Engineering and Uthlaut Professor of Chemical Engineering
Yoon Y. Lee, Professor Emeritus of Chemical Engineering

Abstract

This thesis endeavors to add to the field of equilibrium modeling of coal and biomass gasification by utilizing widely available commercial process modeling software (Aspen Plus®) to evaluate the impacts of various system parameters within a gasification system and by providing an evaluation of general techniques that are used in creating equilibrium-based simulations of gasifiers. From the results presented, the following conclusions and recommendations are made. Air-to-fuel ratio should be concurrently varied with any other system parameter when performing a parametric analysis of a gasification system. The carrier gas utilized in dry-feed systems should not be ignored. The correct representation of the form of sulfur in sulfur-bearing feedstocks is important. Additionally, further work is needed in accounting for the heat of formation of various feedstocks in gasification models, and further work is also needed to allow for simple modifications to equilibrium gasification models to represent various technologies (e.g. entrained flow, fluidized bed, etc.) for use in feasibility studies.

Acknowledgements

I would like to express my gratitude to the entire Auburn University family, particularly the Department of Chemical Engineering. Through both my undergraduate and graduate education, the challenging academic environment has trained me in a manner of thinking that has benefitted me in many aspects of my life. I often express to others that more than the learning of particular concepts such as thermodynamics or process control, it is the training of my mind for rigorous thought that is the most valuable of all of my education. This is not the product of one bulk conveyance of knowledge, but of many, many interactions between my fellow students, alumni, and the faculty.

I would like to thank the graduate students who started with me in the fall semester of 2009. Having been a few years since I had encountered some of the concepts that were required in my first semester, especially differential equations and kinetics, they graciously helped me get back up to speed.

I would like to thank my fellow members in Dr. Eden's group for the help they gave to me at various times. I would particularly like to thank Dr. Subin Hada. Helping one another, bouncing ideas off of one another, joking with one another, and teaching him paper football only to have him become basically unbeatable in our daily match were all parts of what made my time in Dr. Eden's group all the more enjoyable. I can't say

that I ever thought I would have a friend from Kathmandu, but I am thankful to call him "friend".

I would like to thank my advisor, Dr. Mario Eden for his support in this entire endeavor. When I was contemplating the decision to return to Auburn for graduate school, he made the choice an easy one. Being able to return to Auburn for further education has allowed me to realize both personal and professional goals.

I would like to thank Dr. Christopher Roberts, my co-advisor, and Dr. Y. Y. Lee for their willingness to be on my committee. I would particularly like to thank Dr. Roberts for his words of encouragement one night late into my first semester back at graduate school. After the rest of the faculty and staff had long since left for home, I saw his door open, dropped in, and he took some time to talk even though it was already late. At a time when the stress of that first semester was weighing heavily on me, his words of reassurance in his usual, calm demeanor helped me tremendously. I would particularly like to thank Dr. Lee for bearing with me and helping me out as I struggled to get up to speed in his reactions class that first semester.

Special thanks go to my parents, Greg and Teresa Vaughan, who have supported me in my education and made it possible. From my earliest years they have encouraged me to learn and answered countless questions from my curious mind, such as the time when my dad fielded a question about subtracting a larger number from a smaller number when I was in the second grade and responding with a most adept analogy using holes in the ground to explain the concept of negative values!

I would like to give very special thanks to my wife, Sarah, who supports, encourages, and loves me each and every day, and especially so in this work. Any words that I could write could only scratch the surface of the joy that I experience from being with her and the appreciation that I have for being married to her. An excellent wife she certainly is.

Above all, I am most grateful to the eternal, Triune God, Father, Son, and Holy Spirit. All of the faculties that have enabled me to do this work are gifts from him. "For of him, and through him, and to him, are all things: to whom be glory forever. Amen."

Table of Contents

List of Figures

List of Tables

1. Introduction

As the world population continues to grow, the limited natural resources of the planet will continue to be stretched amongst an ever-increasing number of players. Each nation's access to reliable sources of energy, or lack thereof, will be of particular importance. The supply of oil and natural gas, two critical fossil fuels, will be at the heart of the matter. Recent estimates predict that at current production rates, proven world oil reserves will last 54 years and proven world natural gas reserves will last 61 years (World Coal Association, 2014). Not only are these two key commodities and their derivatives used directly for energy, but they are also the feedstocks for producing many chemicals; thus, if their supply is depleted, the impact will be much greater than that of fuel value alone. It is critical, therefore, that new sources of energy be sought and existing methods and sources of alternative energy be improved. One older energy technology that has seen a surge in interest over the last two decades is gasification.

Gasification uses a limited amount of oxidant to partially oxidize a carbonaceous fuel source to produce a product gas with significant fractions of hydrogen (H_2) and carbon monoxide (CO). This gas stream, commonly called synthesis gas, or "syngas", can then be used for a variety of applications including power generation, the manufacture of various chemicals, and the production of transportation fuels. One advantage to gasification is that a wide variety of materials can be used as the carbon source; though there are practical limitations, virtually any carbon-based substance can be

used as a feedstock. Of particular interest as feedstocks are various types of coal and biomass, with each feedstock having its own set of benefits.

As interest in gasification has increased over the last two decades, research and development in this field has grown. Gasification modeling coupled with bench-scale, pilot-scale, and even commercial-scale research systems have been used to further understand the underlying science behind gasification and the various gasification process technologies. With regard to modeling, Lee *et al.* (2007) write, "The influence of design variables and processing conditions on the gasifier performance must be *a priori* determined before any commercial processes are designed. Such models are then used as tools for design modifications, scaling, and optimization". A report from the U.S. Department of Energy listed "development of gasifier models" as the number eight ranked need on a prioritized list of ninety-five needs for research and development in the field of gasification (Clayton *et al.*, 2002). Thus, the availability of reliable models is critical to the widespread commercialization of gasification.

Gasifiers are essentially chemical reactors, and most mathematical gasifier models can be classified as one of two types of traditional mathematical reactor models: 1) equilibrium models or 2) kinetic models. Equilibrium models are not as complex to create as kinetic models, but their accuracy is often doubted because in many systems equilibrium is not actually achieved. Thus, many modelers focus on kinetic models, which often account for very specific system conditions (e.g. particle size); however, because these models are so system specific, their application may be limited to a narrow range of system configurations, conditions, feedstocks, etc.; whereas, equilibrium models offer the potential for a much wider range of application.

This study hopes to add to the collective knowledge of equilibrium gasification modeling in three main respects:

1) Conducting a thorough analysis of the impact of various system parameters on an equilibrium coal/biomass gasification model using commercial process modeling software.
2) Being the first known work to present a robust parametric analysis of an equilibrium gasification model in which the fuel-to-air ratio is simultaneously varied with other system parameters.
3) Proposing hypotheses when model predictions diverge from established observations in coal and biomass gasification.
4) Evaluating equilibrium-based modeling of gasification generally, to suggest areas of particular consideration in developing such models as well as recommending areas of further research in the field.

Though not a main objective, this work will also make general recommendations to aid in the widespread commercialization of gasification technology.

2. Background

2.1 History

The history of gasification goes back to the 1600s, when Jean Baptist van Helmont discovered that heating coal resulted in the release of a "wild spirit or breath" (Kirk-Othmer, 2002). In 1788, the first patent related to gasification was issued to Robert Gardner (NETL, 2015). The work of Scotsman William Murdoch advanced coal gasification technologies in the late 1700s and early 1800s, and as a result of his efforts, "town gas," called synthesis gas today, saw use for lighting in England and especially London in the early 1800s (NETL, 2015).

The first commercial use of gasification in the United States was in Baltimore in 1816 for lighting purposes (NETL, 2015). The technology spread throughout the U.S. and was used for lighting and heating, but in the late 1800s, advances in electric lighting technology and increasing use of natural gas reduced the use of coal generated syngas in the U.S. (NETL, 2015). Perhaps some of the most famous work in the field of gasification came in Germany in the time leading up to and during World War II. Carl von Linde developed a process to cryogenically separate oxygen from air in the 1920s, which allowed the first truly continuous oxygen-blown gasification processes to operate (Higman & van der Burgt, 2003). The predecessors of many of the various types of conventional gasification processes used today were then developed later in the 1920s and the 1930s (Higman & van der Burgt, 2003). It was also during this time, that Franz

Fischer and Hans Tropsch developed the Fischer-Tropsch (FT) process to manufacture liquid fuels from coal-produced syngas (NETL, 2015).

Though worldwide interest in gasification was limited after World War II, South Africa used gasification to produce liquid fuels and chemicals, building one gasification plant in the 1950s and two more in the 1980s, further proving the viability of gasification technology (NETL, 2015). Also, both the Shell and Texaco gasification processes, two important processes, were developed in the 1950s (Higman & van der Burgt, 2003). Both of these processes use an entrained-flow configuration; the Shell process is dry-feed, and the Texaco process is slurry-feed. Interest in gasification in the U.S. rose and fell with crude oil availability and prices during the 1970s and 1980s, but various projects did prove the ability of gasification to adapt to different applications during this time (NETL, 2015).

Figure 2.1 – SASOL II & SASOL III gasification plants in South Africa (NETL, 2015)

Finally, due a variety of economic, political, and environmental forces during the 1990s, the appeal of gasification in the United States and Europe began growing again (NETL, 2015). In recent years, the boom of shale oil and natural gas has drawn much

attention, and it could, once again, shift interest away from gasification, but in the long-term, gasification may yet prove to be a vitally important energy technology.

2.2 Thermochemistry

The principal concept behind gasification is using pressure and a limited supply of oxidant[1] to partially oxidize a carbonaceous feedstock, which, through a complex network of chemical reactions, results in a gaseous product stream that ideally contains large fractions of hydrogen and carbon monoxide, the two desired products. In addition to hydrogen and carbon monoxide, gasification syngas contains large fractions of carbon dioxide (CO_2), water (H_2O), and possibly nitrogen (N_2) and/or methane (CH_4) depending on the process. Other components that may be in the product gas are ammonia (NH_3), nitrogen oxides (NO and NO_2), sulfur oxides (SO_2 and SO_3), hydrogen sulfide (H_2S), and hydrogen chloride (HCl) among others. In addition, ash may be present in the product gas, and its composition varies with feedstock, system conditions, etc. The theory of gasification is commonly explained as occurring in different stages or zones. These zones may be localized to a spatial region inside of the gasifier vessel, as in moving-bed gasifiers, or the reactions in each stage of the process may be occurring throughout the entire volume of the gasifier, as in fluidized-bed gasifiers. These stages, with their

[1] The work presented in this thesis was performed assuming the use of air or a higher oxygen (O_2) content gaseous oxidant stream. Steam-only gasification systems do exist, but were not considered in this work.

associated chemistry, can be summarized as follows (NETL, 2015; Probstein & Hicks, 1990; Higman & van der Burgt, 2003; Adhikari, 2010; Kirk-Othmer, 2002).

1) Drying – The feedstock undergoes dewatering, which often occurs in a process or unit operation prior to the gasifier for dry-feed gasifiers, but any residual moisture remaining in the dried feedstock after pretreatment or liquid water in the feedstock slurry will be vaporized in the gasifier itself.

2) Pyrolysis/Devolatilization – Heat from combustion causes chemical bonds within the feedstock to break, resulting in compounds of various molecular weights. The light components vaporize. Some remain gaseous while others form tars. The heavy components form char.

3) Combustion – The combustible components react with oxygen, releasing the heat which is the driving force for the entire process.

$$C + \tfrac{1}{2} O_2 \rightarrow CO \qquad (\Delta H = -111 \text{ kJ/mol}) \qquad (1)$$

$$CO + \tfrac{1}{2} O_2 \rightarrow CO_2 \qquad (\Delta H = -283 \text{ kJ/mol}) \qquad (2)$$

$$C + O_2 \rightarrow CO_2 \qquad (\Delta H = -394 \text{ kJ/mol}) \qquad (3)$$

$$H_2 + \tfrac{1}{2} O_2 \rightarrow H_2O \qquad (\Delta H = -242 \text{ kJ/mol}) \qquad (4)$$

4) Gasification – Steam and carbon dioxide react with the char (carbon) that has not been oxidized to form hydrogen and carbon monoxide.

Water-Gas Reaction:

$$C + H_2O \leftrightarrow CO + H_2 \qquad (\Delta H = +131 \text{ kJ/mol}) \qquad (5)$$

Boudouard Reaction:

$$C + CO_2 \leftrightarrow 2\ CO \qquad (\Delta H = +172\ kJ/mol) \qquad (6)$$

Additionally, the following reactions are important to the gasification process.

Methane Combustion:

$$CH_4 + 2\ O_2 \rightarrow CO_2 + 2\ H_2O \qquad (\Delta H = -803\ kJ/mol) \qquad (7)$$

Methanation (or Hydrogasification) Reaction:

$$C + 2\ H_2 \leftrightarrow CH_4 \qquad (\Delta H = -75\ kJ/mol) \qquad (8)$$

Methane Reforming Reaction:

$$CH_4 + H_2O \leftrightarrow CO + 3\ H_2 \qquad (\Delta H = +206\ kJ/mol) \qquad (9)$$

Water-Gas Shift Reaction:

$$CO + H_2O \leftrightarrow CO_2 + H_2 \qquad (\Delta H = -41\ kJ/mol) \qquad (10)$$

Other Reactions:

$$C + 2\ H_2O \leftrightarrow CO_2 + 2\ H_2 \qquad (\Delta H = +90.1\ kJ/mol) \qquad (11)$$

$$C + H_2O \leftrightarrow \tfrac{1}{2}\ CO_2 + \tfrac{1}{2}\ CH_4 \qquad (\Delta H = +7.7\ kJ/mol) \qquad (12)$$

$$CH_4 + \tfrac{1}{2}\ O_2 \rightarrow CO + 2\ H_2 \qquad (\Delta H = -36\ kJ/mol) \qquad (13)$$

Previous work has shown that the water-gas shift, Boudouard, and methanation reactions are the "fundamental" reactions in the gasification process (*Perry's*, 7th Ed.).

2.3 Feedstocks

As previously mentioned, a strength of gasification as an energy technology is that a wide variety of solid, liquid, and gaseous materials can be utilized as feedstocks. Coal, petroleum coke, waste plastic, waste paper, biomass, industrial waste, municipal waste, refinery residues, residual heavy oils, sewage sludge, black liquor, natural gas, and refinery off gas have all been used or proposed as feedstocks (Foster Wheeler, 2015; Clayton *et al.*, 2002). This flexibility means that the viability of gasification as an energy platform is not dependent on a few single sources of raw materials; thus, the syngas product is not as susceptible to supply shortages and upset conditions as other energy sources, such as crude oil. Though a wide variety of feedstocks can be used in the gasification process, this study focuses on the use of various types of coal and biomass. Coal and biomass each offer benefits as a potential feedstock.

At current production rates, the world's proven oil and natural gas reserves will last 54 years and 61 years, respectively, but proven coal reserves will last 142 years (World Coal Association, 2014). Thus, the supply of coal will far outlast that of oil or natural gas, so by the sheer amount available for use, coal is an important feedstock for gasification.

While coal is more abundant than either oil or natural gas, the other major feedstock considered in this thesis, biomass, is even more abundant. Most areas of the world have access to biomass of some form or another. In addition, biomass offers two more great advantages as a feedstock: 1) Biomass is renewable; unlike fossil fuels, which have limited total recoverable reserves, the supply of biomass is virtually unlimited, and 2) while the issue of biomass fuels being "carbon-neutral" is debated; it is

certain that using biomass is much closer to carbon-neutral than fossil fuels. In addition, biomass gasification could make use of biomass streams that are often discarded such as hulls, husks, clippings, etc. Additionally, using what would generally be considered as waste biomass, as opposed to food source biomass (e.g. corn), would not affect the availability or the pricing of food crops. This could prove to be of great benefit in countries where food supplies are already limited.

2.4 Feedstock Analyses

There are standard laboratory methods for analyzing feedstock composition and energy content. A basic understanding of these analyses is important in modeling coal and biomass gasification.

2.4.1 Proximate Analysis

The proximate analysis of a feedstock divides the mass of the substance into four categories: 1) moisture, 2) volatile matter, 3) ash, and 4) fixed carbon. The mass of moisture is found by heating the feedstock to between 104-110°C for one hour and determining the change in mass (Higman & van der Burgt, 2003). Volatile matter is then determined by heating the now-dry-feedstock to a much higher temperature (950°C for one method) for a set period of time and determining the change in mass again (Higman & van der Burgt, 2003). Ash is the remaining mass after combustion of the feedstock (Higman & van der Burgt, 2003). Fixed carbon is the mass fraction remaining after subtracting the other three; it is important to note that this not actually a measure of carbon in the substance but is an "artificial concept" used in reporting results (Higman &

van der Burgt, 2003). In fact, a portion of the carbon in the sample is driven off with the volatiles (Gaur & Reed, 1998). The "fixed carbon" concept is intended to represent the amount of char that remains after drying, pyrolysis, and volatilization (Gaur & Reed, 1998). Many reports will also normalize volatile matter, ash, and fixed carbon to give the mass fractions on a dry basis.

2.4.2 Ultimate Analysis

Ultimate analysis is another method of analyzing the composition of a feedstock. The ultimate analysis of a feedstock reports the mass fractions of carbon (C), hydrogen (H), nitrogen (N), oxygen (O), sulfur (S), and ash. Some analyses will also report the mass fraction of chlorine (Cl). It should be noted that there is some variation in how moisture is reported in the ultimate analysis. Some analyses will report moisture as a separate mass fraction unto itself. Other reports will lump the moisture in with the hydrogen and the oxygen. Still other reports will be on a dry basis, thus the moisture is not represented at all in the analysis. Either reporting moisture as a separate fraction or showing results on a dry basis are preferable to including the moisture as portion of the hydrogen and oxygen fractions, because reporting the moisture as hydrogen and oxygen prevents fair comparisons of one specimen against another because of differing moisture contents.

2.4.3 Sulfur Analysis

The sulfur analysis of a feedstock further divides the sulfur content into three classifications: 1) pyritic, 2) organic, and 3) inorganic sulfates (Higman & van der Burgt,

2003). Pyritic sulfur exists as iron sulfide (FeS_2) (*Perry's*, 7th Ed.). Organic sulfur is chemically bound into the structure of the coal (Probstein & Hicks, 1990). The sulfate form generally comprises a very small portion of the sulfur in the sample (*Perry's*, 7th Ed.). In coals of the eastern United States, which are generally higher-sulfur, the majority of the sulfur exists in the pyritic form. In the lower-sulfur coals from the western United States, the majority of the sulfur exists in the organic form. Biomass feedstocks generally have a much lower sulfur content than coal. The process simulation software (See Section 4.1) that was used in the work presented in this thesis requires that the sulfur analysis be provided to use the property set for modeling solids. This can pose a problem, because although proximate and ultimate analysis data is readily available for many potential feedstocks, sulfur analysis data is often not included. Therefore, assumptions had to be made regarding the breakdown of any sulfur present. The impacts of this assumption are further discussed in Section 6.8.

2.4.4 Heating Value

The heating value of a feedstock is usually given as either the higher heating value (HHV) or the lower heating value (LHV). The HHV of a substance indicates the energy per unit mass that is released if that substance is completely combusted and any water formed during the combustion is condensed (*Perry's*, 7th Ed.). The LHV assumes that the water formed during combustion is not condensed; thus, it is inherently less than the HHV by the amount of energy used for vaporizing and increasing the temperature of any water formed as a combustion product. Although in many industrial applications the LHV is more applicable than the HHV because latent heat of any steam formed during

combustion is not recovered, more data is available for the HHV of potential gasification feedstocks than for the LHV of those feedstocks. The work reported in this thesis used HHV due to the requirements of the process simulation software (See Section 4.1).

2.5 Gasifier Types

In the gasification process, a variety of equipment is necessary for feedstock treatment and syngas cleanup and conditioning, but the heart of the gasification process is the gasifier vessel itself, and there are several different types of gasifiers that can be employed. There are different methods for classifying gasifiers, including method of heat delivery, gasifying agent, and reactor type (Probstein & Hicks, 1990).

Classification based on the method of heat delivery divides the gasifiers into two groups, direct or indirect, based on the method in which the heat from the combustion zone is delivered to the drying, pyrolysis, and gasification zones. In processes that utilize direct gasification, the heat from the combustion zone is supplied to the other zones by the fact that a portion of the feedstock is combusted in the gasifier vessel. Conversely, indirect gasification separates the combustion and the drying/pyrolysis/gasification into two separate vessels. In this configuration, the energy needed for the endothermic zones is supplied from the combustion zone by some media that links the two vessels without creating direct contact between the gas phases of the vessels.

Another method of classification is based on the gasifying media that is injected with the feedstock. Air, oxygen, and steam are the most commonly used oxidants. Thus, gasifiers can be classified as “air-blown,” “oxygen-blown,” etc.

Yet another method of classifying gasifiers is to divide them based on whether the feedstock is supplied to the gasifier as dry particles or as a slurry. Dry-feed gasifiers use a transport gas to deliver the feedstock into the gasifier through a series of lock-hoppers. Slurry-feed gasifiers combine the feedstock particles with water to make a slurry, which is pumped into the gasifier.

Gasifiers can also be classified by whether or not the ash from the feedstock is converted to slag. In slagging gasifiers, the temperature is maintained above the melting point of the ash particles, whereby the particles form a liquid slag. In non-slagging gasifiers, the temperature is kept below the temperature at which the ash begins to soften (Higman & van der Burgt, 2003). The ash melting temperatures and the ash softening temperatures are not the same; below the ash softening temperature, the ash particles behave as a solid, but in between the ash softening and ash melting temperatures, the ash particles begin to agglomerate and become sticky but do not behave as a liquid slag; thus, this region of operation for a given feedstock should be avoided (Higman & van der Burgt, 2003).

The most common method of classifying gasification processes is based on the method of contacting the feedstock and the oxidant in the gasifier vessel. By taking this approach, gasifiers can be classified as one of three main types: 1) fixed-bed or moving-bed, 2) entrained-flow, 3) fluidized-bed. The operation of these various classifications of gasifiers is discussed in the following sections.

2.5.1 Moving-Bed/Fixed-Bed

In moving-bed gasifiers, a bed of feedstock particles is moved continuously downward by gravity, and the oxidant is usually injected from the bottom (updraft), creating countercurrent flow between the solid and gas phases (Probstein & Hicks, 1990; Higman & van der Burgt, 2003). A grate at the bottom of the vessel supports the solids (Probstein & Hicks, 1990). Because the bed of solids is maintained at a fixed height by the continuous introduction of feedstock, this type of gasifier is sometimes referred to as a fixed-bed gasifier, which can lead to confusion due to the seemingly contrary terms that are used to describe it.

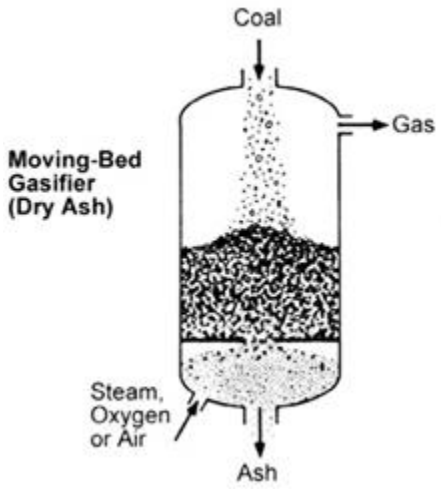

Figure 2.2 – Moving-bed/Fixed-bed gasifier (NETL, 2015)

In the updraft moving-bed gasifier, the reaction zones progress down the length of the reactor from the point of feedstock injection, as shown in the following figure.

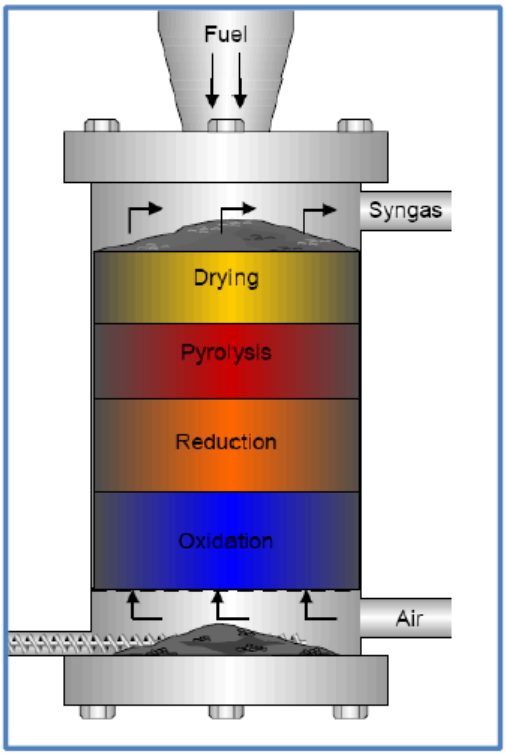

Figure 2.3 – Updraft Gasifier (Adhikari, 2010)

Although the oxidant is usually injected from the bottom of the gasifier, other potential configurations do exist, and it should be noted that the spatial relation of the zones varies depending on the injection point of the oxidant. The following figure shows the orientation of the zones in a crossdraft moving-bed gasifier.

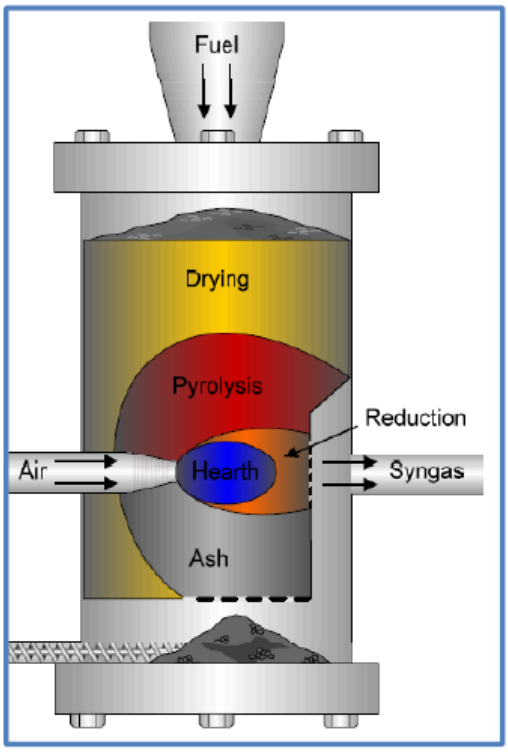

Figure 2.4 – Crossdraft gasifier (Adhikari, 2010)

Note the central combustion zone or "hearth," with the other zones in a somewhat radial orientation to the combustion zone. Although various configurations are possible, most of the literature focuses on the updraft configuration, so it is this configuration that will be discussed in detail.

The combustion zone is near the base of the gasifier, and the heat progresses up the length of the gasifier supplying energy to the endothermic processes of gasification, pyrolysis, and drying, respectively. Because of this configuration of the zones, the feedstock particles can be fed with high moisture content, up to 60% by weight (*Handbook Biomass Gasification*, 2005). This configuration also causes the outlet temperature of the syngas to be relatively lower than other types of gasifiers, because sensible heat is removed from the syngas and dries the feedstock in the upper portion of

the gasifier (Higman & van der Burgt, 2003). The vertically decreasing temperature profile also causes more of the hydrocarbons driven off in the pyrolysis process to be in the liquid state, as opposed to the gaseous state (Lee *et al.*, 2007), and some of these liquids, or tars, may become entrained in the syngas (Higman & van der Burgt, 2003). In coal-fed systems, the average linear velocity of the bed ranges from 0.5 m/h to 5 m/h depending on the combination of pressure and oxidant selection (Probstein & Hicks, 1990). The presence of fines (< 3mm) can pose operational problems in moving-bed gasifiers because of their tendency to agglomerate and impede the flow of gas through the bed and the potential to be carried out with the syngas product (Probstein & Hicks, 1990). The Lurgi dry-ash gasifier, shown in following figure, is an example of a moving-bed gasifier.

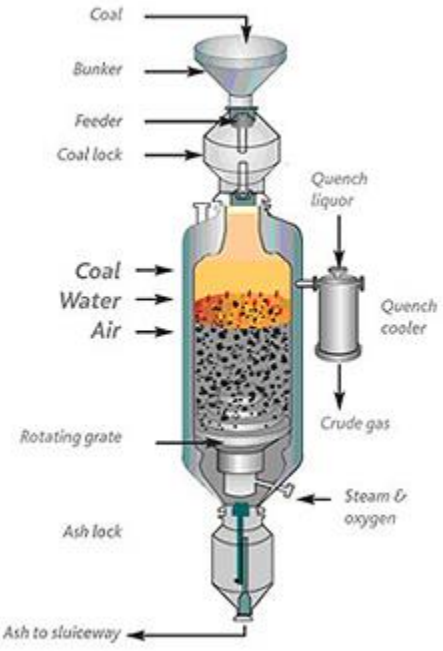

Figure 2.5 – Lurgi Gasifier (NETL, 2015)

The SASOL II & III plants in South Africa have a combined total of 80 Lurgi gasifiers, and the Great Plains Synfuels Plant in North Dakota has 14 Lurgi gasifiers (NETL, 2015).

2.5.2 Entrained-Flow

Entrained-flow gasifiers introduce the feedstock particles and the oxidant concurrently, often from the top of the gasifier. The actual site of the injection port can be changed so that they are top-fired, side-fired, etc. (Higman & van der Burgt, 2003).

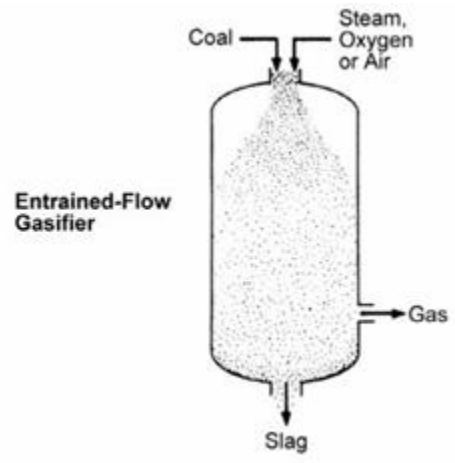

Figure 2.6 – Top-fired entrained-flow gasifier (NETL, 2015)

Entrained-flow gasifiers require that the feedstock particles be very small. Probstein and Hicks (1990) recommend a particle size of approximately 75 μm. Higman and van der Burgt (2003) recommend that particle size be no more than 100 μm. The gasifiers are generally designed for high throughput, with the feedstock particles having very short residence times of roughly a few seconds (Probstein & Hicks, 1990). This short residence time requires that the gasifier operate at a very high temperature to

achieve a high conversion during the small amount of time that the feedstock particles remain in the gasifier (Lee *et al.*, 2007). Outlet gas temperatures can range from 1250 to 1600°C (Higman & van der Burgt, 2003). Using oxygen as the oxidant can help to achieve these high temperatures (Lee *et al.*, 2007). These temperatures are the highest of the main types of gasifiers (Probstein & Hicks, 1990). In addition to enabling a rapid conversion, the high temperature also creates other operational benefits. Methane production is very low; the ratio of CO to CO_2 is high, and the syngas product has low tar or heavies content (Probstein & Hicks, 1990). The high temperature presents some drawbacks as well. Ash is melted into slag, and the hot outlet gas must be quenched, which results in thermal inefficiency (Probstein & Hicks, 1990). Additionally, the H_2/CO ratio in the product syngas from entrained-flow gasifiers is the lowest of the major gasifier types (Probstein & Hicks, 1990). Entrained-flow gasifiers can be either dry-feed or slurry-feed. The following figures depict two well-known entrained-flow gasifier designs.

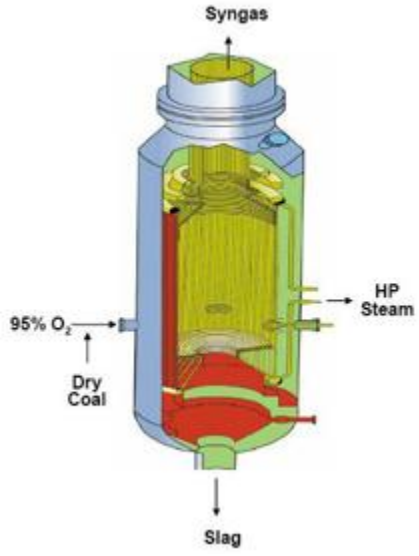

Figure 2.7 – Shell gasifier (NETL, 2015)

The Shell gasifier is a dry-feed, oxygen-blown gasifier than can accept a wide variety of coals (Lee *et al.*, 2007). Worldwide, Shell has sold 27 licenses for their technology (Shell, 2015).

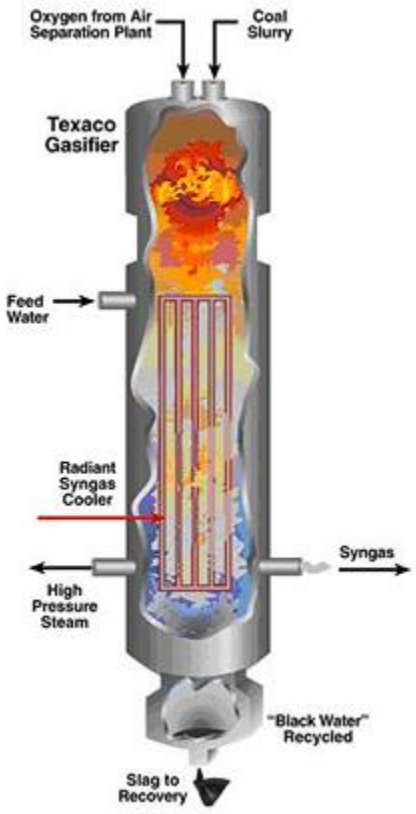

Figure 2.8 – Texaco Gasifier (NETL, 2015)

The Texaco gasifier is a slurry-feed, oxygen-blown gasifier (Probstein & Hicks, 1990). It can use coal, petroleum coke, heavy oil, or natural gas as a feedstock (NETL, 2015). More than 60 units are in operation around the world (NETL, 2015).

2.5.3 Fluidized-bed

Fluidized-bed gasifiers operate by fluidizing a bed of feedstock particles with the oxidant, which enters near the bottom of the gasifier. The oxidant injection can be either co-current or counter-current to the feedstock particles.

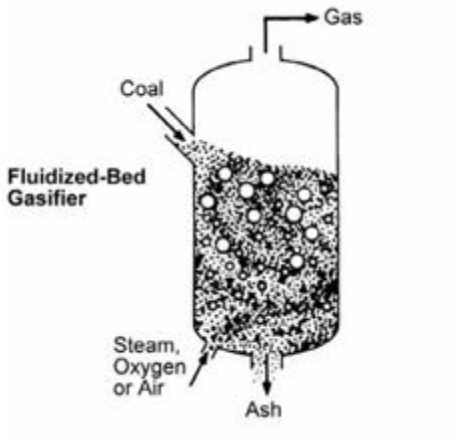

Figure 2.9 – Fluidized-bed gasifier (NETL, 2015)

Particle size is a very important parameter in the operation of a fluidized-bed gasifier (Higman & van der Burgt, 2003). For coal, the particle size is normally less than 6 mm (NETL, 2015). If the particles are too small, it can contribute to the inherent tendency for the carryover of solids into the syngas product (Higman & van der Burgt, 2003). The nature of the fluidized-bed promotes good mixing, and therefore, uniform bed temperature as well as excellent contact between the solid and gas phases (Probstein & Hicks, 1990; Lee *et al.*, 2007). This, in turn, causes the gasification reactions to reach equilibrium rapidly, allowing for high throughputs, but with feedstock residence times that are longer than those of entrained-flow gasifiers (Probstein & Hicks, 1990; Lee *et al.*, 2007). Additionally, the temperature uniformity also prevents clinker formation in higher

temperature zones (Probstein & Hicks, 1990). Two drawbacks of the fluidized gasifier are that it does not perform well with coals that have a tendency to cake or swell, and the carryover of a portion of the feedstock or char into the product (Probstein & Hicks, 1990). This causes decreased overall conversion. Normally, this phenomenon is addressed by solids separation that returns a portion of the unreacted solids to the gasifier (Higman & van der Burgt, 2003). With regard to ash or slag, denser mineral particles drop out of the bed, and the temperature is usually kept below the temperature at which ash begins to soften and form slag because slag formation negatively affects the nature of the fluidized regime (Probstein & Hicks, 1990; Higman & van der Burgt, 2003). Generally, among the various types of gasifiers, fluidized-bed gasifiers have the lowest operating temperatures (Probstein & Hicks, 1990).

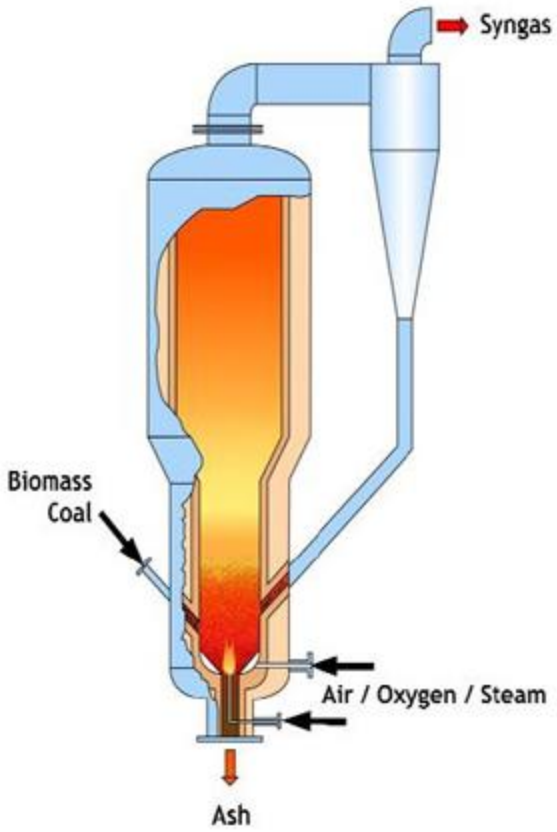

Figure 2.10 – U-GAS® gasifier (NETL, 2015)

The U-GAS® gasifier is a fluidized-bed design that can operate on a variety of feedstocks (NETL 2015). The design has been licensed for two facilities in China (NETL, 2015).

2.5.4 Specialty Gasifiers

In addition to the traditional types of gasifiers, there are also a variety of novel gasifier technologies available such as molten bath, arc furnace, and electric induction (Warnecke, 2000).

2.5.5 In-Situ Gasification

It should be noted that in-situ gasification, where the feedstock (e.g. lignite, bituminous coal, etc.) is gasified in underground seams by injecting the oxidant into the seam, igniting it to begin the partial combustion/gasification process, and collecting the syngas at-grade, is another option. Though it still involves the same thermochemical principles as industrial gasifiers, it is a different technology entirely, and is not considered in this thesis.

2.6 Additional Systems

Though the gasifier vessel itself is the critical component of any gasification process, there are a number of process systems that are vitally important to the operation of the overall process. Some of these systems are discussed in the following sections.

2.6.1 Feedstock Pre-Treatment

Most feedstocks, if not all, require some type of sizing operation to allow for feeding to the gasifier. Shredding, crushing, grinding, and screening are examples of different operations that may take place depending on the selected feedstock. The preferred feedstock particle size varies depending on the type of gasifier (See Sections 2.5.1-2.5.4). Generally, moving-bed gasifiers accept much larger particles than either entrained-flow or fluidized-bed gasifiers.

In addition to sizing operations, some gasifiers also require that the feedstock be dried. Drying is not required for slurry-feed gasifiers (Higman & van der Burgt, 2003). Most dry-feed moving-bed gasifiers also do not require drying because the drying step

takes place within the gasifier (Higman & van der Burgt, 2003). For systems that require a drying step, the most energetically favorable option is to use waste heat from the product gas as opposed to a fired dryer (Higman & van der Burgt, 2003).

2.6.2 Feedstock Handling

One important system in any gasification process is the method of introducing the treated feedstock into the gasifier vessel. Conventional gasifier feed systems are one of two types, dry-feed or slurry-feed.

Dry-feed systems use a carrier gas (or transport gas) to transport the feedstock particles which is pressurized by a lock hopper system. Nitrogen, carbon dioxide, or recycled syngas are used as the carrier gas. If the gasification process has an air separation unit (see next section) to supply high-purity oxygen to the gasifier, then the nitrogen from the air separation unit is an easy option for use as the carrier gas. Nitrogen is more common in gasification for power production, but additional N_2 in the process can be problematic if the downstream application of the syngas is for the production of chemicals other than ammonia (Higman & van der Burgt, 2003). Carbon dioxide is a viable option if the gasification facility has a CO_2 removal process, eliminating the problem of introducing additional nitrogen into the process, but may reduce the H_2/CO ratio of the syngas product (Higman & van der Burgt, 2003). Lastly, recycled syngas can also be used to feed the solids, as in the KBR TRIG™ gasifier (Ariyapadi *et al.*, 2008). Dry-feeding the solids into the gasifier eliminates the energy penalty that is incurred when slurry-feeding is used, but dry-feeding can pose its own challenges. The lock-hoppers that are generally used are expensive, operate discontinuously, and require

increasing quantities of carrier gas for increasing operating pressure of the gasifier, which incurs its own thermal penalty (Higman & van der Burgt, 2003). The U.S. Department of Energy lists this lock hopper delivery system as "a cause of considerable downtime" and recognizes it as a gasification supporting technology that needs improvement (Clayton *et al.*, 2002).

Slurry-feed systems use water as the medium for transporting the feedstock into the gasifier, allowing more conventional and reliable pressurization technology than the lock hopper system used with dry-feed systems. The drawback to slurry-feed systems is the energy penalty that is paid to vaporize the liquid water once it enters the gasifier. This problem can be mitigated by preheating the slurry before introducing it into the gasifier (Higman & van der Burgt, 2003). The standard operation of slurry-feed coal systems is 60-70% solids by weight (Higman & van der Burgt, 2003).

Additional feeding technologies include wet lock-hoppers, which use lock-hoppers to pressurize a slurry, and dynamic hoppers, which use a tall column of feedstock to deliver the solids into the gasifier (Higman & van der Burgt, 2003). However, a survey of gasifier designs reveals that these feeding technologies are much less common than the traditional dry-feed or slurry-feed processes.

2.6.3 Air Separation

For gasifiers that use oxygen-enriched air or nearly pure oxygen as an oxidant, an air separation unit (ASU) is necessary. The most common process for this is cryogenic separation (Higman & van der Burgt, 2003). These cryogenic air separation processes work by compressing and drying the air and then condensing the air into a liquid; this

liquid is then distilled yielding two or three product streams, a nitrogen-rich stream and oxygen-rich stream and, in some processes, an argon-rich stream (Higman & van der Burgt, 2003). The oxygen-rich stream can then be used for the gasification process. When integrated gasification combined cycle (IGCC) power generation is the intended end use of the syngas, 95% oxygen has been reported as the probable economic optimum for use as the oxidant (NETL, 2015). Even higher purity oxygen is often required for the production of clean fuels and chemicals (NETL, 2015). In addition, the ASU is considered a weak link in oxygen-blown gasification systems due to its high cost and energy usage, and a report from personnel at the United States Department of Energy lists air separation as a technology that needs improvement to aid in the widespread commercialization of gasification (Clayton *et al.*, 2002; NETL, 2015).

2.6.4 Syngas Cooling

The syngas stream exiting the gasifier is at a high temperature, ranging from 550°C for certain moving-bed gasifiers to 1600°C for some entrained-flow gasifiers (Higman & van der Burgt, 2003). To perform various cleanup operations on the gas, the temperature must be lowered. For solids removal, the temperature must be less than 500°C (Higman & van der Burgt, 2003). For acid-gas removal (AGR) processes (See Section 2.6.8), the temperature must be reduced to around 100°C (Phillips, 2015). The cooling necessary for particulate removal may be performed separately from the cooling required for AGR (NETL, 2015).

Both direct and indirect heat exchange can be used to cool the syngas. Direct cooling, or quenching, can be accomplished by introducing water, cooled gas recycled

from downstream, or the feedstock slurry (in slurry-feed gasification systems) into the syngas exiting the gasifier (Higman & van der Burgt, 2003; NETL, 2015). Indirect cooling is accomplished by a network of either radiant or convective heat exchangers (or both) which produces steam to be used elsewhere in the process (NETL, 2015). From a heat recovery standpoint, indirect cooling to generate steam is more favorable, but requires additional expensive equipment that can be prone to erosion and fouling from ash particles in the syngas (Higman & van der Burgt, 2003). The capital costs of cooling with a quench are much lower than those of indirect cooling designs, but quenching is less energy-efficient (Higman & van der Burgt, 2003). However, if the downstream application of the syngas requires a higher H_2/CO ratio than the gas has leaving the gasifier, a water-quench will convert a portion of the CO to CO_2, per the water-gas shift reaction, which will increase the H_2/CO ratio. Thus, direct-quenching could also provide this advantage depending on downstream requirements.

2.6.5 Syngas Cleanup

Regardless of the end application of the syngas, it will require cleanup. Particulate matter can be removed by a variety of technologies such as filters, electrostatic precipitators, cyclones, or wet-scrubbers. After particulate removal, further gas cleanup is performed based on the requirements of the downstream systems. Different applications (IGCC, FT, etc.) have different tolerances of the various species that may be present in the syngas; therefore, various technologies are utilized to reduce the levels of oxygen (and/or oxygen-containing species), mercury, nitrogen oxides, chlorides, cyanic compounds, sulfur (and/or sulfur-containing species), and ammonia

(e.g. sorbent injection for mercury removal) (NETL, 2015; *Ullmann's*, 5th Ed.). Some of these species are removed in the AGR system, which is discussed further in Section 2.6.8.

2.6.6 Water-Gas Shift

The water-gas shift (WGS) reaction is very important in the gasification process. Recall that the WGS reaction is as follows:

$$CO + H_2O \leftrightarrow CO_2 + H_2 \qquad (\Delta H = -41 \text{ kJ/mol}) \qquad (10)$$

Since heat is a product when CO is converted into CO_2 and H_2, the reaction is favorable toward hydrogen production at lower temperatures (Higman & van der Burgt, 2003). In addition, because the reaction is equimolar, pressure has a minimal effect on its equilibrium (Higman & van der Burgt, 2003). The effect of this reaction within the gasifier is significant, but it is often used in a reactor network separate from the gasifier to adjust the composition of the syngas. There are multiple reasons why this might be necessary. Many downstream applications require hydrogen to carbon monoxide (H_2/CO) ratios greater than what can be achieved by that gasification process. For some applications, it might be desirable to simply maximize the production of hydrogen from the feedstock. In the case of a power generation application with carbon capture requirements, it might be necessary to convert some of the CO into CO_2, which can be removed by the AGR system, thus allowing the process to meet the specified carbon capture requirements (Grol & Yang, 2009). Whatever the reason for its usage, WGS reactor technology is important to the gasification industry.

The water-gas shift system may be based on a single reactor or multiple reactor configuration (Grol & Yang, 2009). The syngas products from dry-feed systems often

require additional steam to be introduced into the syngas stream prior to entering the WGS system, while the syngas from slurry-feed systems often has enough moisture that adding steam prior to WGS is not necessary (NETL, 2015). WGS systems can be designed to operate over a variety of temperature ranges and can use a variety of catalysts with 500°C as the high end temperature maximum for catalytic conversion (Higman & van der Burgt, 2003). Operating above this temperature causes thermal degradation and deactivation of the catalyst (Higman & van der Burgt, 2003). The WGS system can be placed before the sulfur-removing AGR system, which is called a "sour-shift" or after the AGR system, which is called a "sweet-shift."

2.6.7 Sulfur-Gas Conversion

The majority of the sulfur in a feedstock will be converted to H_2S in the gasifier, but a portion will remain as carbonyl sulfide (COS) (NETL, 2015). Depending on system conditions, the portion of sulfur in the feed that is converted to COS is roughly 3-10% (NETL, 2015). The amount of COS in the syngas is important because although some AGR technologies will effectively remove COS, many AGR technologies do not effectively remove COS but are very effective at removing H_2S (Higman & van der Burgt, 2003). Thus, it sometimes becomes necessary to convert COS into H_2S catalytically by the following reaction:

$$COS + H_2O \leftrightarrow CO_2 + H_2S \qquad (\Delta H = -30\ kJ/mol) \qquad (14)$$

This reaction is also promoted in the WGS system, and depending on system setup, the WGS process alone may convert enough COS to ultimately meet the sulfur removal

requirements in the AGR, or a separate reactor for COS conversion may be necessary (Grol & Yang, 2009).

2.6.8 Acid-Gas Removal

Acid-gases[2] will inevitably be present in syngas; these include H_2S, COS, and CO_2, and there is often a need to remove these gases. In converting syngas to fuels and chemicals, sulfur compounds can cause catalyst poisoning and deactivation. In power production applications, carbon capture requirements may be in place. In either case, an acid-gas removal (AGR) system is used to remove the undesirable species from the syngas. Three common acid-gas removal technologies are absorption, adsorption, and diffusion (Higman & van der Burgt, 2003). The following list examines criteria for comparing different technologies (Higman & van der Burgt, 2003).

- Inlet Gas Composition – The removal technology must be able to remove the impurities in the form and concentration in which they exist in the inlet gas. For example, a particular technology is only effective at removing H_2S, but a significant fraction of the sulfur is in the form of COS. Additionally, the effects of any impurities that foul, decompose, or otherwise negatively impact the removal equipment, solvent(s), etc. must be considered.

[2] In the context of gasification, the terms "acid-gas" or "acid-gases" can be used to refer specifically to sulfur-containing species or can include CO_2 as well. This thesis adopts the latter approach.

- Selectivity – The effectiveness with which a given technology removes one species in the syngas relative to the other species in the syngas. This can be of particular importance relative to the desire to remove CO_2 or leave it in the syngas.

- Outlet Gas Requirements – Downstream applications have varying requirements relative to total sulfur and/or CO_2 content.

- Regeneration/Utility Requirements – For AGR technologies that have an associated regeneration process, the equipment and utilities necessary for regeneration varies between different technologies.

Absorption-based AGR processes use a solvent in an absorption/regeneration setup where a solvent contacts the syngas in a trayed or packed column, removing targeted impurities; the impurities are removed from the solvent in a regeneration process that typically involves steam stripping or pressure reduction, thus allowing the solvent to be sent back to the absorber to restart the cycle (Higman & van der Burgt, 2003). Solvents are generally classified into one of three types: 1) chemical, 2) physical, or 3) physical-chemical hybrid.

Chemical solvents chemically bond to the acid-gases, and the regeneration step uses heat to break the bonds to release the impurities and regenerate the solvent (NETL, 2015). Various primary, secondary, and tertiary amines are used as chemical solvents, with methyldiethanolamine (MDEA) being the most widely used (Higman & van der Burgt, 2003; NETL, 2015). Additionally, one non-amine chemical solvent for AGR is potassium carbonate (NETL, 2015).

Physical solvent technologies use high acid-gas partial pressure in the inlet gas to drive absorption of the impurities into an organic solvent (NETL, 2015). Solvent regeneration is performed by pressure reduction (NETL, 2015). Rectisol® (methanol), Selexol™ (dimethyl ethers of polyethylene glycol), and Purisol® (n-methyl-pyrrolidone) are all examples of physical AGR solvents (NETL, 2015).

Physical-chemical solvents, or hybrid solvents, are a blend of a physical solvent and a chemical solvent, thus allowing the solvent to work as both a physical and chemical solvent (Higman & van der Burgt, 2003). Sulfinol® (mixture of diisopropanolamine [DIPA] and Sulfolane [tetrahydrothiophene dioxide]) and m-Sulfinol® (mixture of MDEA, Sulfolane, and water) are examples of physical-chemical solvents (Higman & van der Burgt, 2003; Shell, 2015).

Adsorption is another option for AGR. The impurities are absorbed onto various potential sorbents in a packed bed. Alumina, zeolite, activated carbon, silica gel, zinc oxide, and copper oxide are common sorbents (Higman & van der Burgt, 2003; NETL, 2015).

Diffusion removal technologies utilize the rate at which different species within the syngas permeate a polymeric membrane (Higman & van der Burgt, 2003). Thus certain species pass through the membrane relatively quickly, while others pass through more slowly, thus removing the quickly-permeating species from the gas stream (Higman & van der Burgt, 2003). The following table gives a comparison of the relative permeability of common syngas species relative to one another:

Relative Permeation Rates of Syngas Components		
Quick	**Intermediate**	**Slow**
H_2	CO_2	CO
H_2S		CH_4
		N_2

Table 2.1 – Relative rates of membrane permeation (Higman & van der Burgt, 2003)

2.7 Downstream Technologies

One of the strengths of gasification is that the product it produces can be used for a variety of applications. The following figure gives an overview of the possible downstream applications of a coal/petcoke gasification process.

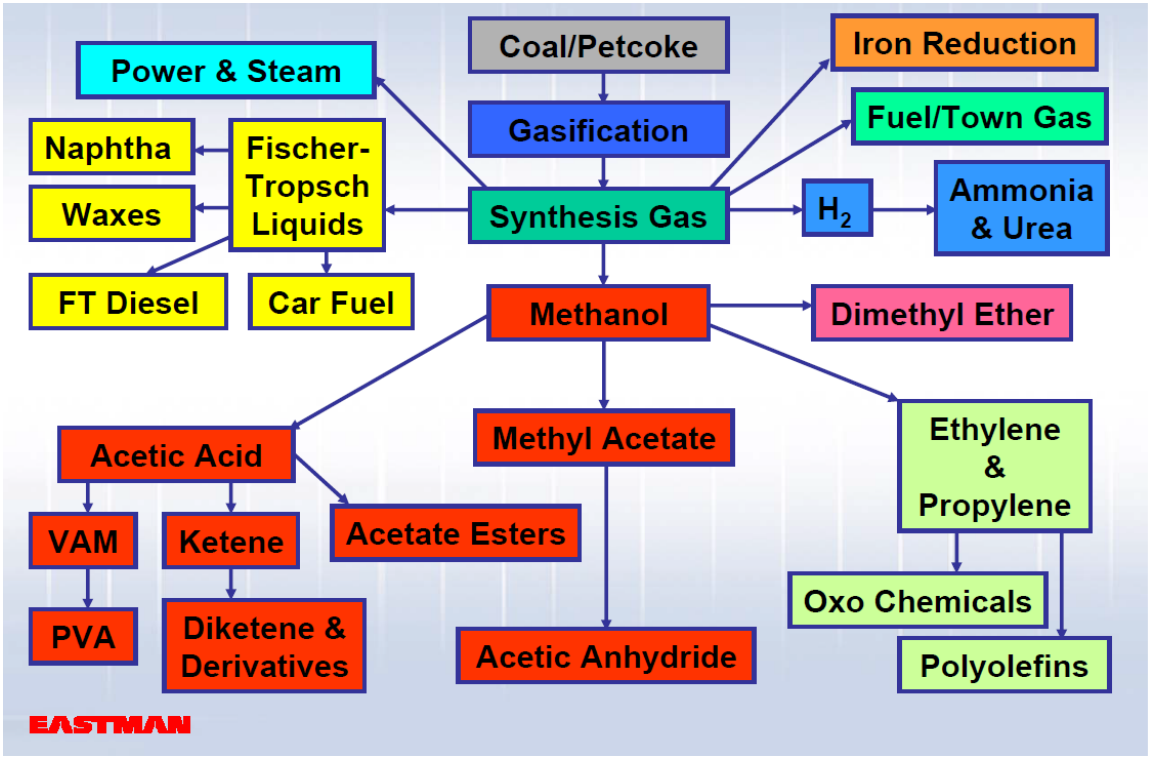

Figure 2.11 – Potential applications of gasification (Eastman, 2005)

As shown in the figure, there are numerous possibilities for utilizing the syngas product from gasification, which can be divided into three broad categories: 1) power generation, 2) synthetic chemical production, and 3) synthetic fuel production. These applications are discussed in the following sections.

2.7.1 Power Generation

The most common downstream technology for electric power generation from gasification is the integrated gasification combined cycle (IGCC) power plant. These plants operate on a similar theory as traditional combined cycle power plants, which often operate using natural gas. In the IGCC system, the syngas is fully combusted in a gas-turbine and the heat from this combustion is recovered to produce steam which drives a steam turbine. One particular advantage of IGCC over conventional combustion boilers is that contaminants can be removed from the syngas prior to combustion in the gas-turbine (NETL, 2015). Additionally, coal-based IGCC plants are more efficient than conventional coal-fired power plants (NETL, 2015).

2.7.2 Synthetic Chemical Production

A wide variety of chemicals can be produced from synthesis gas. Ammonia (NH_3) can be produced by the following reaction over an iron or ruthenium catalyst (Higman & van der Burgt, 2003).

$$N_2 + 3\,H_2 \leftrightarrow 2\,NH_3 \qquad (\Delta H = -92\ kJ/mol) \qquad (15)$$

Additionally, if NH_3 is produced, it can be reacted with CO_2 from the syngas to produce urea (NH_2CONH_2) as shown (Higman & van der Burgt, 2003).

$$2\ NH_3 + CO_2 \leftrightarrow NH_2CONH_2 + H_2O \quad (16)$$

Methanol is another chemical that can be produced from syngas. Methanol has a wide variety of uses, including serving as an intermediate (or platform chemical) in the production of other chemicals. It is produced from syngas by using a copper catalyst to react H_2 with CO or CO_2 according to the following reactions (Higman & van der Burgt, 2003).

$$CO + 2\ H_2 \rightarrow CH_3OH \qquad (\Delta H = -91\ kJ/mol) \quad (17)$$

$$CO_2 + 3\ H_2 \rightarrow CH_3OH + H_2O \qquad (\Delta H = -50\ kJ/mol) \quad (18)$$

Additional chemicals that can be produced from syngas include acetic anhydride, acetic acid, and mixed alcohols, which range from C_3-alcohols to C_{18}-alcohols (NETL, 2015; Higman & van der Burgt, 2003).

2.7.3 Synthetic Fuel Production

Syngas can also be converted to liquid transportation fuels. This use of syngas may become increasingly important as competition for the world's oil reserves continues to grow. One method of creating transportation fuel, converts methanol, which can be produced as described in the previous section, into gasoline. Another technology for fuel production from syngas involves much older technology that has seen a great resurgence in interest over the last decade. Fischer-Tropsch (FT) reactors can be used to convert syngas into a variety of hydrocarbons, including fuels, oils, and waxes according to the following reaction (Irankhah *et al.*, 2007):

$$n\ CO + \left(\frac{n+m}{2}\right) H_2 \rightarrow C_nH_m + n\ H_2O \quad (19)$$

A variety of catalysts can be used in the FT process, with different catalysts requiring different H_2/CO ratios in the syngas.

2.8 Environmental Considerations

As with any industrial process, understanding environmental impacts is important. Though only a few considerations will be discussed briefly here, there are many environmental issues that play a role in the implementation and operation of gasifiers and the downstream application of the syngas product. As was previously mentioned, two environmental benefits can be found in biomass gasification, which utilizes a renewable energy source and is closer to carbon-neutral than the combustion of fossil fuels. Another eco-friendly aspect of gasification is that AGR technologies make carbon sequestration possible. In addition, as a source of power generation, gasification allows for easier capture of sulfur than does conventional coal-fired power generation because the removal of H_2S from syngas is much more easily accomplished than removing SO_2 from flue gas (Higman & van der Burgt, 2003).

3. Modeling Approach

3.1 General Approach

The research presented in this thesis is aimed toward general observations in equilibrium modeling of coal and biomass gasification using commercial process simulation software. The model configuration used for this work is not intended to reflect the configuration of a particular style of gasifier but is intended to be used to evaluate the equilibrium phenomena of equilibrium-based gasification modeling at large with a focus on comparing results to established observations and suggesting limitations of and areas of improvement for equilibrium gasification modeling.

3.2 Selected Feedstocks

The abundant supply of coal and the flexible and nearly ubiquitous supply of biomass make them ideal feedstocks for gasification. This work was done using two coal feedstocks and two biomass feedstocks. Montana sub-bituminous coal and Illinois bituminous coal were used as the two coal feedstocks. Southern pine wood and switchgrass were used as the two biomass feedstocks. The characterization of each of these feedstocks is given in the following tables.

Montana Sub-Bituminous Coal					
Proximate Analysis	**As Received**	**Dry Basis**	**Ultimate Analysis**	**As Received**	**Dry Basis**
% Moisture	10.50		% Moisture	10.50	
% Ash	11.20	12.51	% Carbon (C)	59.82	66.84
% Volatiles	34.70	38.77	% Hydrogen (H)	4.38	4.89
% FixedCarbon	43.60	48.72	% Nitrogen (N)	1.33	1.49
	100.00	100.00	% Sulfur (S)	1.10	1.22
			% Ash	11.20	12.51
% Sulfur (S)	1.10	1.22	% Oxygen (O)	11.67	13.04
				100.00	100.00
HHV (BTU/lb)	8600.00				

Table 3.1 – Montana sub-bituminous coal (MTC) characterization

Illinois Bituminous Coal					
Proximate Analysis	**As Received**	**Dry Basis**	**Ultimate Analysis**	**As Received**	**Dry Basis**
% Moisture	13.00		% Moisture	13.00	
% Ash	10.70	12.30	% Carbon (C)	59.82	68.76
% Volatiles	37.00	42.53	% Hydrogen (H)	4.12	4.74
% FixedCarbon	39.30	45.17	% Nitrogen (N)	1.07	1.23
	100.00	100.00	% Sulfur (S)	3.74	4.30
			% Ash	10.70	12.30
% Sulfur (S)	3.74	4.30	% Oxygen (O)	7.55	8.68
				100.00	100.00
HHV (BTU/lb)	11000.00				

Table 3.2 – Illinois bituminous coal (ILC) characterization

Southern Pine Wood					
Proximate Analysis	**As Received**	**Dry Basis**	**Ultimate Analysis**	**As Received**	**Dry Basis**
% Moisture	8.20		% Moisture	8.20	
% Ash	0.30	0.33	% Carbon (C)	42.47	46.26
% Volatiles	72.39	78.86	% Hydrogen (H)	5.16	5.62
% FixedCarbon	19.10	20.81	% Nitrogen (N)	0.12	0.13
	100.00	100.00	% Sulfur (S)	0.00	0.00
			% Ash	0.30	0.33
% Sulfur (S)	0.00	0.00	% Oxygen (O)	43.75	47.66
				100.00	100.00
HHV (BTU/lb)	8100.00				

Table 3.3 – Southern pine wood (SPW) characterization

Switchgrass					
Proximate Analysis	**As Received**	**Dry Basis**	**Ultimate Analysis**	**As Received**	**Dry Basis**
% Moisture	8.18		% Moisture	8.18	
% Ash	2.72	2.96	% Carbon (C)	40.86	44.50
% Volatiles	77.18	84.06	% Hydrogen (H)	5.17	5.63
% FixedCarbon	11.92	12.98	% Nitrogen (N)	1.10	1.20
	100.00	100.00	% Sulfur (S)	0.00	0.00
			% Ash	2.72	2.96
% Sulfur (S)	0.00	0.00	% Oxygen (O)	41.97	45.71
				100.00	100.00
HHV (BTU/lb)	8250.00				

Table 3.4 – Switchgrass (SWG) characterization

These four materials cover a diverse range of feedstock options: a low-middle rank coal, a high-middle rank coal, and two potentially large biomass resources.

4. Software & Simulation Techniques

4.1 General Information

All process modeling was done with Aspen Plus®, a commercial process simulation software package. This software is widely used in academics and industry, and can be used to model a variety of processes. The software enables the user to model a wide range of processes by allowing the user to choose from a variety of sub-models to represent the necessary unit operations in the overall process. These sub-models or subroutines (or "blocks" as they are referred to within the software) are interconnected by material and energy streams, thus producing an overall process flowsheet. System components and the governing thermodynamic model(s) must be specified, and once all necessary input has been completed, the software uses rigorous mathematics to determine the simulation output. In addition, Aspen Plus® has the ability to model nonconventional solids, which was integral in studying coal and biomass gasification.

4.2 Modeling Tools

A tool incorporated in the software package that was extensively used in generating the data was the "sensitivity analysis" function. This tool allows the user to specify independent and dependent variables within the process (e.g. material flows, unit operation conditions, feedstock parameters, etc.) and generate a pool of data that shows

the response of each dependent variable to the manipulation of the independent variable over a given range.

4.3 Thermodynamic Model

The Peng-Robinson model with the Boston-Mathias modification (PR-BM) is one of the software's suggested models for coal systems and was used to generate the data in this study.

4.4 System Components

Creating an accurate model is dependent on including the components (i.e. chemical species) that may be found in the system. The following components were included in creating each of the simulations: ammonia (NH_3), argon (AR), carbon (C [modeled as graphite]), carbon monoxide (CO), carbon dioxide (CO_2), hydrogen (H_2), hydrogen sulfide (H_2S), methane (CH_4), nitrogen (N_2), nitric oxide (NO), nitrogen dioxide (NO_2), oxygen (O_2), sulfur (S), sulfur dioxide (SO_2), sulfur trioxide (SO_3), and water (H_2O). Each simulation also included ash as a nonconventional inert component.

4.5 Feedstock Modeling

In addition to the previously specified components, one additional component was also included in each simulation—coal; however, coal is not a traditional component in the sense that the others are. The "coal" component is simply a way for the user to introduce the feedstock of choice into the system, whether it is actually coal, biomass, or another feedstock. Due to a nearly unlimited number of possible feedstocks and an

infinite number of possible characterizations of the feedstocks, each feedstock is introduced into the model as a material with known fractions of various chemical species via the previously discussed proximate, ultimate, and sulfur analyses. The higher heating value of each feedstock is also included as part of the data that is entered for each feedstock. Thus, the coal component in each simulation is actually used to represent each type of feed for the gasification process. Because the software cannot handle this nonconventional component as a standalone species in material and energy balances or chemical reactions, it must be broken down into its constituent chemical species. This process is discussed in further detail in the following section.

4.6 Subroutines

The two following blocks within the software were the key units involved in modeling the gasification process:

RYIELD – This unit is a chemical reactor that is used when the yield of each product is known and can be specified. Within the scheme of gasification modeling, it is used to break down the nonconventional feed component into components that the software can actually use in running simulations. It should be noted that this reactor is not an actual separate piece of equipment that would be present in a gasification system, but is needed to accurately model the gasification process because of the inability of the modeling software to handle each possible feedstock as a unique species. In this thesis, the RYIELD unit will be referenced as the DECOMP block.

RGIBBS – This unit is a chemical reactor that operates by determining the product stream composition, that under specific conditions (temperature, pressure, heat

duty), minimizes the Gibbs free energy of the system. In addition, it does not require knowledge of the kinetics that take place within a given reaction system, so it allows the user to model systems with complex chemistry that is not well described or not documented. This makes this block an ideal choice for use in coal and biomass gasification modeling. It should be noted that this unit assumes that thermochemical equilibrium is achieved. In this thesis, the RGIBBS unit will be referenced as the GASIFIER block.

The RYIELD and RGIBBS blocks together model what would be the gasification vessel in a given coal or biomass gasification system.

4.7 Additional Considerations

As previously stated, the DECOMP and GASIFIER blocks would be one vessel in a real gasification system. (See Figure 4.1 for a simplified simulation flowsheet). To account for this, the DECOMP and GASIFIER blocks were linked by an energy stream. This was necessary to prevent the software from returning a solution that would not occur in reality. Because two blocks must be used to model what is actually one unit operation, gasification, it is possible for the software to find numerical solutions for each unit separately that are actually thermodynamically unfeasible for the gasifier as a whole. If the two blocks were not linked, the GASIFIER block would have more heat available for use in energy balances because it would not account for the energy required to break the feedstock into its constituent components. In standalone operation, the RGIBBS subroutine allows the user to specify any two of the following parameters: temperature, pressure, and/or duty, but when the RGIBBS unit is linked to the RYIELD unit via an

energy stream, the user is allowed to specify only the pressure. When configured as such, the simulation achieves a solution by taking whatever heat is needed by the DECOMP block from the GASIFIER block, and the residual is available to the GASIFIER block for energy balances. Thus, this strategy mitigates the previously mentioned problem of thermodynamically unfeasible solutions. This approach does sacrifice the flexibility of being able to set both the temperature and the pressure of the gasification process, but it is necessary to realistically simulate the system.

4.8 Ambient Conditions

All simulations in this study assumed an ambient temperature of 25°C and an ambient pressure of 1 atm. All streams into the model are assumed to be at ambient temperature unless otherwise stated. The COALFEED stream is assumed to be at both ambient temperature and pressure as is the DECOMP reactor.

4.9 Model Assumptions

The following assumptions were made in creating the simulations. The composition of standard air was assumed to be 78 mol% N_2, 21 mol% O_2, and 1 mol% argon. For slurry-feed systems, the slurry was set at 70% solids by weight, unless the solids content of the slurry stream itself was the variable of the sensitivity analysis. This assumed solids content falls within the range of 60-70% solids by weight which is the normal range of operation for coal slurries (Higman & van der Burgt, 2003). Lastly, for all feedstocks containing sulfur, an assumption was made for the breakdown of the three types of sulfur within the sulfur analysis. This was necessary because sulfur analysis

data is very difficult to find for most gasification feedstocks, but Aspen Plus® requires that sulfur analysis data be provided to use the non-conventional solid functionality. Therefore, the sulfur in each sulfur-containing feedstock was assumed to have the following composition by weight: 45% pyritic, 10% sulfate, and 45% organic (Eden, 2010). The effects of the various sulfur types are examined further in the results and discussion section.

4.10 Simulation Flowsheet

The following figure shows a simplified version of the simulation software flowsheet for both dry-feed and slurry-feed setups. It is not the exact flowsheet that was used to generate the data presented in this thesis, but it is functionally the same and is simplified for ease of viewing.

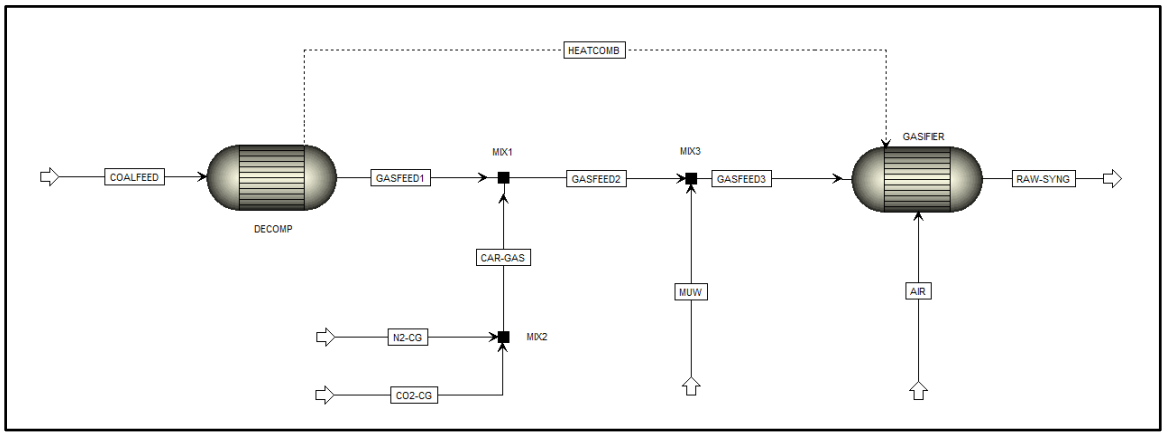

Figure 4.1 – Simplified simulation screenshot

Note that the configuration allows the addition of carrier gas and/or slurrying water between the "DECOMP" and "GASIFIER" blocks.

5. Literature Review

Damiani and Trucco (2010) developed a modified-equilibrium-based biomass gasification model. The model assumed that the gasifier operates at atmospheric pressure and that all tar is converted to gases. The authors note that traditional equilibrium models of downdraft biomass gasifiers give lower gasifier temperatures and lower values for solid carbon and methane out of the gasifier than what is observed experimentally. The suggested cause for these discrepancies is that a portion of the carbon and the hydrogen fed to the gasifier do not actually reach equilibrium. The base equilibrium model utilizes constant atomic ratios of C/O, H/O, and N/O into and out of the gasifier in conjunction with interdependent expressions for temperature dependent rate constants and the overall system energy balance to calculate the temperature of the gasifier and the composition of the product. A modification to yield more accurate predictions was achieved by determining a correlation between the equivalence ratio and the amounts of solid carbon and methane that exit the gasifier, which were obtained empirically. Thus, for a given equivalence ratio, the model removes a calculated amount of the carbon and the hydrogen from being available for equilibrium calculations, and adds these molecules back to the equilibrium predicted stream composition in the form of solid carbon and methane. Compared to the experimental data that was used as the basis for the modifications, the modified model more accurately predicted values for C, H_2O, N_2, CO, CO_2, H_2, CH_4, and temperature than the original equilibrium model. When compared to two additional sets

of experimental data from literature for the gasification of rubber wood, the modified model had mixed results compared to the equilibrium model. For one data set, the modified model more accurately predicted N_2, H_2, and CH_4, and the simple equilibrium model more accurately predicted CO and CO_2. For another data set, the modified model more accurately predicted N_2, CO, and CH_4, and the simple equilibrium model more accurately predicted CO_2 and CH_4. The modified model more accurately predicted the lower heating value of the syngas in both data sets. The authors note that the application of the modified model to systems with equivalence ratios around 0.4 is limited because the model predicts negative values for the moles of carbon not in equilibrium.

Shen *et al.* (2012) used a pilot-scale entrained-flow gasifier to evaluate the effects of blending various gasification feedstocks. The gasifier was configured to be either air-blown or oxygen-blown, and 95% oxygen was used as the oxidant for the experimental work. One major system parameter that was evaluated was the effect of O_2/carbon ratio on the composition of the syngas. In one set of experimental data, increasing the O_2/carbon ratio from 0.5 to 0.75 Nm^3/kg clearly decreased the concentration of H_2 and CO while increasing the concentration of CO_2, while the results of the other data set do not show an easily-described trend. The authors also created an equilibrium-based model in Aspen Plus® that showed good agreement with the experimental results.

Barman, Ghosh, and De (2012) generated an equilibrium model and a modified-equilibrium model. The initial model was evaluated against published experimental data for two different feedstocks, and the authors noted relatively good correlation with their model, with 7.2% being the largest error of predicted mole fraction against observed mole fraction for any species in the syngas except CH_4, which had error values of 51.1%

and 54.1%. The authors modified their model to better predict the non-equilibrium behavior of CH_4, and compared the results to experimental data from five different feedstocks. The modification to the model resulted in much more accurate predictions of CH_4 in the syngas, but the impact on the accuracy of the other species in the syngas was varied.

Vaezi *et al.* (2011) developed a numerical, modified-equilibrium model of the downdraft gasification of heavy fuel oil. The formation of char, H_2S, and NH_3 were assumed to be negligible, with the syngas comprised of H_2, CO, CO_2, CH_4, H_2O, and N_2. Because of the assumed absence of carbon in the product gas, the researchers consider only the water-gas shift reaction and the methane reforming reaction. The model was evaluated against previous experimental results from a gasification system with a configuration similar to that of the model, showing good agreement between the two, with the exception that the model predicted a much lower quantity of methane in the syngas than was found experimentally. The overall root mean square (RMS) error of the values of syngas component fractions and HHV predicted by the model against the experimental data was 0.54. The model was augmented by the addition of factors that relate the model results to the experimental results. Additionally, the researchers performed parametric studies to examine the impact of varying equivalence ratio, oxygen-enrichment of gasification air, and gasifier pressure. By varying the equivalence ratio, the authors found a value of ER (0.37) that yielded the maximum fraction of H_2 in the syngas. The authors then evaluated the effects of varying oxygen content of the gasifying agent while maintaining this optimum equivalence ratio, and found that the model predicted increasing H_2 and CO in the syngas with increasing oxygen content of

the oxidant. Increasing gasifier pressure up to 80 atm at the same equivalence ratio resulted in decreased fractions of H_2 and CO in the syngas, and greatly increased fractions of CO_2, CH_4, and H_2O in the syngas.

Schuster *et al.* (2001) report their results of creating an equilibrium-based model of a dual fluidized-bed steam gasifier in IPSEpro™. The model assumed that 15% of the carbon in the feedstock remained in the syngas product as char. H_2, CO, CO_2, CH_4, and H_2O were considered in equilibrium calculations, with all the sulfur and the nitrogen in the feedstock assumed to be converted to H_2S and NH_3, respectively. Tar formation was not considered. Increasing gasifier temperature resulted in finding a temperature that resulted in the maximum fraction of H_2 in the syngas. CO and H_2O generally increased with increasing temperature over the entire range of evaluated temperatures while CO_2 and CH_4 decreased with increasing temperatures. Increasing moisture content in the feedstock increased the fractions of H_2 and CO_2 in the syngas and decreased the fractions of CO and CH_4.

Doherty *et al.* (2009) developed an equilibrium model of a CFB gasifier using Aspen Plus®. The model breaks the gasification process into multiple blocks, and assumes that 2% of the carbon in the feedstock is lost with the ash and that 3% of the heat input is lost from the gasifier. Additionally, all sulfur was assumed to form H_2S, and NOX was not considered. The model was evaluated using available experimental data, and the model results generally compared favorably with the experimental results, with the exception that the model's calculated value for the fraction of methane in the syngas was more than double that of the empirical data. The model used a gasifier pressure of 1.05 bar. The effects of equivalence ratio, air temperature, and feedstock moisture

content were all evaluated. Increasing equivalence ratio was found to increase the fractions of H_2 and CO up their maximum values, at a common ER, and increasing the ER beyond this value, decreased the fraction of both. Increasing air temperature at an ER=0.29 increased the fractions of H_2 and CO in the syngas over the entire input range.

Ramanan *et al.* (2008) developed two equilibrium gasification models, one based on chemical equilibrium and the other based on Gibbs free energy minimization. Both models were evaluated against data from the gasification of cashew nut shell char in a downdraft gasifier. The Gibbs free energy minimization model was generally more accurate in predicting syngas composition, with the chemical equilibrium model showing much larger error in predicting CO and CO_2 fractions in particular. Both models yielded estimates of CH_4 in the syngas that were much lower than was observed in the experimental results. Qualitatively, both models showed the same results when evaluating the effect of equivalence ratio and feedstock moisture on the syngas composition, although the actual values differed. Increasing ER from 0.1 to 1.0 caused a steady decrease in the fractions of both H_2 and CO in the syngas, while the fraction of CO_2 in the syngas increased with increasing ER. Higher feedstock moisture resulted in increasing H_2 and CO_2 and decreasing CO in the product gas.

Radmanesh *et al.* (2006) created two kinetic models based on two separate sets of background data for the gasification of beech wood in a bubbling fluidized-bed. The researchers modeled the gasifier as two parts, the fluidized-bed region where both heterogeneous and homogeneous reactions occur, and the freeboard region of the gasifier, where only homogenous reactions occur. The models use both fluid dynamics and reaction kinetics. The results of both models were examined against experimental data

for the system with regard to gas composition as a function of height in the reactor, with one model clearly proving to be more accurate. Additionally, a comparison of the results of one of the models against empirical data is presented for various parametric studies, including the effect of equivalence ratio. As the ER was increased from 0.1 to 0.5 the models predicted decreasing fractions of H_2, CO, and CH_4 in the syngas while the fraction of CO_2 in the syngas increased over the same range.

Shen, Gao, and Xiao (2008) present an equilibrium-based model of a twin-bed gasifier created using Aspen Plus®. The authors use Gibbs free energy minimization blocks to simulate both the combustion bed and the gasification bed. Tars were not considered and the gasifier pressure was set to 0.1 MPa. Sand was used as the circulating energy carrier between the beds, although the authors note that other solids such as limestone could be used and would have an added catalytic effect. Increasing gasifier temperature from 650 to 800°C was shown to increase H_2 and CO fractions in the syngas while decreasing the fractions of CO_2 and CH_4. Further temperature increase from 800 to 900°C continued to increase the fraction of CO and decrease the fractions of CO_2 and CH_4, although the fraction of hydrogen remained relatively constant.

Puig-Arnavat *et al.* (2012) developed a modified-equilibrium-based model of a fluidized-bed gasifier using Engineering Equation Solver. Initially, a true equilibrium model was created assuming chemical equilibrium of the Boudouard, water-gas, water-gas shift, and methanation reactions in the gas phase. This model was modified by adding a pyrolysis unit between the drying and gasification units within the model. The products of the pyrolysis unit were calculated using correlations from previous work. Additionally, a set fraction of the char and tar produced in the pyrolysis block were

assumed to be present in the syngas product of the gasifier. An additional modification from true equilibrium basing the CH_4 in the syngas on user input; thus the equilibrium constant of the methanation reaction was ignored. The model was evaluated by comparing its predictions to experimental results from various literature sources; the accuracy of the model varied depending on the case. Also, the model was used to perform parametric studies on various system conditions, including equivalence ratio, air temperature, and oxygen content of air. With a feedstock of woodchips with 10% moisture, increasing ER from 0.3 to 0.6 decreased H_2 and CO fractions in the syngas, while increasing CO_2 fractions in the syngas. Using the same feedstock, increasing air temperature from 25 to 825°C increased H_2 and CO in the product gas while decreasing CO_2 and CH_4. For hemlock woodchips with 11.7% moisture, with ER varied from 0.1 to 0.6, both the fractions of both H_2 and CO were highest at an ER of roughly 0.3. The CH_4 fraction decreased over the entire range, while the fraction of CO_2 decreased with increasing ER from 0.1 to 0.4 and increased as ER was increased further from 0.4 to 0.6. In another study with the same feedstock, enriching the oxygen content of the gasification air from 25% to 50% (volume) significantly increased fractions of H_2 and CO over the entire range. The fraction of CO_2 increased only slightly over the range, and the fraction of CH_4 decreased significantly.

Lee, Choi, and Paek (2010) discuss the use of commercially available process simulation, software for gasification modeling. The authors mention various process simulation packages but particular focus is given to examining the adequacy of equilibrium-based models of coal gasification in Aspen Plus®. The authors note the usefulness of such models in predicting the thermodynamic limits of a given process but

also examine the potential limitations of such models. They note that some gasifier configurations will not reach equilibrium and present estimates of the relative reaction rates of the heterogeneous reactions of carbon (char) within the gasifier system. The reaction rates of carbon with H_2O and carbon with CO_2 were estimated to be 1000 fold greater than that of carbon with H_2. Additionally, the authors note the inability of equilibrium models to predict the differences in the temperature and composition at various points within the geometry of the gasifier. The authors conclude that for more accurate results, kinetic models should be used but also suggest the potential of a two-stage equilibrium model, where the heterogeneous reactions are all solved in the first equilibrium stage and the homogenous reactions are solved in the second equilibrium stage.

Li *et al.* (2001) present a thermodynamic equilibrium model that is evaluated against experimental data and used for various parametric studies. The model uses a Gibbs energy minimization approach to model the gasification of Highvale and Pittsburgh Seam coals in a circulating fluidized-bed. C, H, O, N, and S were the elements that were considered in the model. From these elements, 42 gaseous components and 2 solid components were included. Ash was considered to be chemically inert. The equilibrium model was modified by including a parameter to account for the fractional approach to equilibrium of the carbon in the system. For the model the authors present, the value of the parameter was regressed from experimental data, but the authors note that to develop a fully predictive model, an algorithm would need to be developed to accurately predict the value of the parameter for a given system.

The authors conclude that the developed model showed good agreement with experimental results with the exception of CH_4.

Nikoo and Mahinpey (2008) used Aspen Plus® to create a model of an atmospheric, fluidized-bed biomass gasifier. A yield reactor was used to simulate the decomposition of the biomass into its constituent components. The stream leaving the yield reactor is separated into volatile components and solids using a separation unit. The volatiles enter a Gibbs reactor while the solids bypass the Gibbs unit. The product of the Gibbs reactor and the solids from the separation unit are combined and fed to two CSTR units in series. One unit represents the fluidized-bed region and the other represents the freeboard region of the gasifier. FORTRAN code was used to incorporate fluid dynamics into the CSTRs. The model accurately predicted the qualitative effect of increasing temperature from 700-900°C on the fractions of H_2, CO, and CH_4. Experimental data showed a decrease in the fraction of CO_2 in the product gas over the temperature range, but the model predicted an increase. The effects of varying equivalence ratio from 0.19-0.27 were also presented, although the model was not as accurate in predicting the general trends of the fractions of the components in the syngas in response to varying ER as it was in predicting the response to varying gasifier temperature. The authors suggest various measures to increase the accuracy of their model, including accounting for tar formation and wall effects.

Hannula and Kurkela (2010) developed a modified-equilibrium model of an air-blown, fluidized-bed biomass gasifier using Aspen Plus®. Experimental data from the gasification of sawdust was incorporated into the model to more accurately predict the incomplete conversion of carbon and the formation of hydrocarbons and ammonia using

FORTRAN subroutines. The authors report an average relative error from the model of 14% for the concentrations of H_2, CO, CO_2, and CH_4 compared to the experimental data. Further data was presented in evaluating the model's ability to predict the overall carbon conversion of other biomass feedstocks, with the researchers concluding that the model could accurately predict the carbon conversion of 3 of the 5 additional feedstocks. The authors conclude that while parameters for modifying an equilibrium model can be extrapolated to similar feedstocks (e.g. feedstocks with similar moisture content or reactivity), attempting to use the same parameters for dissimilar feedstocks does introduce error.

Gungor *et al.* (2012) created a chemical equilibrium model of coal gasification using FORTRAN. Air gasification and air-steam gasification were evaluated parametrically. Gasifier temperature, gasifier pressure, air-to-fuel ratio, steam-to-fuel ratio, and coal properties were the inputs to the model. Four Turkish coals were used as the feedstocks. At 1400°K and roughly atmospheric pressure, varying the air-to-fuel ratio from 0.2 to 1.2 on a mass basis increased both the H_2 and the CO in the syngas, but the overall molar ratio of H_2/CO in the syngas did not vary significantly. Holding the AFR at 1.2 at the same temperature and pressure and increasing steam-to-fuel ratio on a mass basis from 0 to 0.4 greatly increased the H_2 in the syngas while also increasing the CO. Because the response of the H_2 was more significant, increasing steam also increased the H_2/CO ratio. At Increasing gasifier pressure up to 4053 kPa decreased both H_2 and CO in the syngas. Lastly, the authors varied the gasifier temperature at atmospheric pressure while holding the AFR at 1.2 and the SFR at 0.4. Increasing temperature had little impact on the syngas.

Azzone *et al.* (2012) report their findings of developing a chemical equilibrium gasification model to perform parametric evaluations and compare them with empirical data from literature. The authors modeled a downdraft, fixed-bed gasifier. They assumed that no tar will be present in the syngas, which is comprised of H_2, CO, CO_2, CH_4, H_2O, and N_2. A factor to account for the lack of complete carbon conversion was included. Increasing process temperature decreased H_2 and CH_4 in the syngas, while increasing CO up to an optimum temperature and then decreasing as temperature was increased beyond that point. Increasing gasifier pressure resulted in decreased H_2 and CO but increased CH_4. Varying the moisture content of the feedstock at constant temperature and pressure decreased H_2 and CO in the syngas. When the model was configured to the same settings as were used in an actual gasifier with results presented in the literature, the model was shown to generally predict more hydrogen in the syngas, but less carbon dioxide and methane that was observed in the empirical data. The model predicted the carbon monoxide and water content of the syngas fairly accurately.

6. Results & Analysis

6.1 Approach to Results & Analysis

A consistent approach is taken for reviewing each sensitivity analysis. The results are presented, analyzed, and then any points particularly pertinent to gasification modeling or commercialization are discussed.

6.2 Initial Sensitivity Studies

Initially, various sensitivity studies were performed for each of the four selected feedstocks based on the as-received analyses (See Section 3.2). After evaluating the results of these sensitivity studies, it was determined that the sensitivity studies should be performed using the same moisture content for each of the four feedstocks. Thus, all of the following studies were performed by adjusting the moisture content of each of the feedstocks to 5% weight-basis and normalizing the values of the other components.

6.3 Varying AFR

To evaluate the effects of air-to-fuel ratio (AFR) on the system, a sensitivity analysis was performed to vary the air flow rate to the gasifier.

6.3.1 Varying AFR – Dry-Feed – Results

6.3.1.1 Varying AFR – Dry-Feed – Effect on Syngas Components

The following figures show the effects of varying AFR on syngas component flows for each of the four feedstocks at 30 atm.

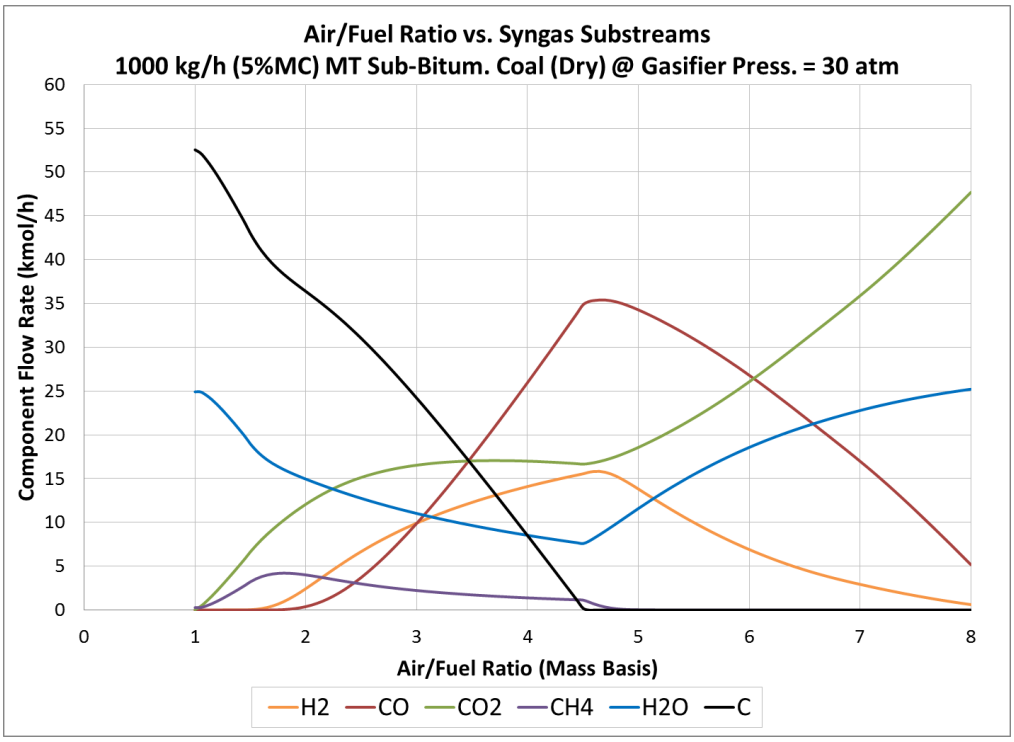

Figure 6.1 – MTC: AFR vs. syngas component flows (dry-feed)

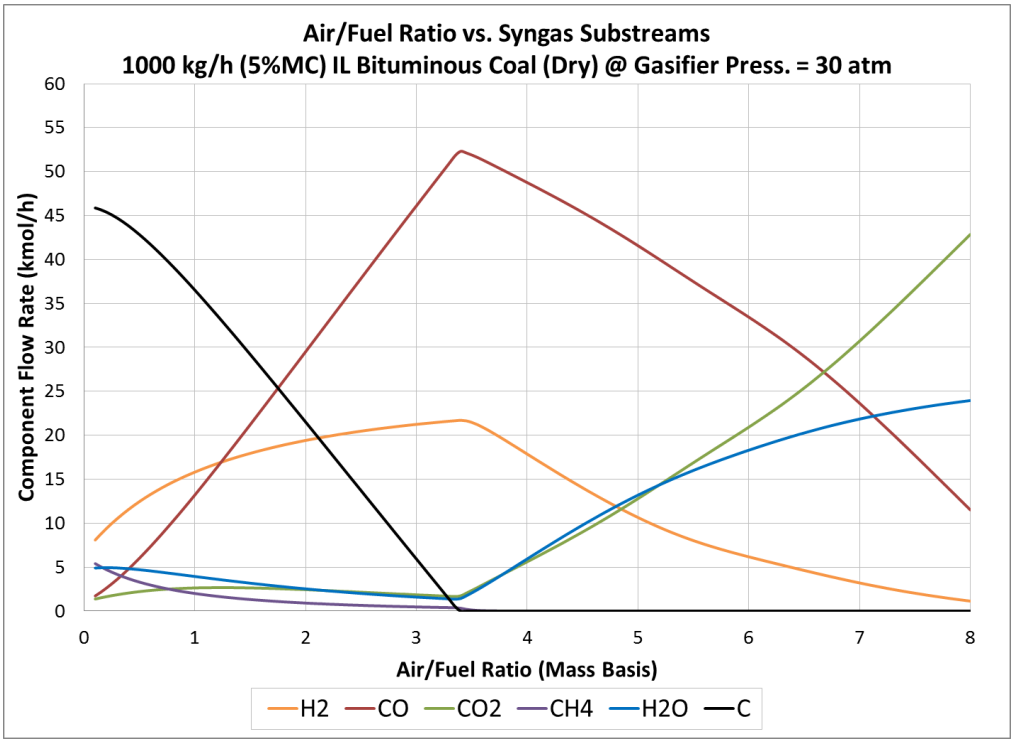

Figure 6.2 – ILC: AFR vs. syngas component flows (dry-feed)

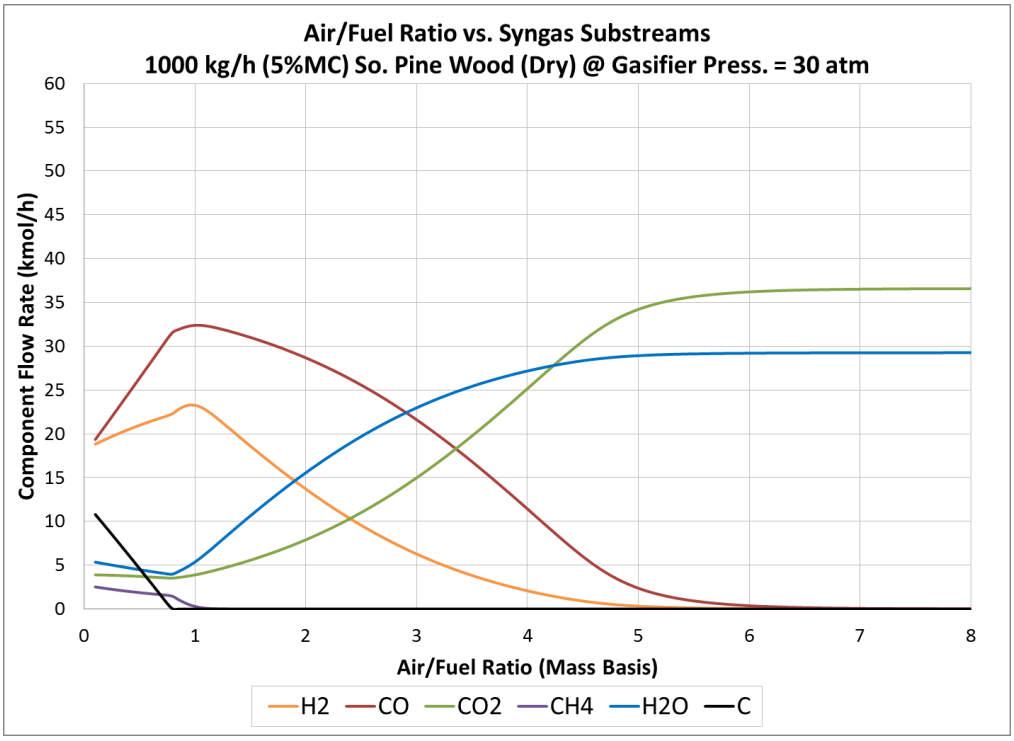

Figure 6.3 – SPW: AFR vs. syngas component flows (dry-feed)

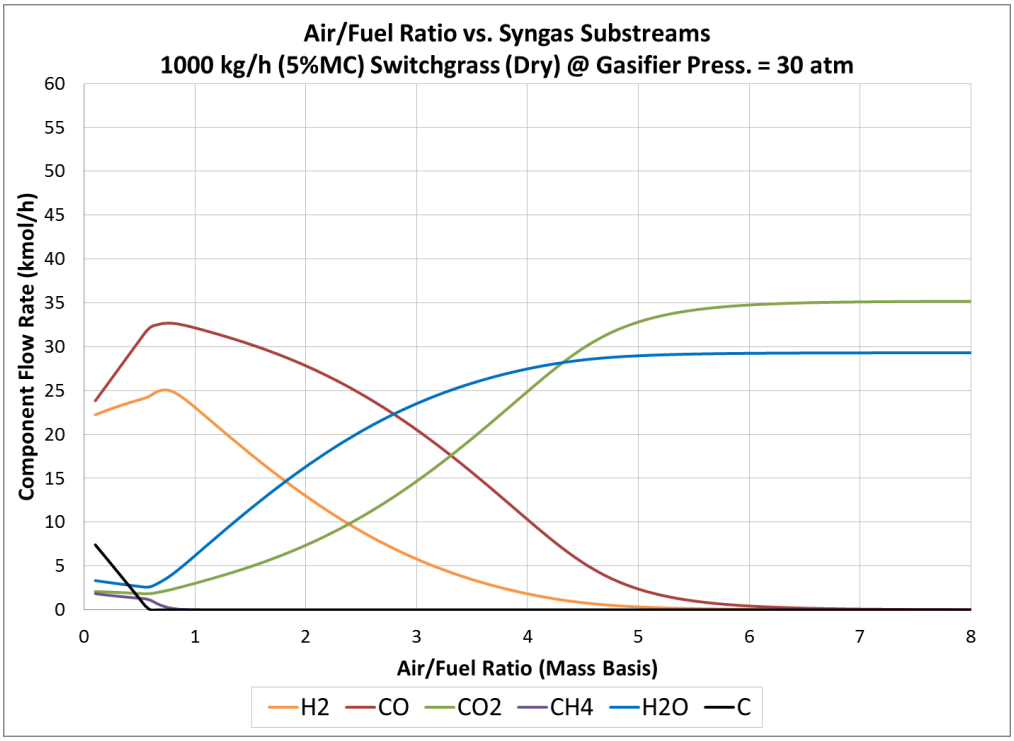

Figure 6.4 – SWG: AFR vs. syngas component flows (dry-feed)

For all of the feedstocks, unconverted carbon in the product decreases as the air-to-fuel ratio is increased. Additionally, in each case the maximum flow of both hydrogen and carbon monoxide is very near to the AFR at which 100% carbon conversion is achieved.[3] Methane is present in the product gas at AFR values less AFR_{CC}, but at an AFR only marginally greater than AFR_{CC}, methane is essentially eliminated as a product. Water formation decreases with increasing AFR, up to the point of complete carbon conversion, and then increases dramatically as AFR is increased beyond that point. In the Montana sub-bituminous coal, carbon dioxide formation increases with increasing air

[3] AFR_{CC} will be used to designate the air-to-fuel ratio that results in 100% conversion of the carbon in the feedstock.

flow up to an AFR of roughly 3.5, at which point it levels off until the AFR increases above AFR_{CC}. For the other three feedstocks, the flow rate of CO_2 in the product is relatively constant at values less than AFR_{CC}. For all of the feedstocks, increasing the AFR beyond AFR_{CC} causes the formation to CO_2 to increase rapidly with increasing AFR.

6.3.1.2 Varying AFR – Dry-Feed – Effect on Gasifier Temperature

The following figure shows the effects of varying AFR on gasifier temperature for each of the four feedstocks at 30 atm.

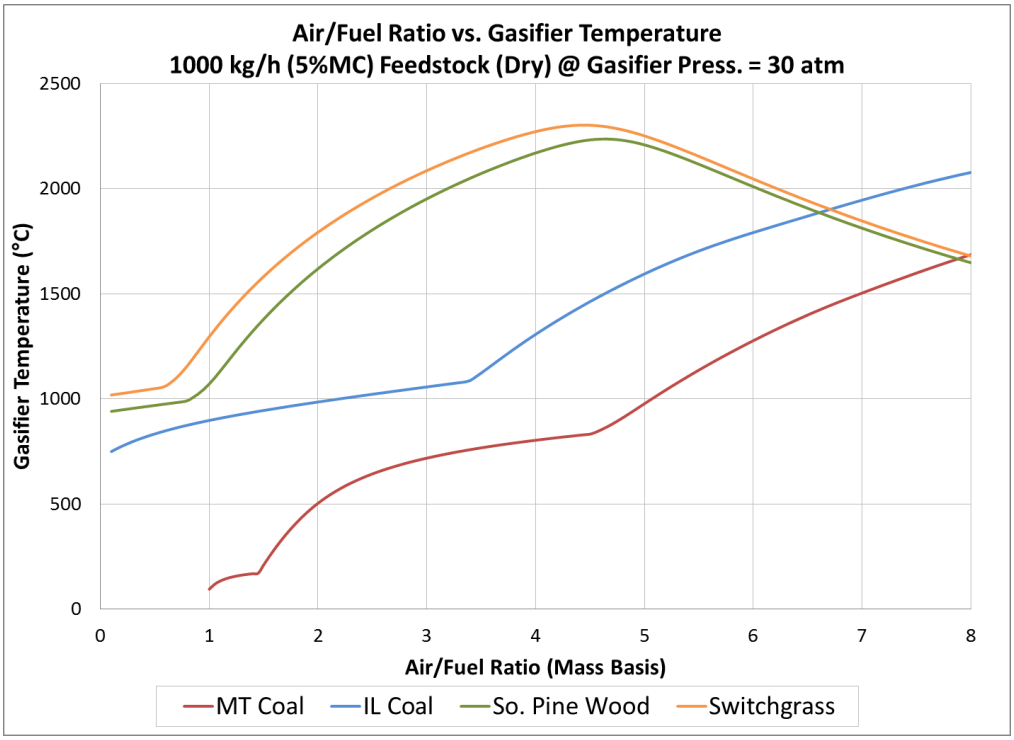

Figure 6.5 – AFR vs. gasifier temperature (dry-feed)

For each of the feedstocks, increasing AFR increases the temperature up to AFR_{CC}. Increasing the AFR above AFR_{CC} continues to increase the temperature of the gasifier, but the effect is greater than what is seen at air-to-fuel ratios less than AFR_{CC}. For the two biomass feedstocks, the data also shows the points at which the temperature begins to decrease with increasing air flow. If the range of AFR data were extended, this point would be shown for the coal feedstocks as well.

6.3.2 Varying AFR – Slurry-Feed – Results

6.3.2.1 Varying AFR – Slurry-Feed – Effect on Syngas Components

The following figures show the effects of varying AFR on syngas component flows for each of the four feedstocks at 30 atm.

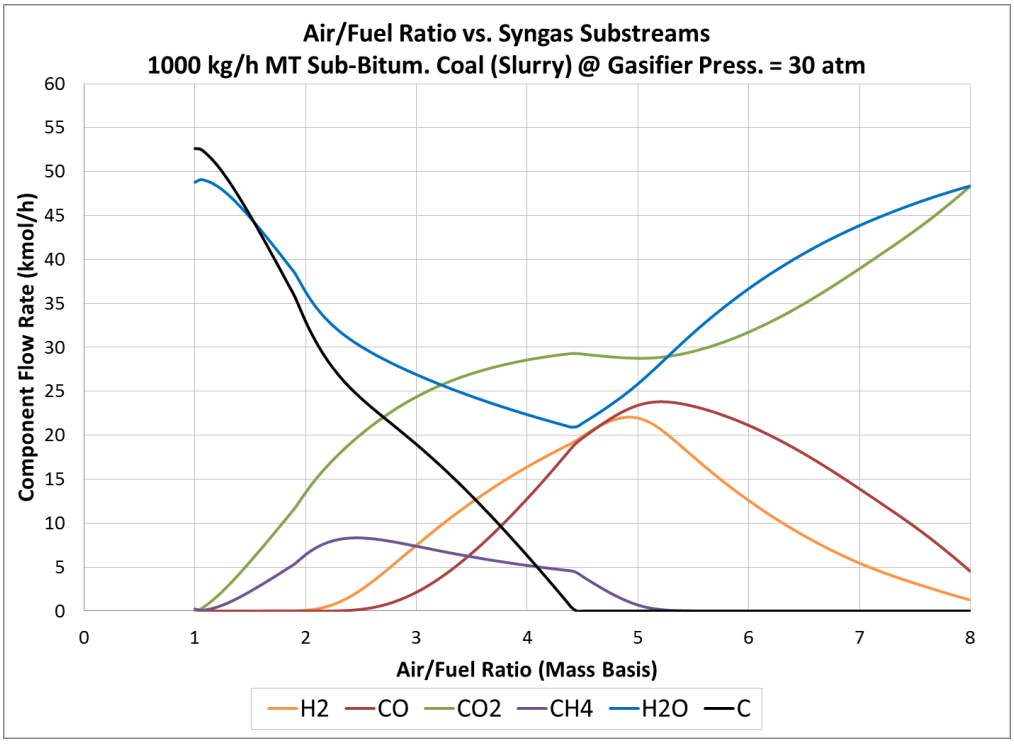

Figure 6.6 – MTC: AFR vs. syngas component flows (slurry-feed)

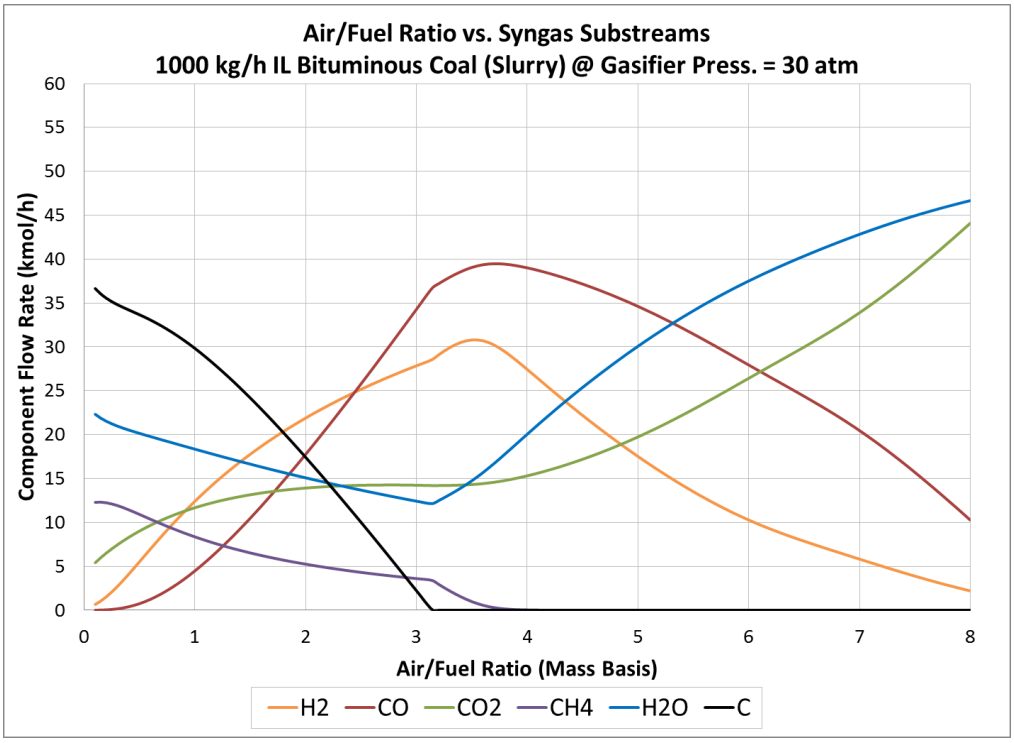

Figure 6.7 – ILC: AFR vs. syngas component flows (slurry-feed)

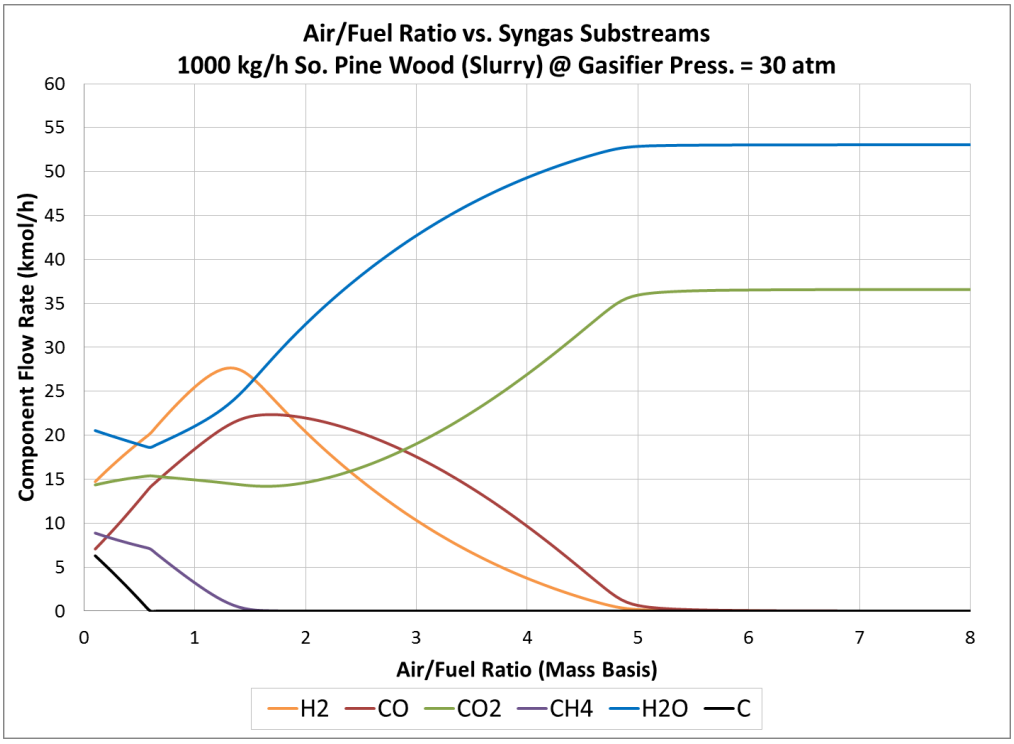

Figure 6.8 – SPW: AFR vs. syngas component flows (slurry-feed)

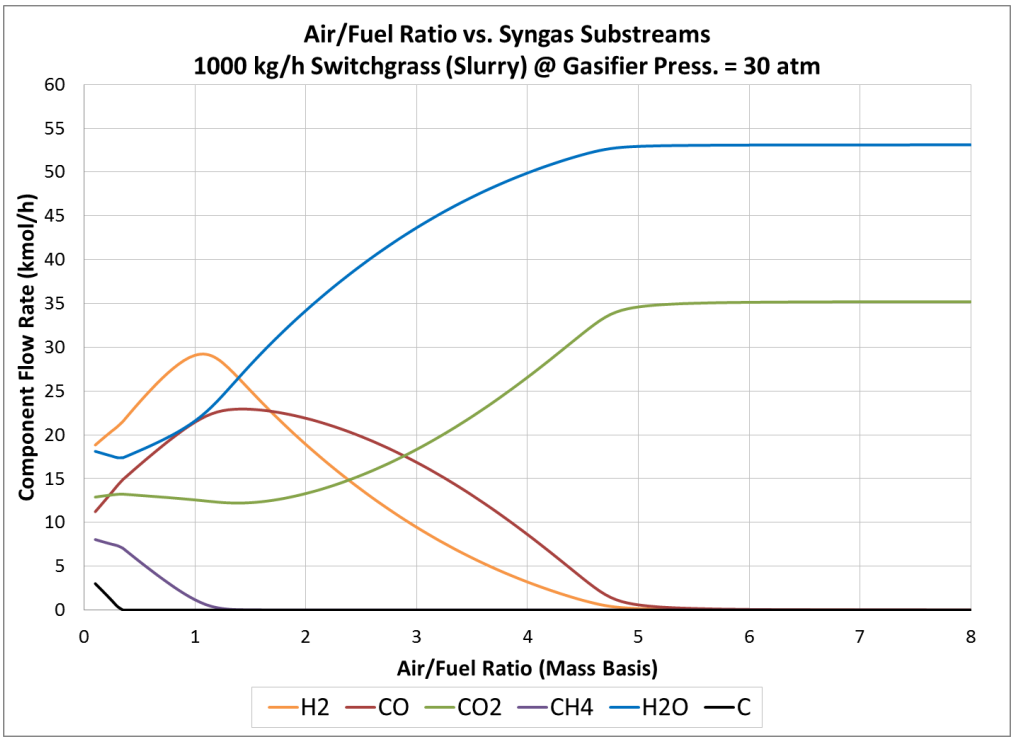

Figure 6.9 – SWG: AFR vs. syngas component flows (slurry-feed)

Relative to the dry-feed configuration, for all four feedstocks, the H_2 and H_2O flows are greater and the CO flow is lower. The flow rate of CO_2 is greater across the most of the range, but the maximum flow stays roughly the same. The AFR that eliminates CH_4 from the syngas is higher, and in the range of AFRs where CH_4 does exist, the flow rate is significantly higher than is seen in the dry-feed configuration.

6.3.2.2 Varying AFR – Slurry-Feed – Effect on Gasifier Temperature

The following figure shows the effects of varying AFR on gasifier temperature for each of the four feedstocks at 30 atm.

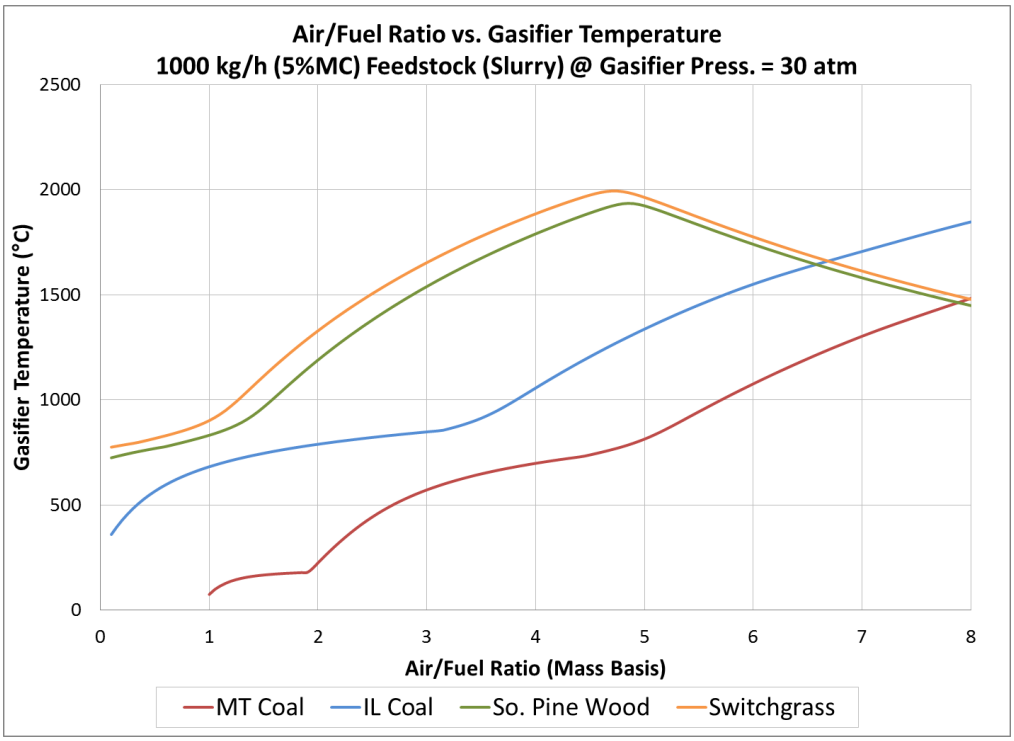

Figure 6.10 – AFR vs. gasifier temperature (slurry-feed)

Compared to the results from the dry-feed simulations, the gasifier temperatures are lower for all four feedstocks.

6.3.3 Varying AFR – Analysis

Generally, the results fit well with gasification/combustion theory. At lower AFRs, the gasification reactions dominate; H_2 and CO comprise a large fraction of the syngas, and CH_4 is also a product. As the AFR is increased beyond this region, complete combustion reactions begin to dominate as opposed to gasification reactions, and the combustibles are oxidized to H_2O and CO_2. The shift in the system from being gasification reactions dominant, which are endothermic, to combustion reactions dominant, which are exothermic, causes the temperature to increase dramatically as the AFR is increased above AFR_{CC}. The data from the biomass feedstocks also shows the point at which the temperature of the gasifier begins to decrease with increased air flow. Increasing the AFR above the value required for complete combustion of all of the components causes this temperature decrease because the additional air dilutes the system. Thus, the same amount of heat is spread throughout an increasingly larger quantity of gas, resulting in lower temperatures. The biomass feedstocks yield higher H_2/CO ratios because the coal feedstocks have a higher content of carbon. Additionally, the biomass feedstocks require less air to fully oxidize the combustibles relative to the coal feedstocks. This is attributed to the higher combined hydrogen and carbon content of the coal feedstocks, which presents as a larger amount of fuel to be oxidized, and the much higher oxygen content of the biomass feedstocks, which means that much of the oxygen required for combustion is contained within the structure of the biomass.

The slurry-feed configuration has lower gasifier temperatures, as would be expected due to the energy required to vaporize the liquid water. The larger amount of water going into the system also shifts more CO into CO_2 and H_2. Methane content is greater presumably because the system temperature is lower. Even though there is more steam present to drive the methane reforming reaction, the heat available for this highly endothermic reaction is less than that of the dry-feed systems, resulting in greater methane in the syngas.

6.3.4 Varying AFR – Gasification Modeling Implications

Air-to-fuel ratio has a critical impact on the performance of gasification systems, and it must be taken into account in the study of any other parameter. The value of any study of a gasification system parameter, without considering the air-to-fuel ratio at which the parameter is evaluated, is limited. Further research into gasification modeling, or empirical gasification research for that matter, should take this point into particular consideration. When evaluating the impact of another system parameter (e.g. feedstock moisture content), care should be taken to evaluate the impact of the system parameter at a range of different air-to-fuel ratios because the effects of manipulating said parameter could be dramatically different with only a marginal change to the system AFR.

6.4 Varying AFR & Gasifier Pressure

To evaluate the effects of pressure, the air-to-fuel ratio and the pressure were varied for each of the four feedstocks in both dry-feed and slurry-feed configurations.

6.4.1 Varying AFR & Gasifier Pressure – Dry-Feed – Results

6.4.1.1 Varying AFR & Gasifier Pressure – Dry-Feed – Effect on Carbon in Syngas

Generally, increasing pressure increases the unconverted carbon in the syngas, with the one notable exception being Illinois bituminous coal at very low air-to-fuel ratios (<0.6), where increasing pressure decreases the carbon in the syngas. The following figures show the results for the coal feedstocks.

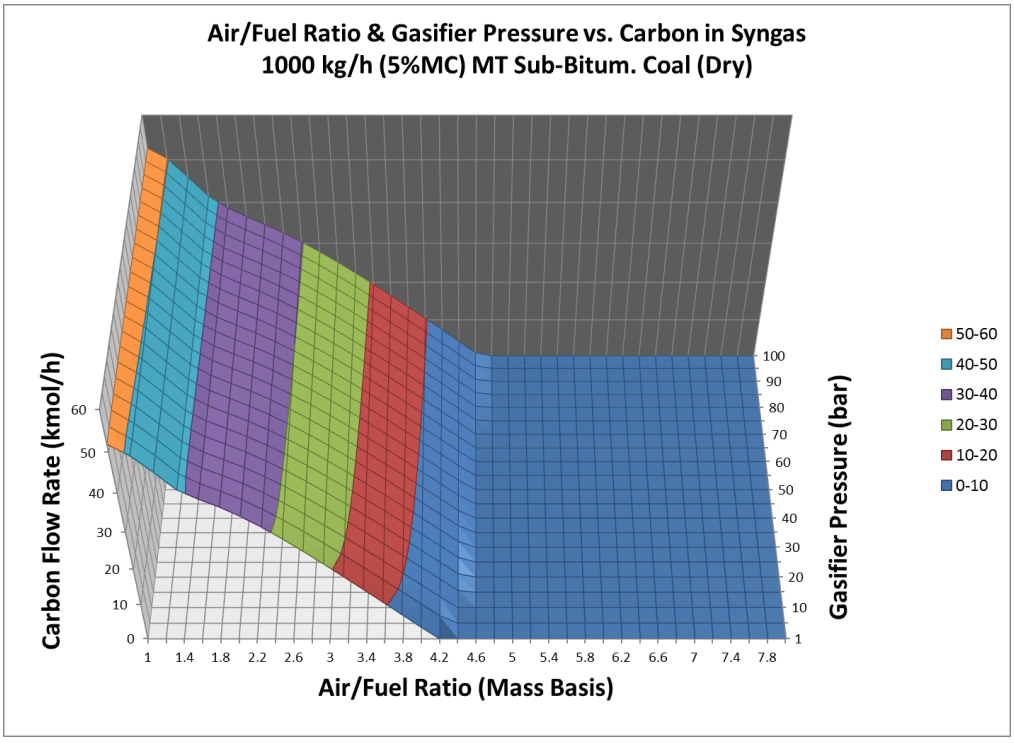

Figure 6.11 – MTC: AFR & gasifier pressure vs. carbon in syngas (dry-feed)

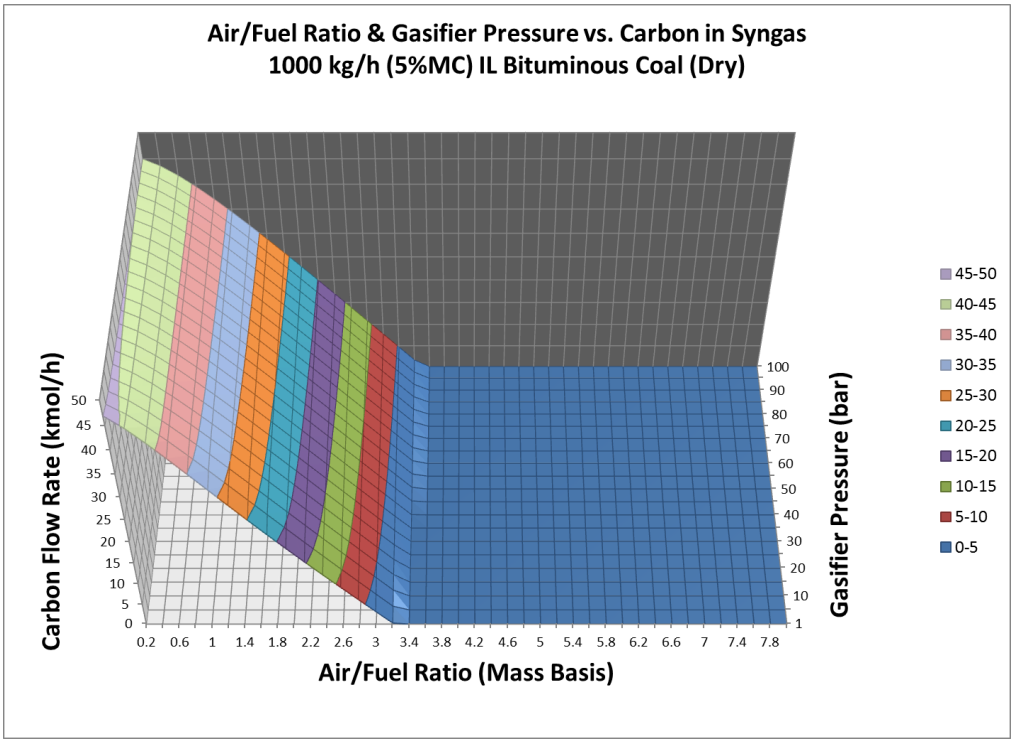

Figure 6.12 – ILC: AFR & gasifier pressure vs. carbon in syngas (dry-feed)

6.4.1.2 Varying AFR & Gasifier Pressure – Dry-Feed – Effect on H_2 in Syngas

The same trend was observed for all four feedstocks. The following figures show the results for Illinois bituminous coal and Southern pine wood as representative of the coal feedstocks and biomass feedstocks respectively.

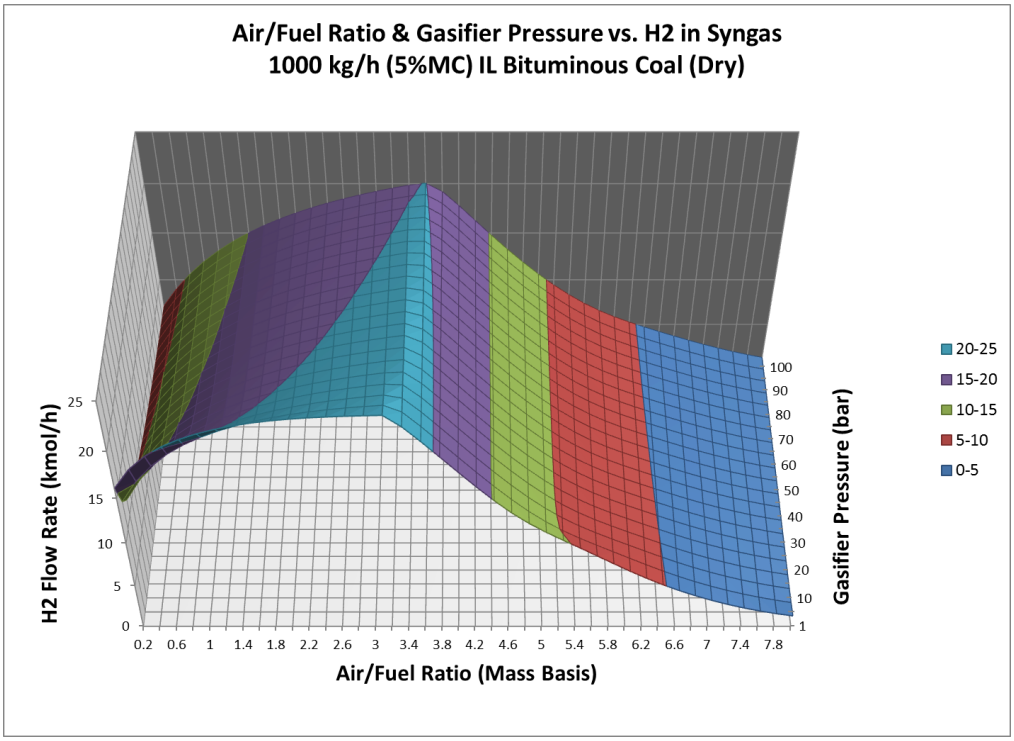

Figure 6.13 – ILC: AFR & gasifier pressure vs. H_2 in syngas (dry-feed)

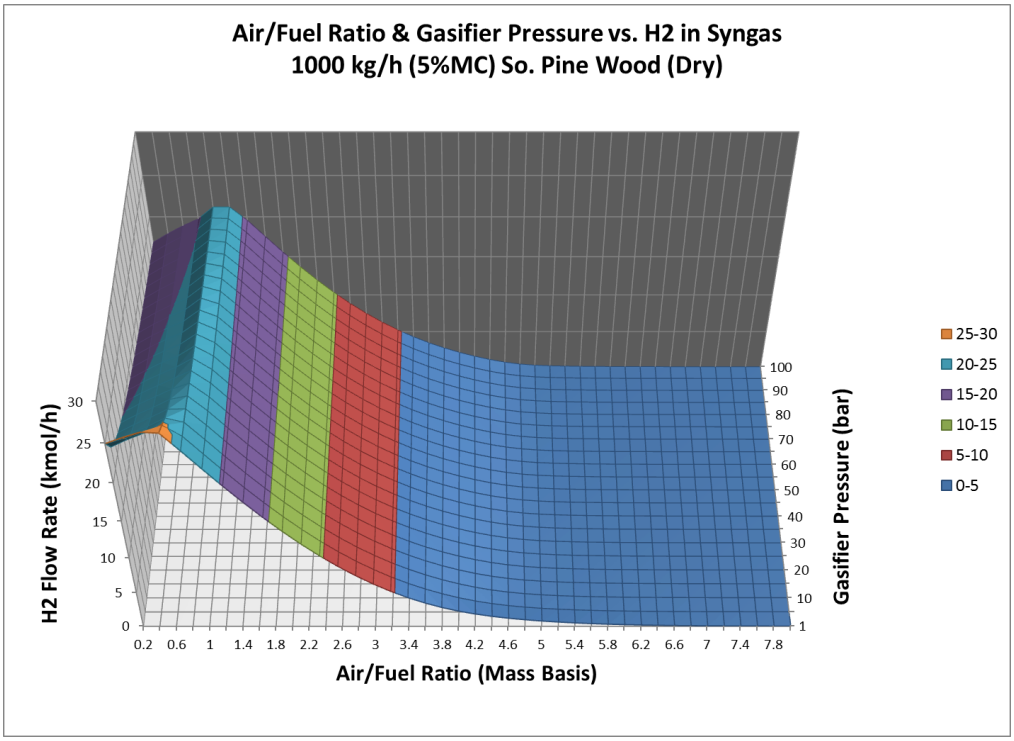

Figure 6.14 – SPW: AFR & gasifier pressure vs. H_2 in syngas (dry-feed)

Increasing gasifier pressure decreases hydrogen in the syngas. The effect at AFRs less than AFR_{CC} is much greater than at AFRs greater than AFR_{CC}.

6.4.1.3 Varying AFR & Gasifier Pressure – Dry-Feed – Effect on CO in Syngas

Increasing gasifier pressure decreases CO in the syngas for all of the feedstocks. The response to increasing pressure is greater at AFRs less than AFR_{CC} than at AFRs greater than AFR_{CC}. The results for Montana sub-bituminous coal are shown in the following figure.

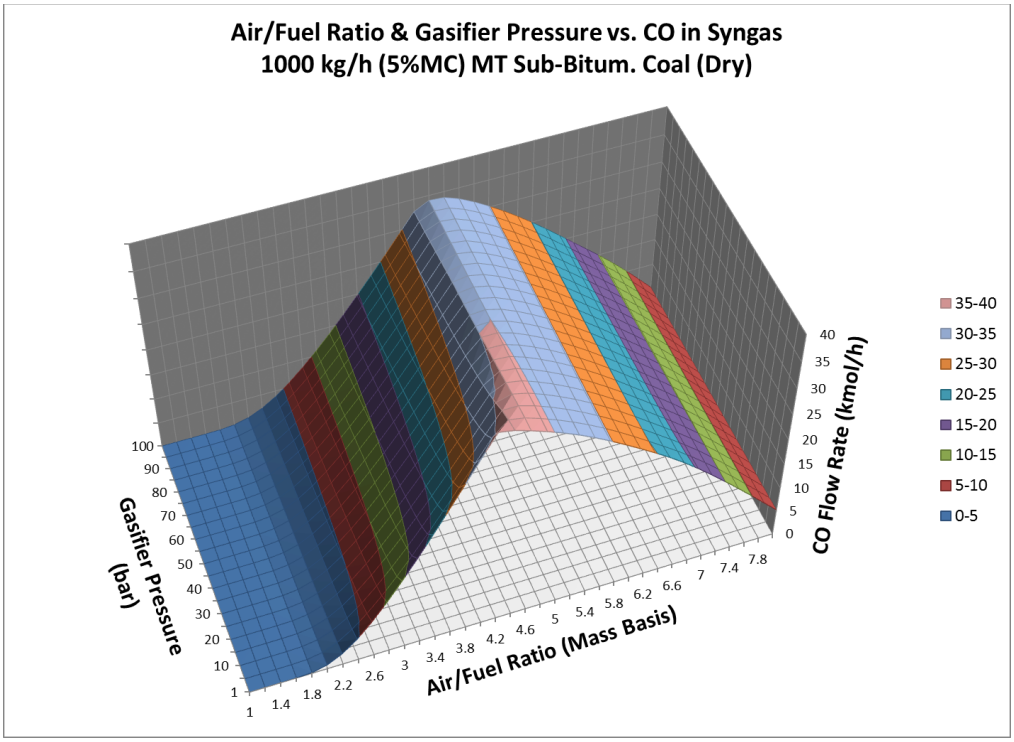

Figure 6.15 – MTC: AFR & gasifier pressure vs. CO in syngas (dry-feed)

6.4.1.4 Varying AFR & Gasifier Pressure – Dry-Feed – Effect on CO_2 in Syngas

For all of the feedstocks, at AFRs approaching AFR_{CC}, increasing pressure increases CO_2 formation. Additionally, in the biomass feedstocks, increased pressure causes CO_2 flow in the syngas to reach its maximum at a lower AFR. Except for these noted effects, the effect of pressure on CO_2 formation is negligible, as seen in the following figures.

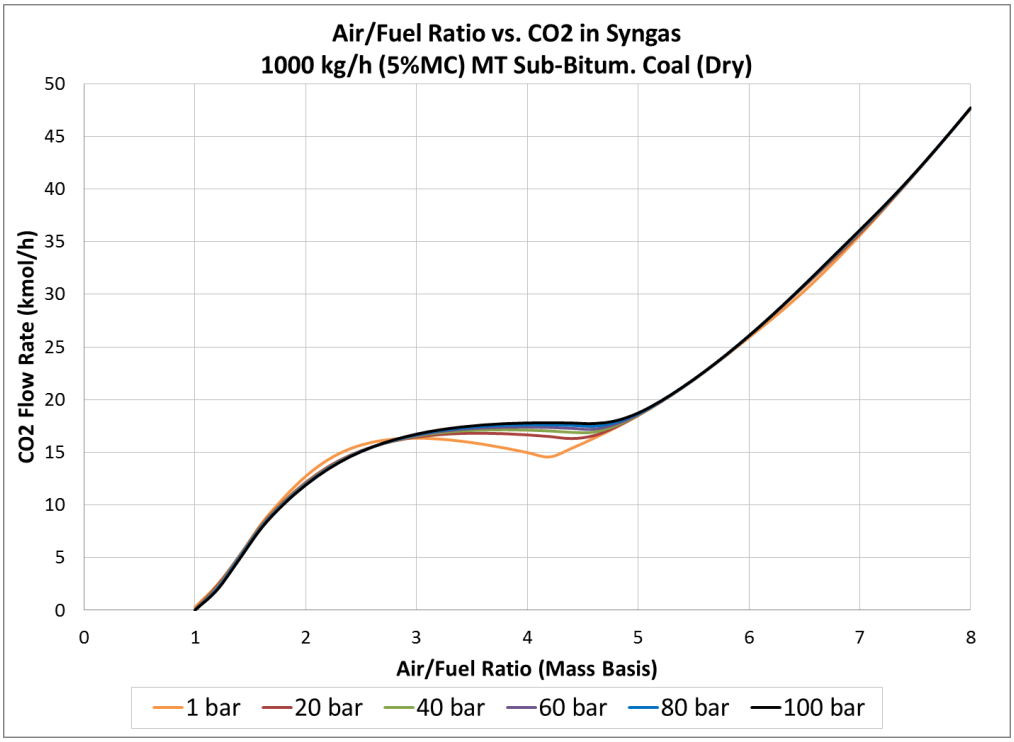

Figure 6.16 – MTC: AFR & gasifier pressure vs. CO_2 in syngas (dry-feed)

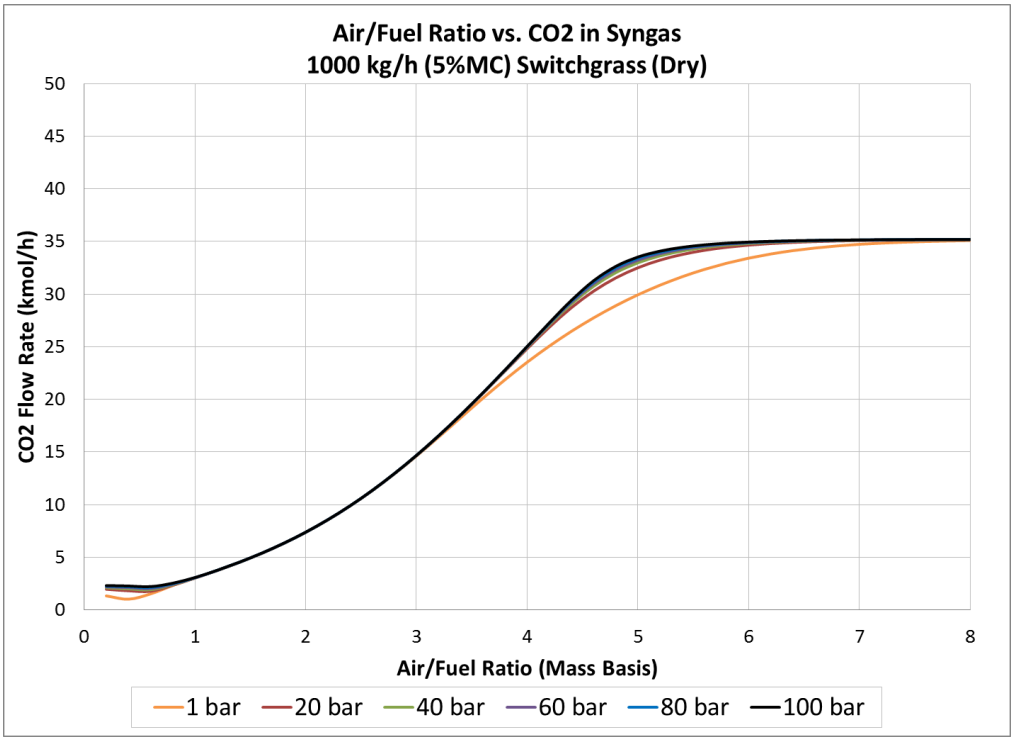

Figure 6.17 – SWG: AFR & gasifier pressure vs. CO_2 in syngas (dry-feed)

6.4.1.5 Varying AFR & Gasifier Pressure – Dry-Feed – Effect on CH_4 in Syngas

With the exception of Montana sub-bituminous coal at lower AFRs, increasing gasifier pressure results in increased methane in the syngas. For Montana sub-bituminous coal at very low AFRs (1.0-1.6) relative to AFR_{CC}, methane formation decreases with increasing pressure. Increasing the AFR beyond these values, up to roughly AFR_{CC}, while increasing the gasifier pressure, increases CH_4 as in the other three feedstocks. The results from Montana sub-bituminous coal and Southern pine wood are shown in the following figures.

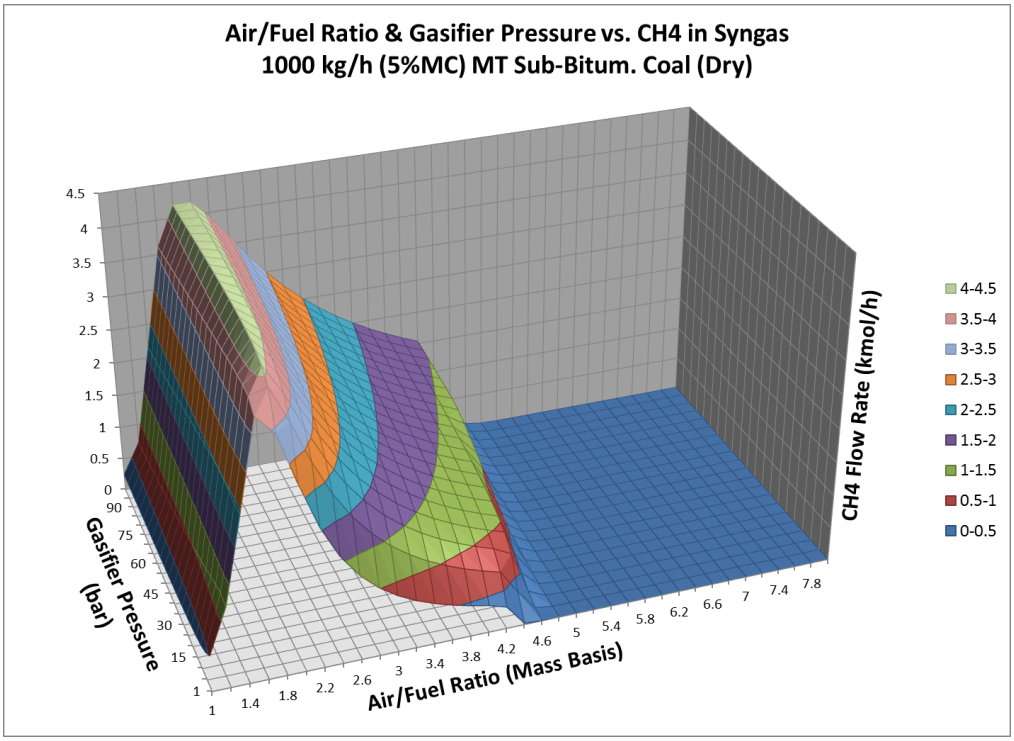

Figure 6.18 – MTC: AFR & gasifier pressure vs. CH_4 in syngas (dry-feed)

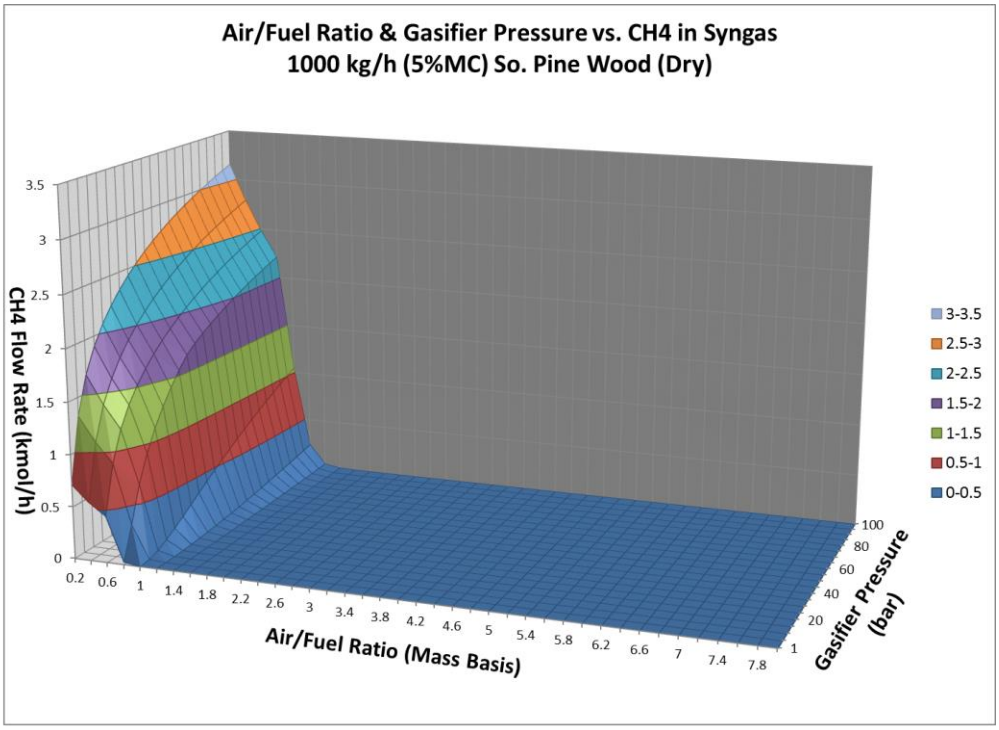

Figure 6.19 – SPW: AFR & gasifier pressure vs. CH_4 in syngas (dry-feed)

6.4.1.6 Varying AFR & Gasifier Pressure – Dry-Feed – Effect on H_2O in Syngas

The effects of increasing gasifier pressure on water formation are similar for each of the feedstocks. The results for Montana sub-bituminous coal are shown in the following figure.

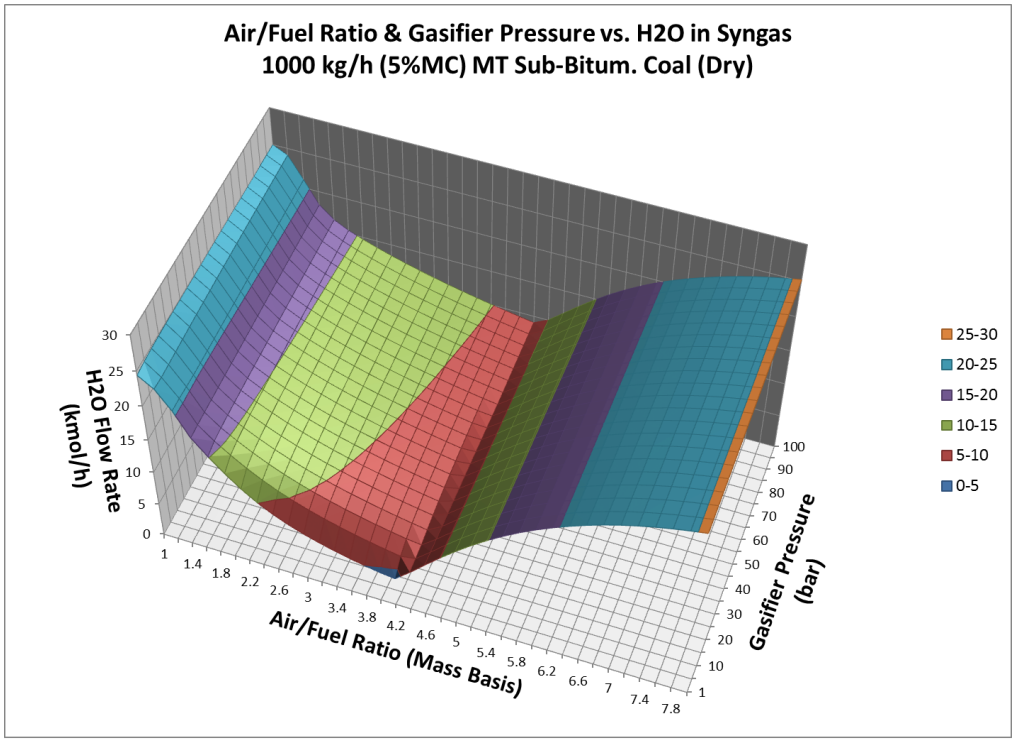

Figure 6.20 – MTC: AFR & gasifier pressure vs. H_2O in syngas (dry-feed)

For AFRs up to AFR_{CC}, the amount of water in the syngas increases as pressure increases. Beyond the 100% conversion AFR, increasing the pressure has little effect on the water content of the syngas.

6.4.1.7 Varying AFR & Gasifier Pressure – Dry-Feed – Effect on Gasifier Temperature

The same response is seen in each of the feedstocks. Up to AFR_{CC}, increasing gasifier pressure increases the gasifier temperature. At air-to-fuel ratios greater than AFR_{CC}, increasing the gasifier pressure has little effect on the gasifier temperature. The results for Montana sub-bituminous coal are shown in the following figure.

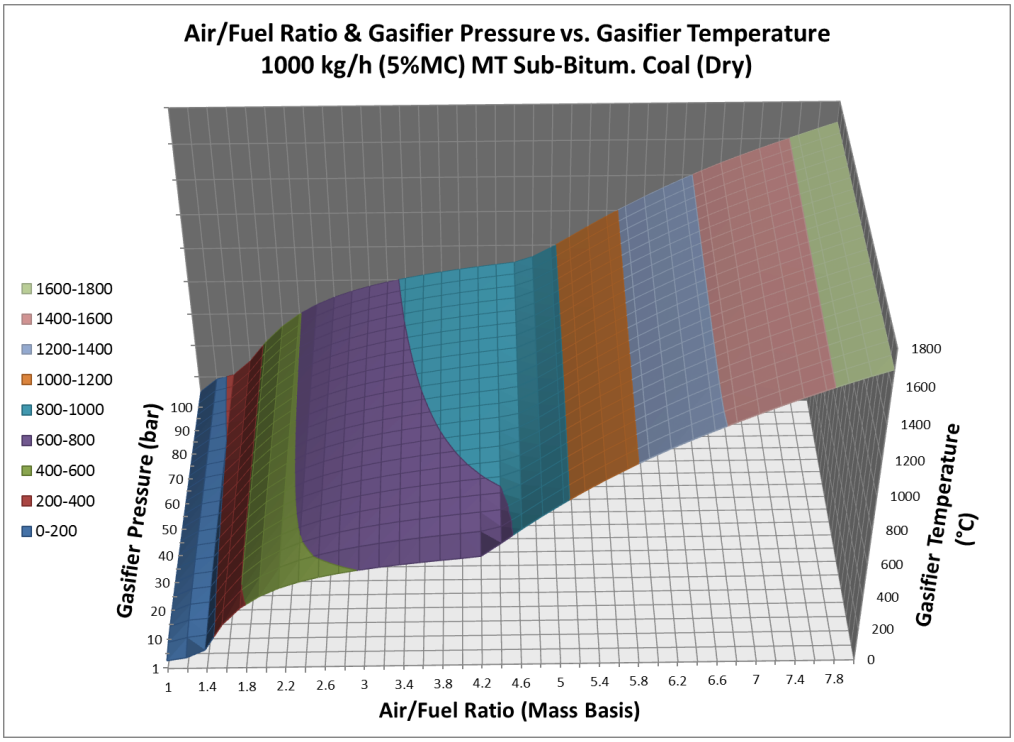

Figure 6.21 – MTC: AFR & gasifier pressure vs. gasifier temperature (dry-feed)

6.4.2 Varying AFR & Gasifier Pressure – Slurry-Feed – Results

6.4.2.1 Varying AFR & Gasifier Pressure – Slurry-Feed – Effect on Carbon in Syngas

In the Montana sub-bituminous coal, the effect of increasing pressure on carbon varies at lower AFRs, increasing with increasing pressure at some and decreasing with increasing pressure at others, but as the AFR neared AFR_{CC}, the effect is consistent, with carbon increasing with increasing gasifier pressure. For the Illinois coal, carbon in the syngas is negatively related to pressure at lower AFRs and positively related to pressure at higher AFRs less than AFR_{CC}. For both of the biomass feedstocks, increasing pressure causes less carbon in the syngas. The results for both of the coal feedstocks and Southern pine wood are shown in the following tables.

Air/Fuel Ratio & Gasifier Pressure vs. Carbon in Syngas												
1000 kg/h (5%MC) MT Sub.-Bitum. Coal (Slurry)												
AFR (Mass Basis)	Pressures (bar)											Δ (100 bar - 1 bar)
	1	10	20	30	40	50	60	70	80	90	100	
1.0	52.18	52.55	52.60	52.62	52.63	52.63	52.63	52.63	52.63	52.63	52.63	0.46
1.2	49.60	50.16	50.50	50.71	50.87	50.98	51.07	51.14	51.20	51.25	51.29	1.68
1.4	46.47	46.46	46.76	47.02	47.25	47.44	47.61	47.76	47.89	48.02	48.13	1.65
1.6	43.23	42.41	42.51	42.69	42.88	43.06	43.24	43.40	43.56	43.71	43.85	0.61
1.8	39.19	38.21	38.05	38.09	38.19	38.32	38.46	38.60	38.74	38.88	39.02	-0.17
2.0	32.51	32.54	32.68	32.83	32.98	33.12	33.27	33.41	33.55	33.69	33.83	1.31
2.2	28.55	28.23	28.29	28.39	28.50	28.61	28.73	28.85	28.97	29.09	29.21	0.66
2.4	26.03	25.39	25.34	25.37	25.43	25.50	25.58	25.66	25.75	25.83	25.92	-0.11
2.6	23.93	23.21	23.10	23.08	23.10	23.14	23.18	23.24	23.29	23.35	23.41	-0.52
2.8	21.75	21.16	21.05	21.02	21.03	21.05	21.08	21.12	21.16	21.21	21.26	-0.50
3.0	19.33	18.99	18.93	18.92	18.94	18.97	19.00	19.04	19.08	19.12	19.17	-0.16
3.2	16.64	16.64	16.65	16.69	16.73	16.77	16.82	16.87	16.92	16.97	17.01	0.38
3.4	13.72	14.09	14.20	14.28	14.36	14.43	14.49	14.56	14.62	14.68	14.74	1.02
3.6	10.61	11.37	11.58	11.72	11.83	11.94	12.03	12.11	12.19	12.27	12.34	1.72
3.8	7.37	8.50	8.82	9.02	9.18	9.31	9.43	9.54	9.63	9.73	9.81	2.45
4.0	4.01	5.52	5.94	6.21	6.41	6.57	6.72	6.85	6.97	7.08	7.18	3.17
4.2	0.57	2.43	2.97	3.29	3.54	3.74	3.91	4.07	4.21	4.34	4.45	3.88
4.4	0.00	0.00	0.00	0.30	0.59	0.83	1.03	1.21	1.37	1.51	1.65	1.65
4.6	0.00	0.00	0.00	0.00	0.00	0.00	0.00	0.00	0.00	0.00	0.00	0.00
4.8	0.00	0.00	0.00	0.00	0.00	0.00	0.00	0.00	0.00	0.00	0.00	0.00
5.0	0.00	0.00	0.00	0.00	0.00	0.00	0.00	0.00	0.00	0.00	0.00	0.00
Note: Carbon flows in (kmol/h)												

Table 6.1 – MTC: AFR & gasifier pressure vs. carbon in syngas (slurry-feed)

Air/Fuel Ratio & Gasifier Pressure vs. Carbon in Syngas												
1000 kg/h (5%MC) IL Bituminous Coal (Slurry)												
AFR (Mass Basis)	Pressures (bar)											Δ (100 bar - 1 bar)
	1	10	20	30	40	50	60	70	80	90	100	
0.2	36.81	35.72	35.58	35.56	35.58	35.62	35.68	35.74	35.81	35.89	35.96	-0.85
0.4	36.28	34.70	34.37	34.23	34.17	34.14	34.13	34.14	34.15	34.18	34.20	-2.08
0.6	35.36	33.65	33.25	33.06	32.96	32.89	32.85	32.83	32.82	32.82	32.82	-2.53
0.8	33.78	32.21	31.81	31.62	31.50	31.43	31.38	31.35	31.33	31.32	31.32	-2.46
1.0	31.63	30.34	30.00	29.83	29.73	29.66	29.62	29.60	29.58	29.58	29.57	-2.05
1.2	29.04	28.13	27.86	27.73	27.66	27.62	27.59	27.58	27.58	27.58	27.58	-1.45
1.4	26.14	25.64	25.48	25.40	25.36	25.34	25.34	25.34	25.35	25.37	25.38	-0.75
1.6	23.02	22.95	22.89	22.87	22.87	22.88	22.90	22.93	22.95	22.98	23.01	0.00
1.8	19.74	20.09	20.14	20.18	20.23	20.27	20.32	20.36	20.41	20.45	20.50	0.76
2.0	16.35	17.10	17.26	17.37	17.46	17.54	17.61	17.68	17.75	17.81	17.87	1.52
2.2	12.88	14.01	14.29	14.46	14.59	14.71	14.81	14.90	14.99	15.07	15.14	2.26
2.4	9.35	10.84	11.23	11.47	11.65	11.79	11.92	12.04	12.15	12.24	12.34	2.99
2.6	5.78	7.61	8.11	8.41	8.63	8.81	8.97	9.11	9.24	9.36	9.47	3.69
2.8	2.17	4.32	4.93	5.29	5.56	5.78	5.96	6.13	6.27	6.41	6.54	4.36
3.0	0.00	1.00	1.71	2.13	2.44	2.69	2.91	3.09	3.26	3.42	3.56	3.56
3.2	0.00	0.00	0.00	0.00	0.00	0.00	0.00	0.02	0.21	0.38	0.54	0.54
3.4	0.00	0.00	0.00	0.00	0.00	0.00	0.00	0.00	0.00	0.00	0.00	0.00
3.6	0.00	0.00	0.00	0.00	0.00	0.00	0.00	0.00	0.00	0.00	0.00	0.00
3.8	0.00	0.00	0.00	0.00	0.00	0.00	0.00	0.00	0.00	0.00	0.00	0.00
Note: Carbon flows in (kmol/h)												

Table 6.2 – ILC: AFR & gasifier pressure vs. carbon in syngas (slurry-feed)

Air/Fuel Ratio & Gasifier Pressure vs. Carbon in Syngas												
1000 kg/h (5%MC) So. Pine Wood (Slurry)												
AFR (Mass Basis)	Pressures (bar)											Δ (100 bar - 1 bar)
	1	10	20	30	40	50	60	70	80	90	100	
0.2	7.26	5.74	5.32	5.11	4.99	4.91	4.85	4.82	4.79	4.78	4.77	-2.48
0.4	4.32	3.12	2.76	2.59	2.48	2.42	2.37	2.35	2.33	2.32	2.32	-2.00
0.6	1.16	0.31	0.03	0.00	0.00	0.00	0.00	0.00	0.00	0.00	0.00	-1.16
0.8	0.00	0.00	0.00	0.00	0.00	0.00	0.00	0.00	0.00	0.00	0.00	0.00
1.0	0.00	0.00	0.00	0.00	0.00	0.00	0.00	0.00	0.00	0.00	0.00	0.00
1.2	0.00	0.00	0.00	0.00	0.00	0.00	0.00	0.00	0.00	0.00	0.00	0.00
Note: Carbon flows in (kmol/h)												

Table 6.3 – SPW: AFR & gasifier pressure vs. carbon in syngas (slurry-feed)

6.4.2.2 Varying AFR & Gasifier Pressure – Slurry-Feed – Effect on H_2 in Syngas

The same trend was observed for all four feedstocks. The following figures show the results for Illinois bituminous coal and Southern pine wood as representative of the coal feedstocks and biomass feedstocks, respectively.

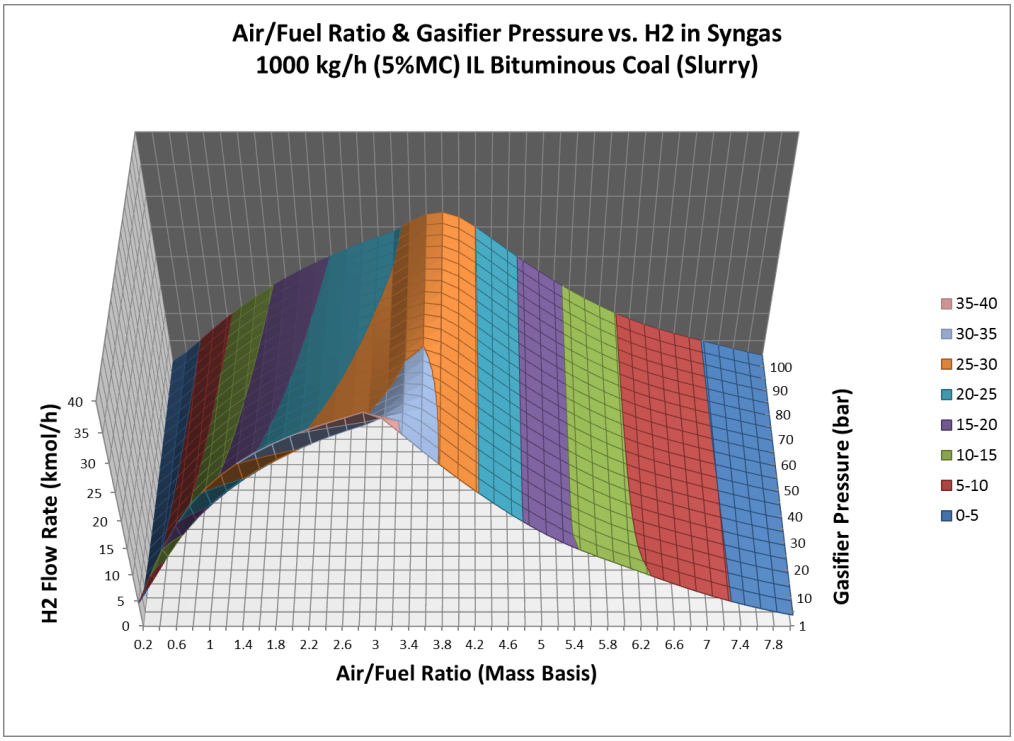

Figure 6.22 – ILC: AFR & gasifier pressure vs. H_2 in syngas (slurry-feed)

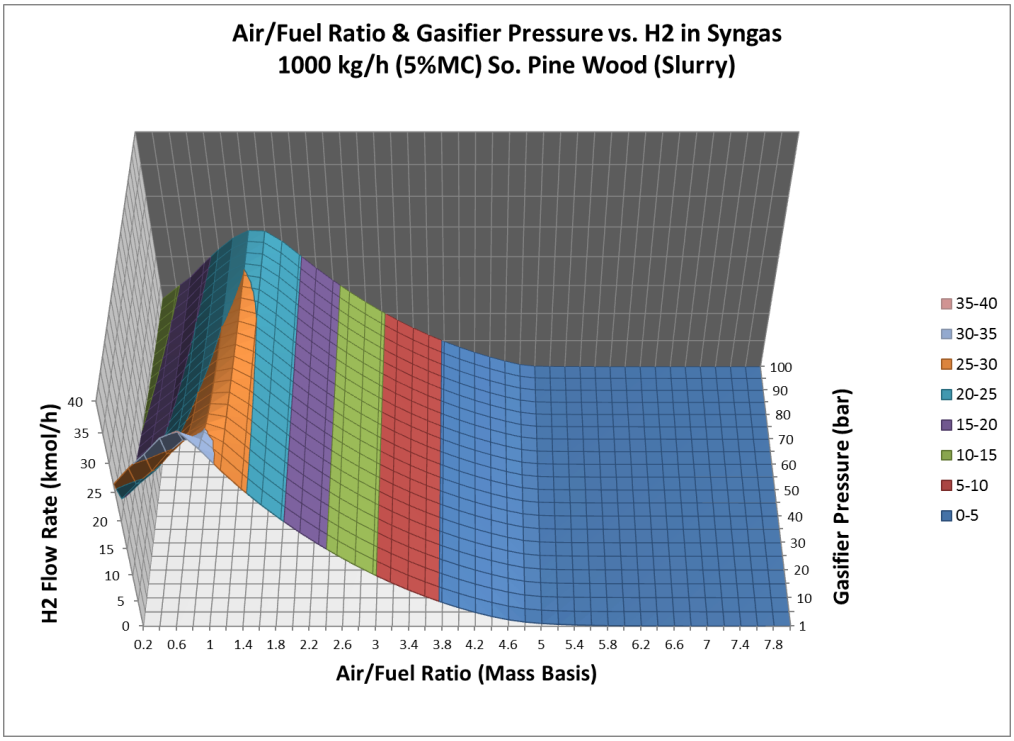

Figure 6.23 – SPW: AFR & gasifier pressure vs. H_2 in syngas (slurry-feed)

Increasing gasifier pressure decreases hydrogen in the syngas. The effect at AFRs less than AFR_{CC} is much greater than at AFRs greater than AFR_{CC}.

6.4.2.3 Varying AFR & Gasifier Pressure – Slurry-Feed – Effect on CO in Syngas

Increasing gasifier pressure decreases CO in the syngas for all of the feedstocks. The response to increasing pressure is greater at AFRs less than AFR_{CC} than at AFRs greater than AFR_{CC}. The results for Montana sub-bituminous coal are shown in the following figure.

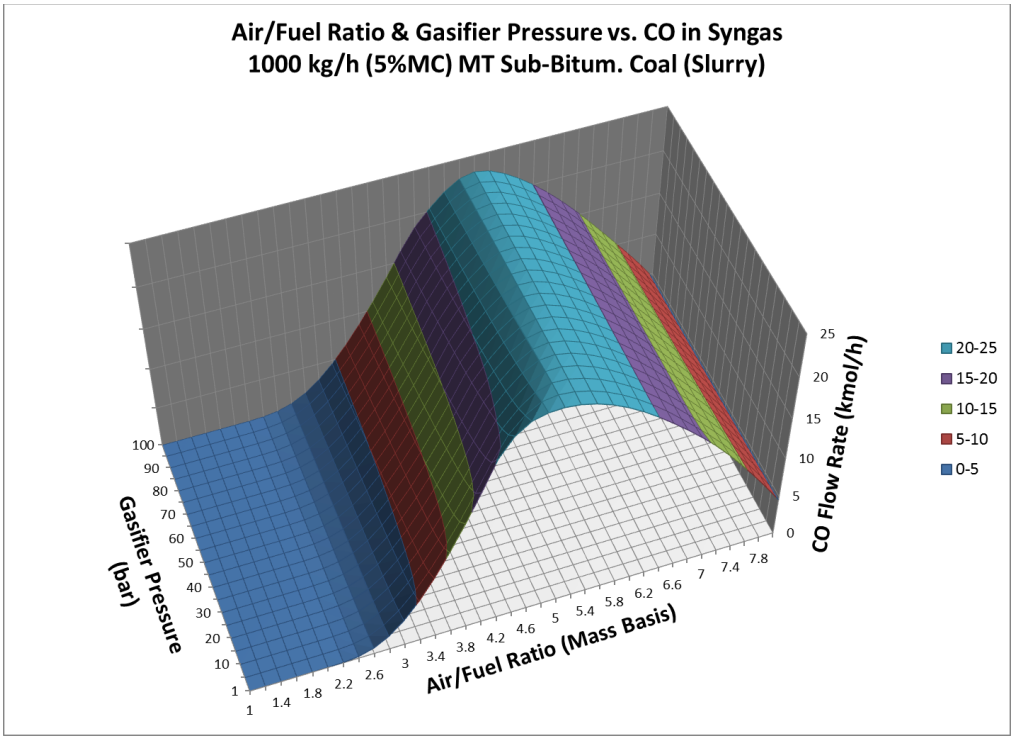

Figure 6.24 – MTC: AFR & gasifier pressure vs. CO in syngas (slurry-feed)

6.4.2.4 Varying AFR & Gasifier Pressure – Slurry-Feed – Effect on CO_2 in Syngas

For Montana coal and the biomass feedstocks, at AFRs approaching AFR_{CC}, increasing pressure decreases CO_2 formation. In the Illinois coal, increasing pressure causes a decrease in CO_2 formation at AFRs less than approximately 2.4, but at AFRs between 2.4 and AFR_{CC}, increasing pressure causes increased CO_2 formation. Additionally, in the biomass feedstocks, increased pressure causes CO_2 flow in the syngas to reach its maximum at a lower AFR. Except for these noted effects, the effect of pressure on CO_2 formation was negligible, as seen in the following figures.

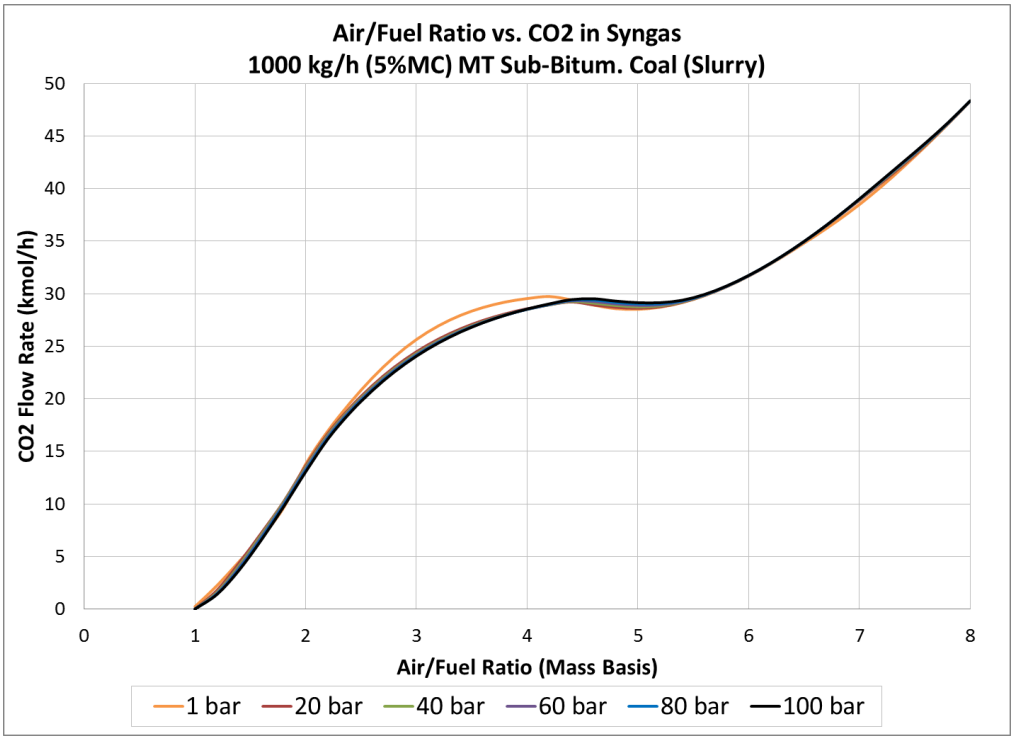

Figure 6.25 – MTC: AFR & gasifier pressure vs. CO_2 in syngas (slurry-feed)

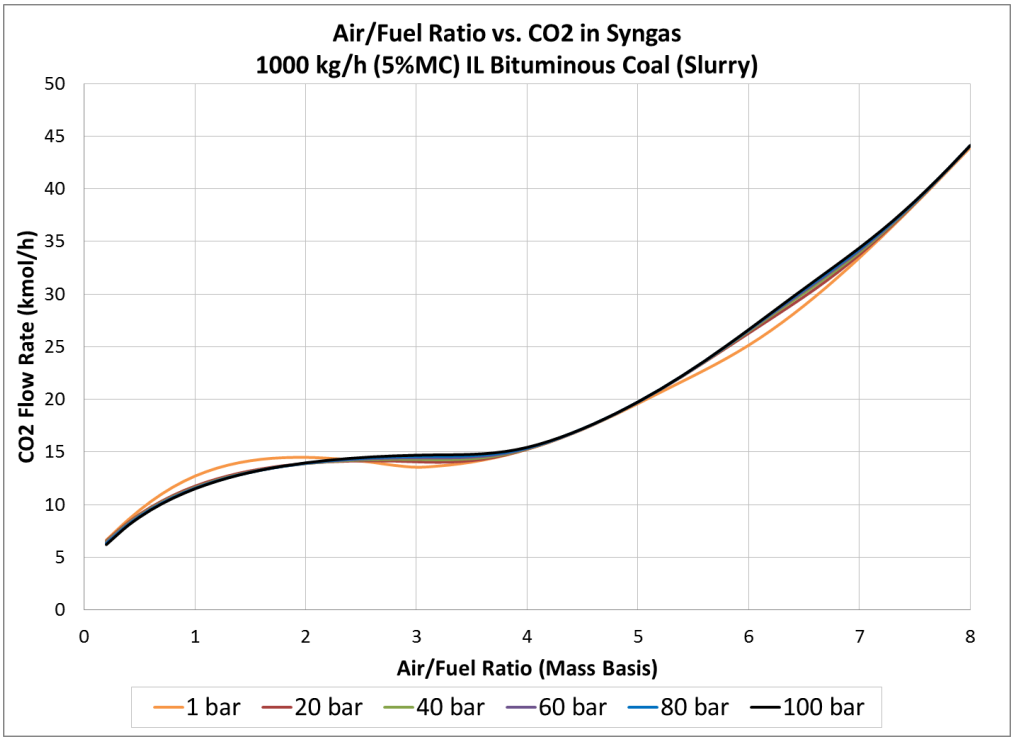

Figure 6.26 – ILC: AFR & gasifier pressure vs. CO_2 in syngas (slurry-feed)

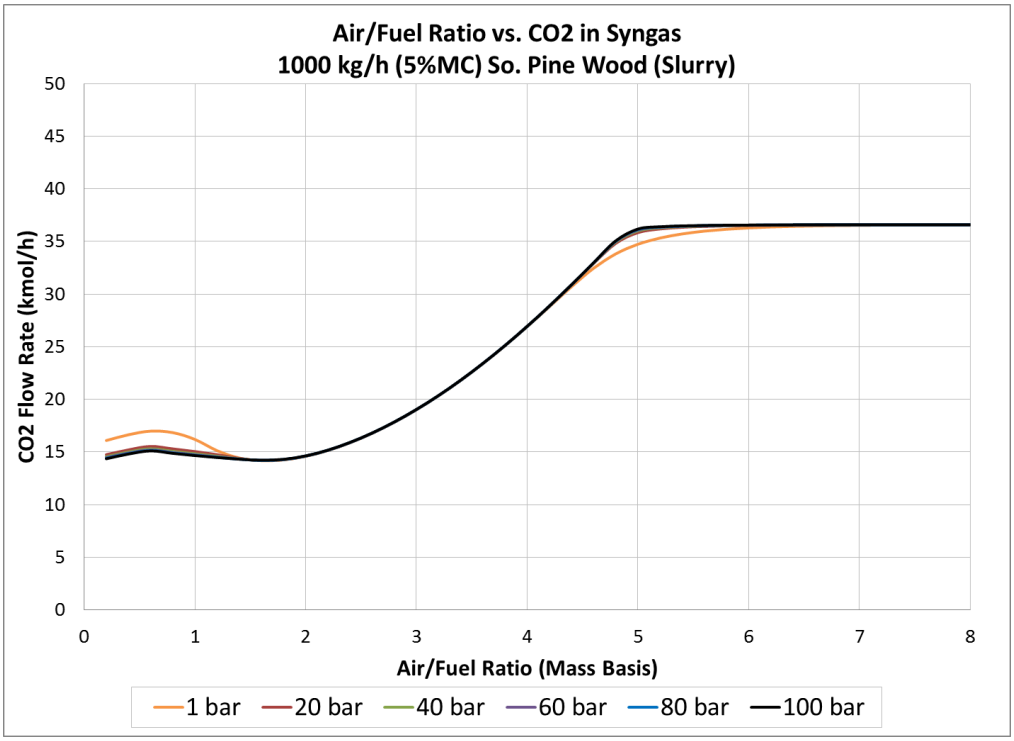

Figure 6.27 – SPW: AFR & gasifier pressure vs. CO_2 in syngas (slurry-feed)

6.4.2.5 Varying AFR & Gasifier Pressure – Slurry-Feed – Effect on CH_4 in Syngas

With the exception of Montana sub-bituminous coal at lower AFRs increasing gasifier pressure results in increased methane in the syngas. For Montana sub-bituminous coal at very low AFRs (1.0-2.0) relative to AFR_{CC}, methane formation generally decreases with increasing pressure. Increasing the AFR beyond these values, up to roughly AFR_{CC}, while increasing the gasifier pressure, results in increased CH_4 as in the other three feedstocks. The results from Montana sub-bituminous coal and Southern pine wood are shown in the following figures.

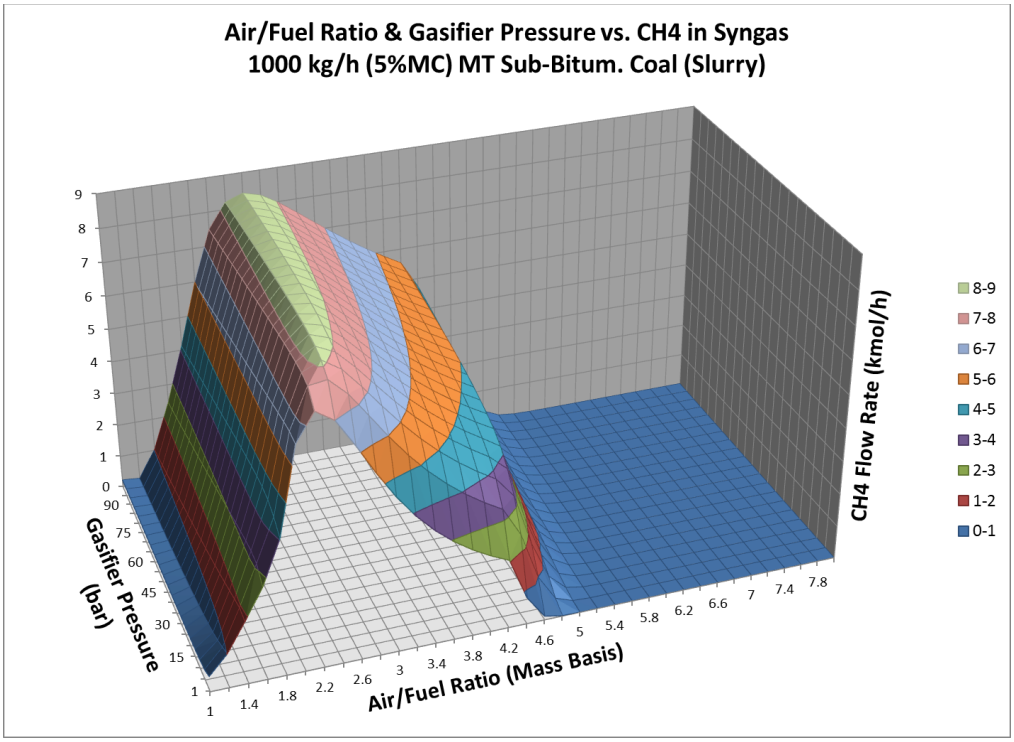

Figure 6.28 – MTC: AFR & gasifier pressure vs. CH_4 in syngas (slurry-feed)

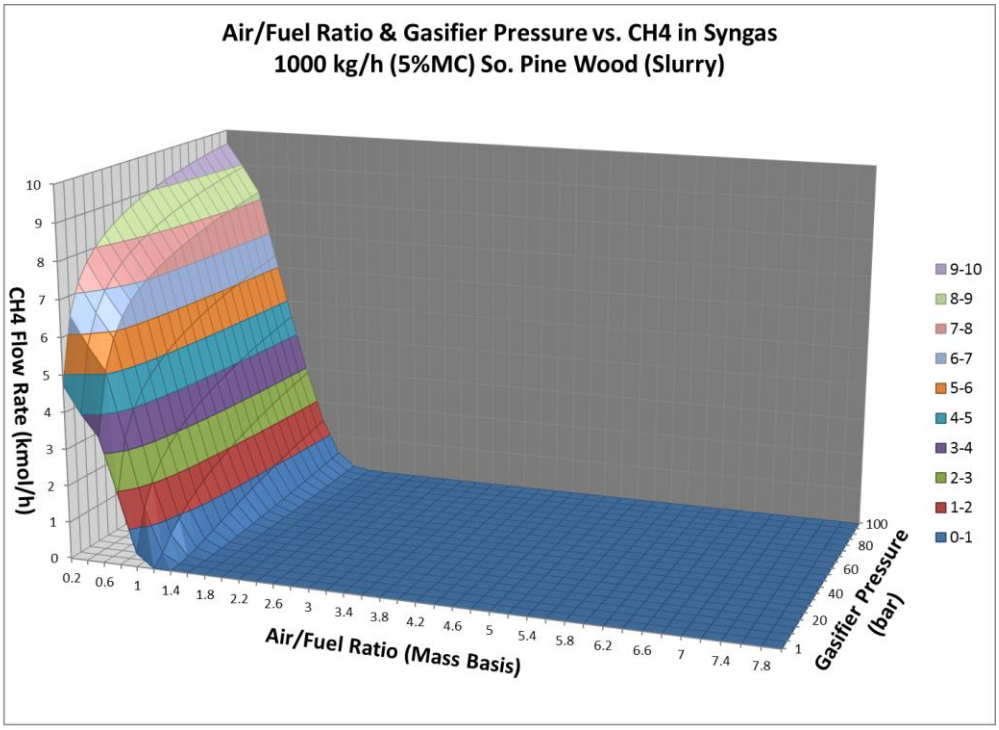

Figure 6.29 – SPW: AFR & gasifier pressure vs. CH_4 in syngas (slurry-feed)

6.4.2.6 Varying AFR & Gasifier Pressure – Slurry-Feed – Effect on H_2O in Syngas

The effects of increasing gasifier pressure on water formation are similar for each of the feedstocks. The results for Montana sub-bituminous coal are shown in the following figure.

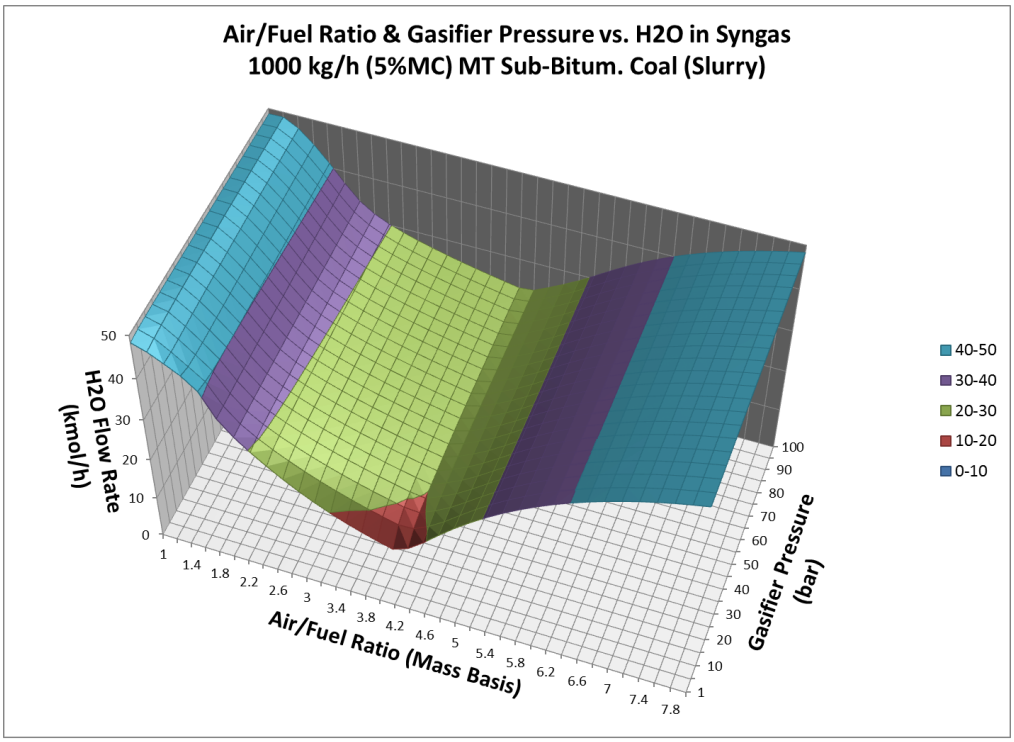

Figure 6.30 – MTC: AFR & gasifier pressure vs. H_2O in syngas (slurry-feed)

For AFRs up to AFR_{CC}, the amount of water in the syngas increases as pressure increases. Beyond the 100% conversion AFR, increasing the pressure has little effect on the water content of the syngas.

6.4.2.7 Varying AFR & Gasifier Pressure – Slurry-Feed – Effect on Gasifier Temperature

The same response is seen in each of the feedstocks. Up to AFR_{CC}, increasing gasifier pressure increases the gasifier temperature. At air-to-fuel ratios greater than AFR_{CC}, increasing the gasifier pressure has little effect on the gasifier temperature. The results for Montana sub-bituminous coal are shown in the following figure.

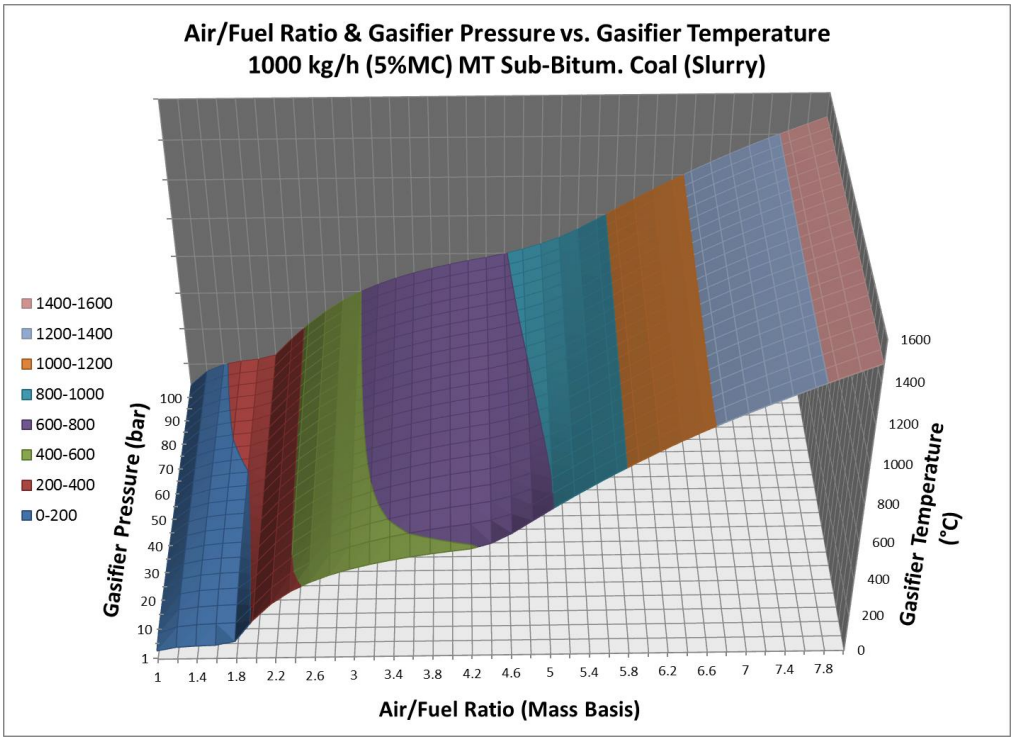

Figure 6.31 – MTC: AFR & gasifier pressure vs. gasifier temperature (slurry-feed)

6.4.3 Varying AFR & Gasifier Pressure – Analysis

Generally, the simulations performed showed that increasing gasifier pressure noticeably decreases both H_2 and CO in the syngas at air-to-fuel ratios that are less than that which is required to completely convert all of the solid carbon to other compounds (AFR_{CC}). These results are similar to the results from equilibrium models presented by Vaezi *et al.* (2011), Gungor *et al.* (2012), and Azzone *et al.* (2012). Two reactions account for this phenomenon. Recalling the methanation and methane reforming reactions:

$$C + 2\ H_2 \leftrightarrow CH_4 \qquad (\Delta H = -75\ kJ/mol) \qquad (8)$$

$$CH_4 + H_2O \leftrightarrow CO + 3\ H_2 \qquad (\Delta H = +206\ kJ/mol) \qquad (9)$$

As the system pressure increases, the equilibrium of the systems shifts away from hydrogen and carbon monoxide and toward methane and water. (i.e. The system moves to increase the fraction of total system pressure accounted for by the partial pressures of methane and water.) This is consistent with Le Chatelier's principle. As system pressure increases, the equilibrium of non-equimolar reactions shifts toward the side of the reaction that will results in fewer molecules.

At first glance, one might assume that the following reaction would also be impacted by increasing pressure:

$$C + H_2O \leftrightarrow \tfrac{1}{2} CO_2 + \tfrac{1}{2} CH_4 \qquad (\Delta H = +7.7 \text{ kJ/mol}) \qquad (12)$$

Of the reactions listed in Section 2.2, it is the only other reversible reaction where the sums of the stoichiometric coefficients of the products and the reactants are not equal. However, when evaluating only the gaseous components, the sum of the stoichiometric coefficients of carbon dioxide and methane is equal to the stoichiometric coefficient of water. With carbon existing in the solid phase, it does not exert a partial pressure on the system. Thus, Reaction 12 would not respond to changing gasifier pressure.

6.4.4 Varying AFR & Gasifier Pressure – Implications

The simulation results show the same trends as other equilibrium gasification models presented in the literature. Vaezi *et al.* (2011) report that increasing pressure decreases hydrogen and carbon monoxide in the syngas while increasing carbon dioxide, methane, and water. Gungor *et al.* (2012) report that increasing gasifier pressure results in decreasing hydrogen and carbon monoxide. However, another report from the literature which presents empirical data offers conflicting results with regard to hydrogen.

Valin *et al.* (2010) report an increase in hydrogen in the syngas with increasing pressure in the gasification of wood sawdust in a fluidized-bed gasifier. The authors also report that through analysis of their data, they show that their system operated "very far from thermodynamic equilibrium constants". With a variety of factors affecting how closely a gasification system approaches equilibrium (e.g. feed/air flow configuration, temperature, etc.), one focus area for equilibrium gasification modeling is to continue to develop approximations to help account for known non-equilibrium conditions, for example, the tendency of solid carbon in the gasifier to not be in equilibrium in specific gasifier configurations. Working to improve equilibrium models with modifications to account for equilibrium approach will allow for the greater use of equilibrium models over and against kinetic models, which are much more time and labor intensive to create.

6.5 Varying AFR & Feedstock Moisture Content

The effects of varying feedstock moisture content were evaluated for each of the four feedstocks at 30 atm.

6.5.1 Varying AFR & Feedstock Moisture Content – Dry-Feed – Results

6.5.1.1 Varying AFR & Feedstock Moisture Content – Dry-Feed – Effect on Carbon in Syngas

For all the feedstocks, increasing moisture content causes carbon in the syngas to decrease. The following figure shows the results for IL bituminous coal.

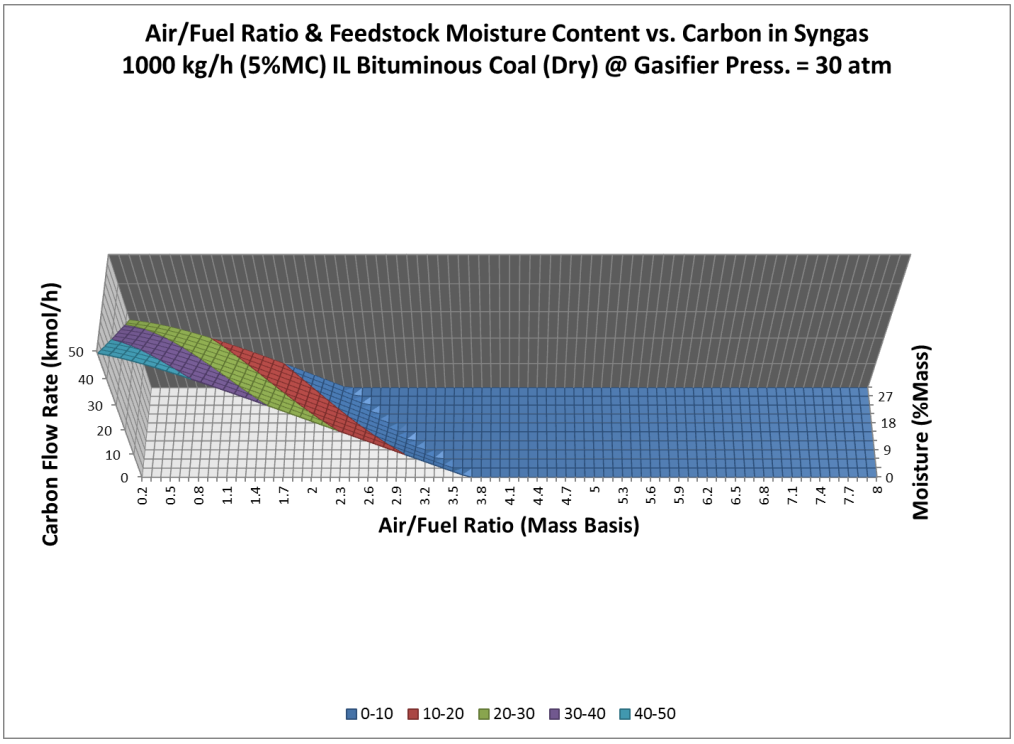

Figure 6.32 – ILC: AFR & feedstock moisture vs carbon in syngas (dry-feed)

6.5.1.2 Varying AFR & Feedstock Moisture Content – Dry-Feed – Effect on H_2 in Syngas

In the Montana sub-bituminous coal, increasing moisture content causes an increase in H_2 in the syngas at AFR values less than AFR_{CC}. In the Illinois coal, at low AFRs ($\leq$ 1.9), increasing moisture content causes a decrease in H_2, but as the AFR is increased from 1.9 up to AFR_{CC}, increasing moisture content causes an increase in H_2. At values greater than AFR_{CC}, increasing moisture causes decreased H_2 for both coals. For both of the biomass feedstocks, increasing moisture causes decreased H_2. The results for both coals and switchgrass are shown in the following figures.

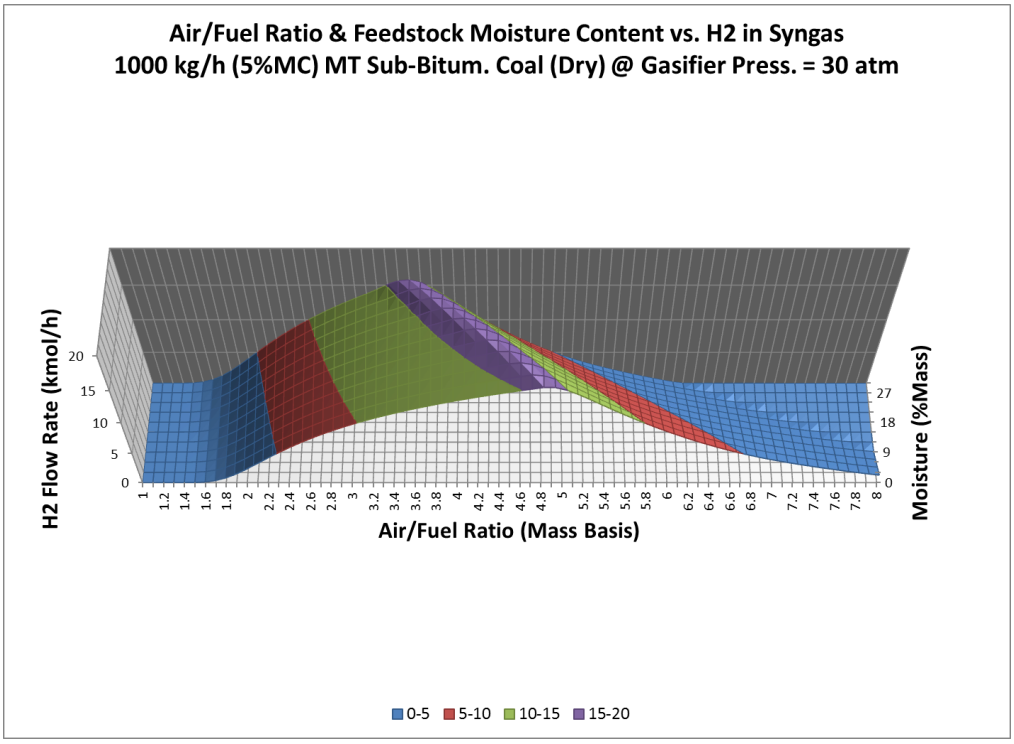

Figure 6.33 – MTC: AFR & feedstock moisture vs H_2 in syngas (dry-feed)

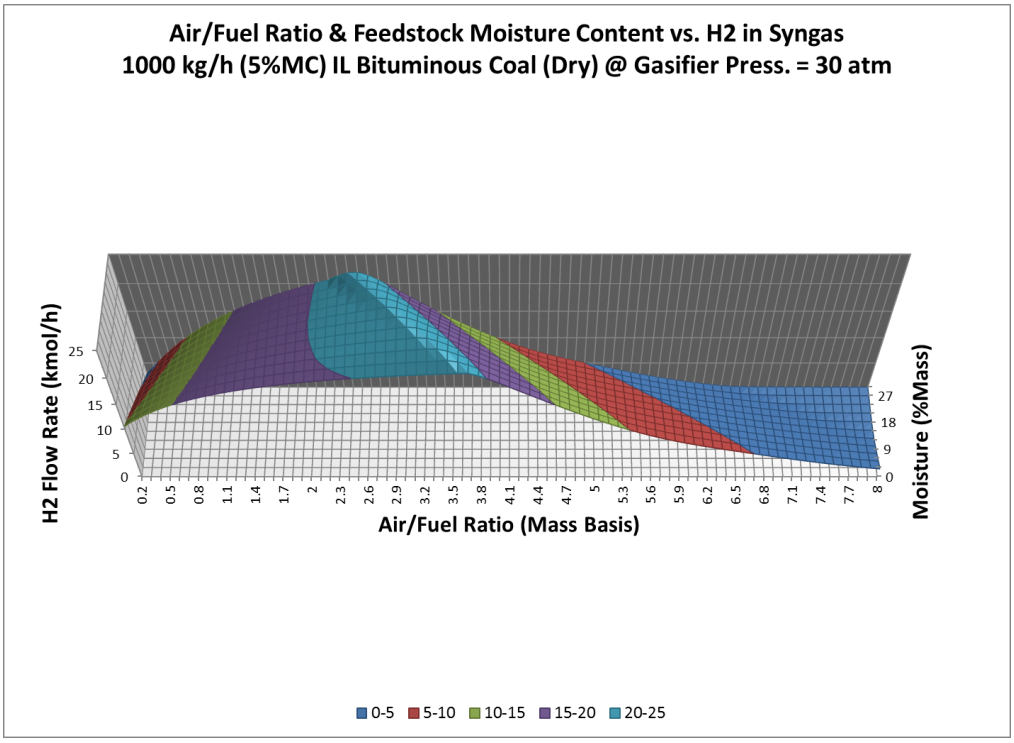

Figure 6.34 – ILC: AFR & feedstock moisture vs H_2 in syngas (dry-feed)

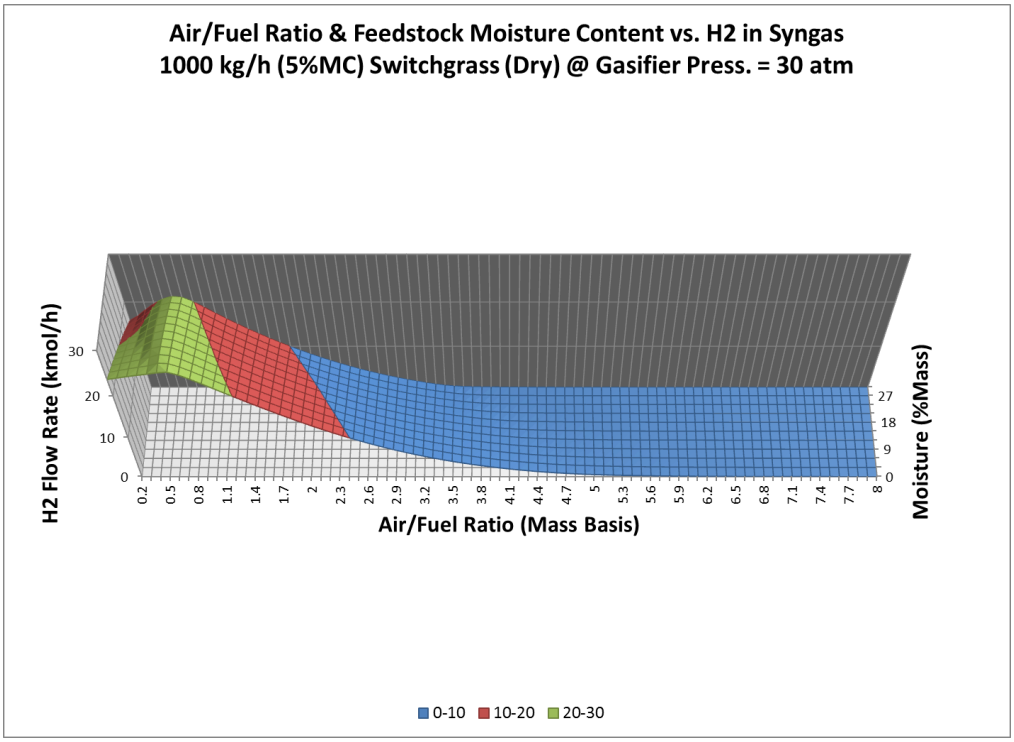

Figure 6.35 – SWG: AFR & feedstock moisture vs H_2 in syngas (dry-feed)

6.5.1.3 Varying AFR & Feedstock Moisture Content – Dry-Feed – Effect on CO in Syngas

For Montana sub-bituminous coal, increasing moisture content causes an increase in CO in the syngas at air-to-fuel ratios less than AFR_{CC}. For Illinois bituminous, Southern pine wood, and switchgrass, increased moisture content results in decreasing CO in the syngas at AFRs less than AFR_{CC}. For all of the feedstocks, increasing moisture content causes decreased CO at AFRs greater than AFR_{CC}. The following figures show the results for Montana coal and switchgrass.

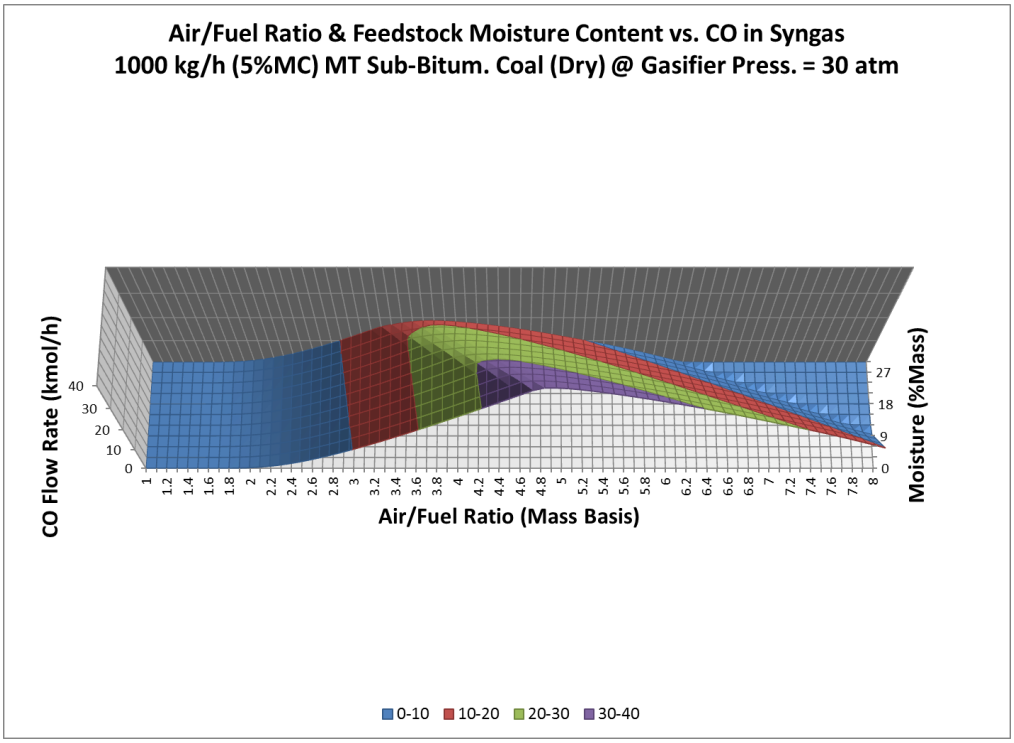

Figure 6.36 – MTC: AFR & feedstock moisture vs CO in syngas (dry-feed)

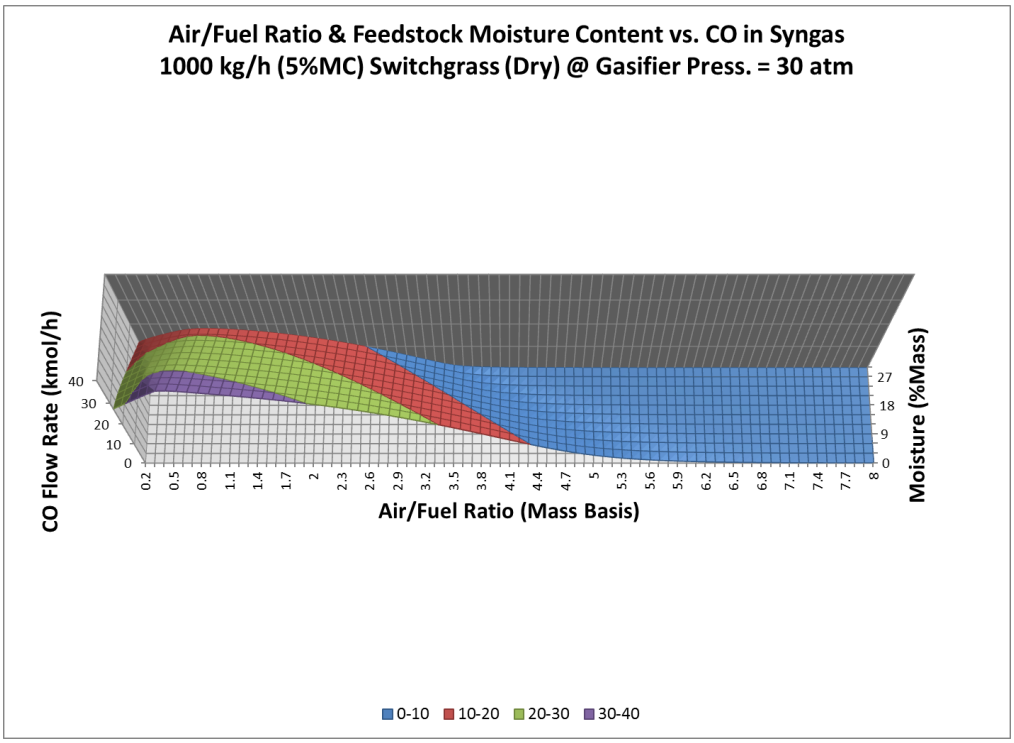

Figure 6.37 – SWG: AFR & feedstock moisture vs CO in syngas (dry-feed)

6.5.1.4 Varying AFR & Feedstock Moisture Content – Dry-Feed – Effect on CO_2 in Syngas

For all four feedstocks, at AFRs less than the value that results in the maximum flow of CO_2 in the syngas, increasing feedstock moisture content causes increased CO_2 in the syngas. At AFR values greater than this, increasing moisture content causes decreased CO_2 in the syngas.

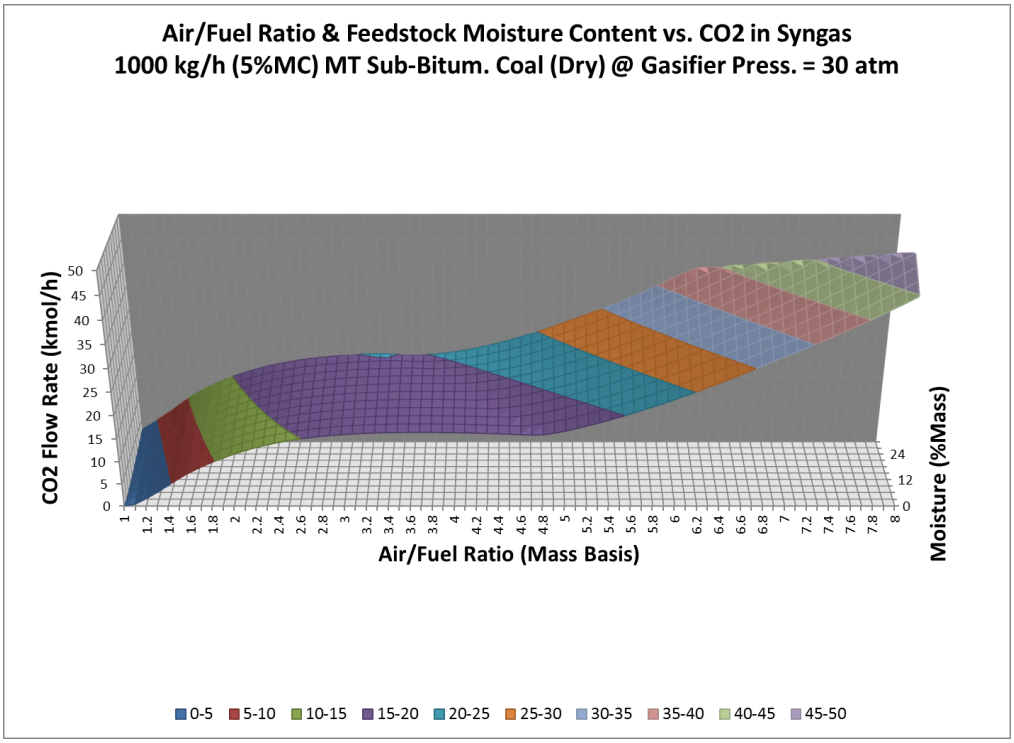

Figure 6.38 – MTC: AFR & feedstock moisture vs CO_2 in syngas (dry-feed, 1 of 2)

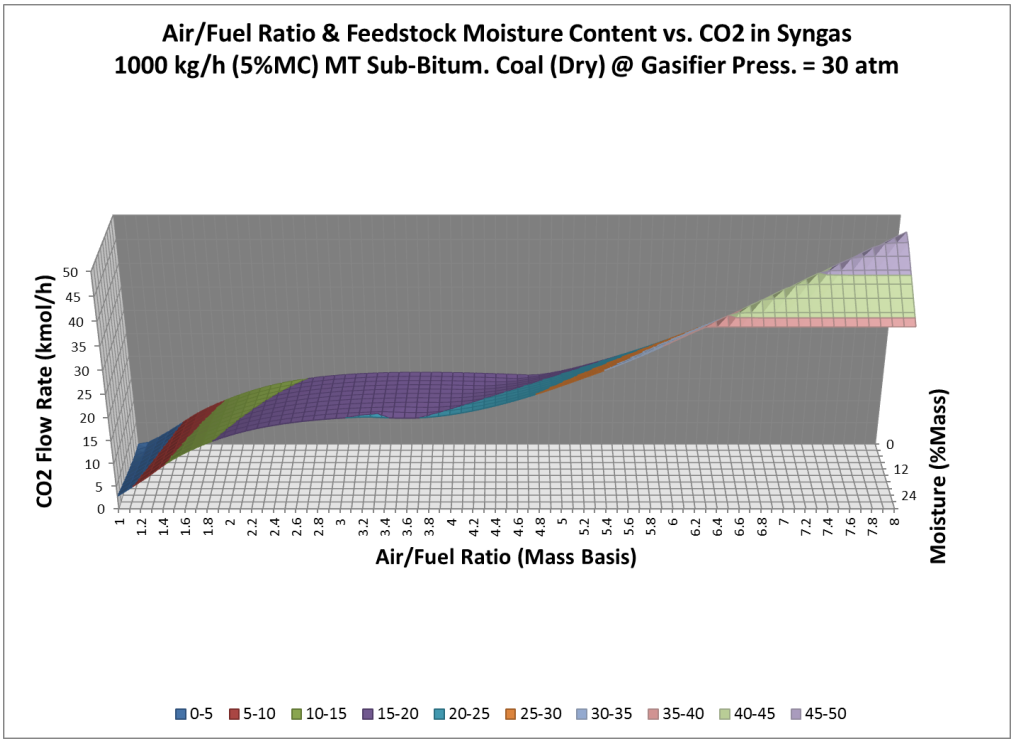

Figure 6.39 – MTC: AFR & feedstock moisture vs CO_2 in syngas (dry-feed, 2 of 2)

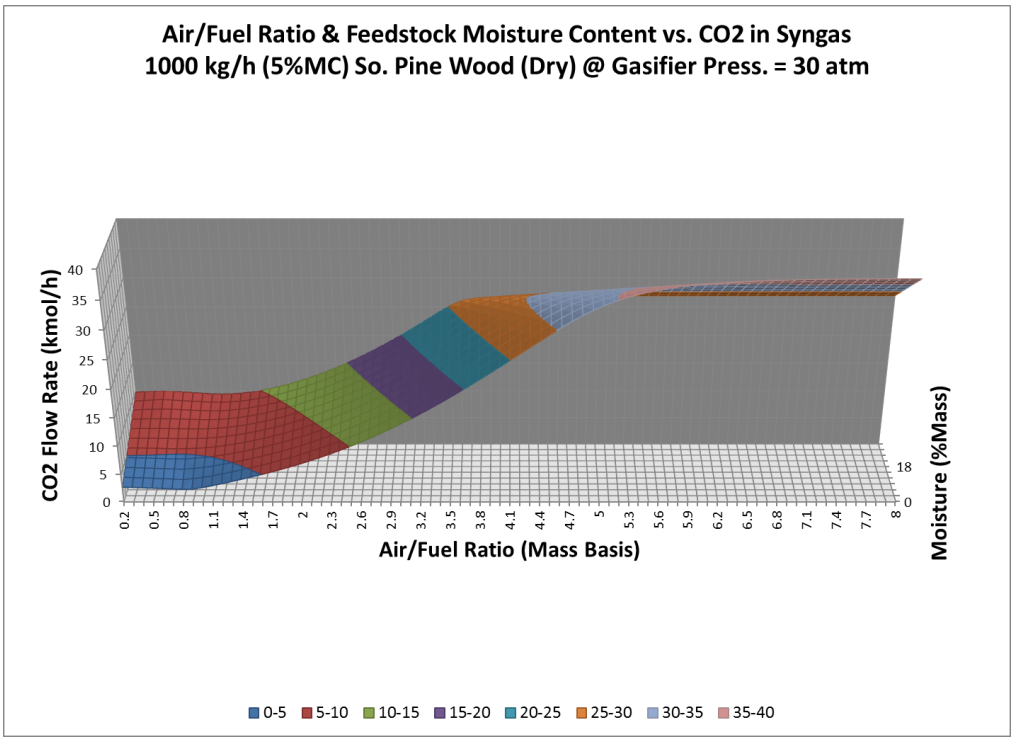

Figure 6.40 – SPW: AFR & feedstock moisture vs CO_2 in syngas (dry-feed, 1 of 2)

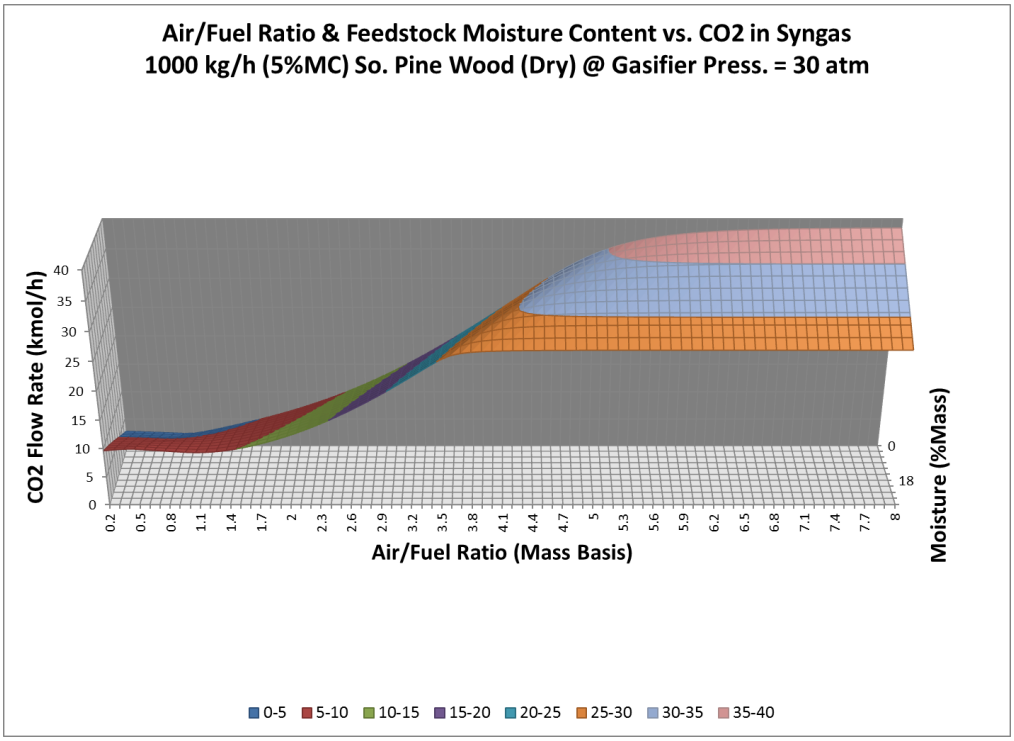

Figure 6.41 – SPW: AFR & feedstock moisture vs CO_2 in syngas (dry-feed, 2 of 2)

6.5.1.5 Varying AFR & Feedstock Moisture Content – Dry-Feed – Effect on CH_4 in Syngas

For all of the feedstocks, increasing feedstock moisture content increases CH_4 in the syngas at AFRs less than AFR_{CC}. At AFRs greater than AFR_{CC}, the effect is reversed, methane decreases with increasing feedstock moisture, although there is very little methane present. The results for the coal feedstocks are shown in the following figures.

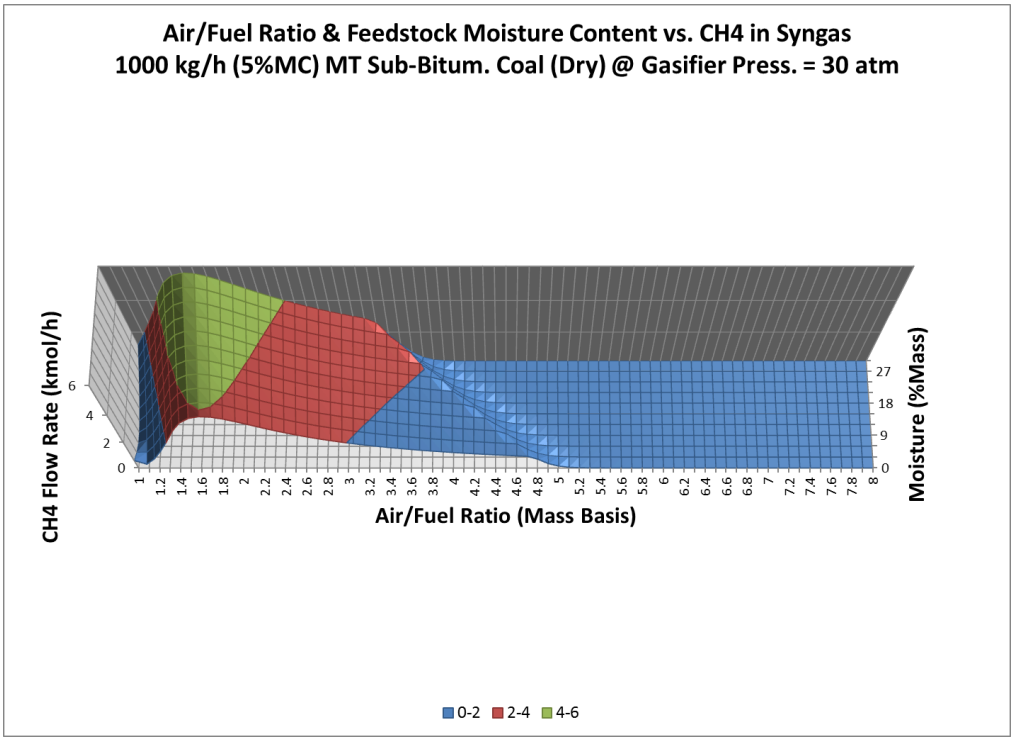

Figure 6.42 – MTC: AFR & feedstock moisture vs CH_4 in syngas (dry-feed)

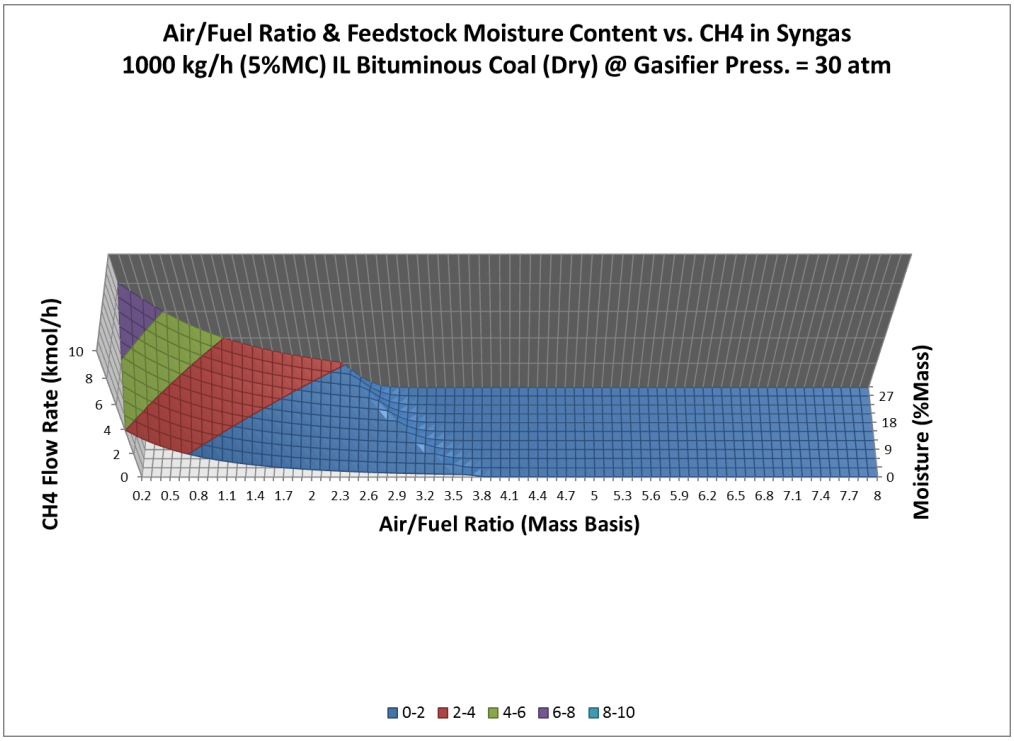

Figure 6.43 – ILC: AFR & feedstock moisture vs CH_4 in syngas (dry-feed)

6.5.1.6 Varying AFR & Feedstock Moisture Content – Dry-Feed – Effect on H_2O in Syngas

Increasing feedstock moisture results in increasing H_2O in the syngas for all of the feedstocks. The results for Illinois bituminous coal are shown in the following figure.

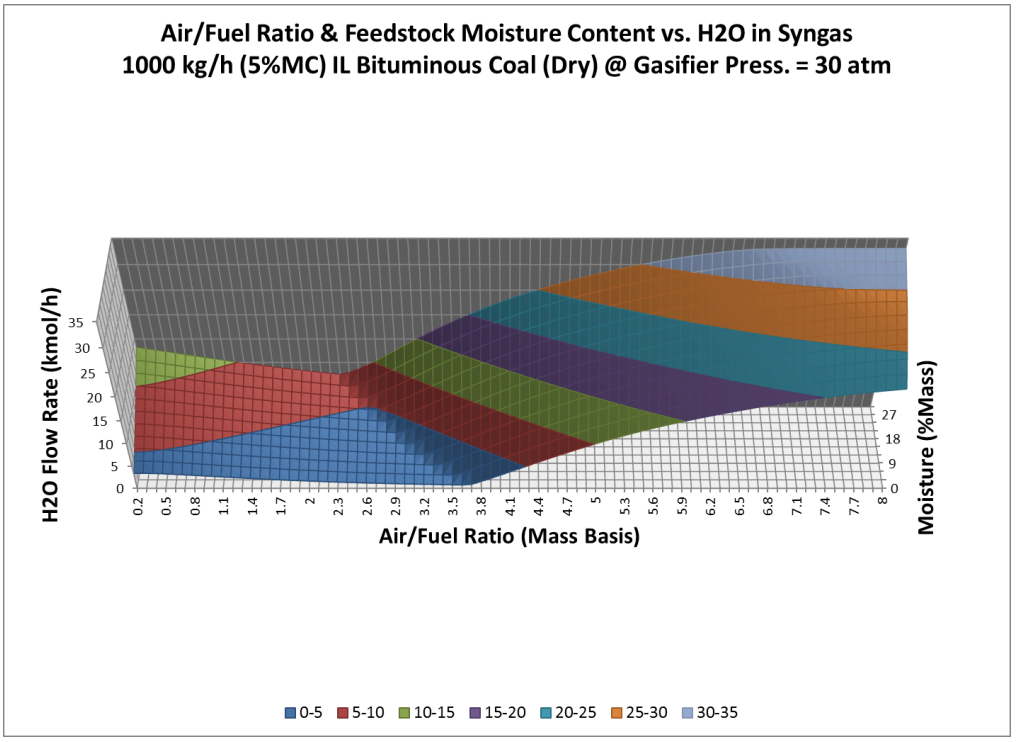

Figure 6.44 – ILC: AFR & feedstock moisture vs H_2O in syngas (dry-feed)

6.5.1.7 Varying AFR & Feedstock Moisture Content – Dry-Feed – Effect on Gasifier Temperature

For the Montana coal, increasing moisture content in the feed increases the temperature of the gasifier at all AFRs lower than the AFR for complete combustion ($AFR_{COMBUST}$). For a given moisture content, increasing the AFR beyond the value

required for complete combustion causes decreasing temperature. The temperature increase over the range of moisture values is more dramatic at AFRs greater than AFR_{CC}. In the Illinois coal, increasing moisture content causes decreasing gasifier temperature at AFRs less than AFR_{CC} and increases the temperature at AFRs greater than AFR_{CC} but less than $AFR_{COMBUST}$. Similarly to the Montana coal, for a specified feedstock moisture, increasing AFR beyond $AFR_{COMBUST}$ causes decreasing temperature. For both of the biomass feedstocks, increasing moisture content decreases the gasifier temperature, with a more pronounced effect at AFRs greater than $AFR_{COMBUST}$. The results for both of the coal feedstocks and switchgrass are shown in the following figures.

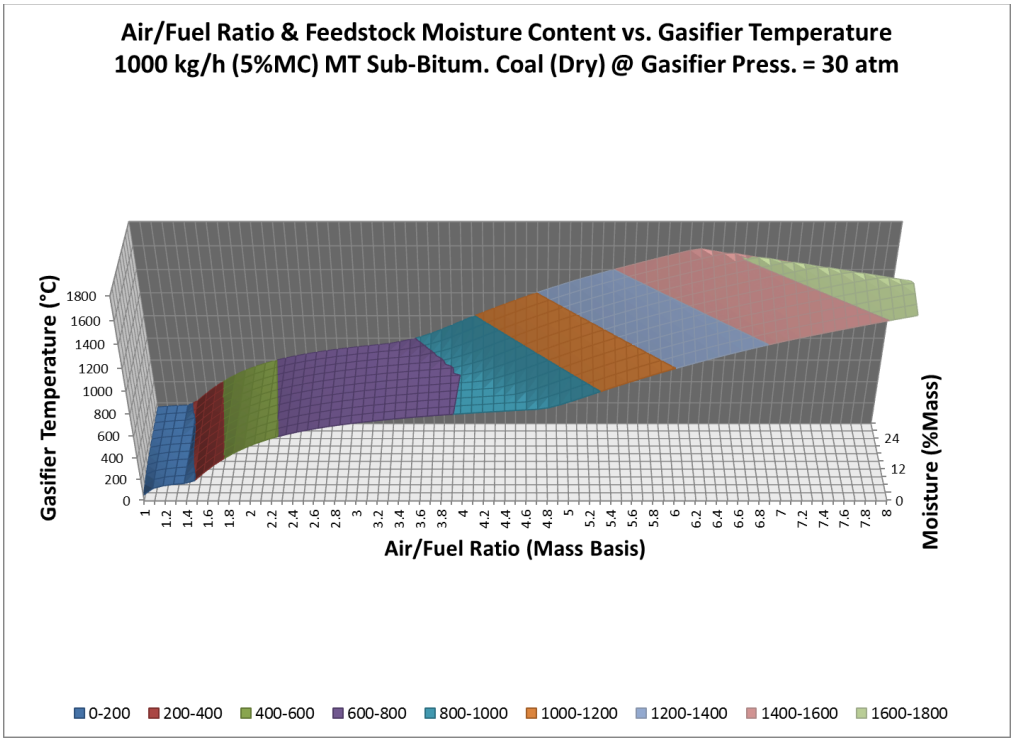

Figure 6.45 – MTC: AFR & feedstock moisture vs gasifier temperature (dry-feed)

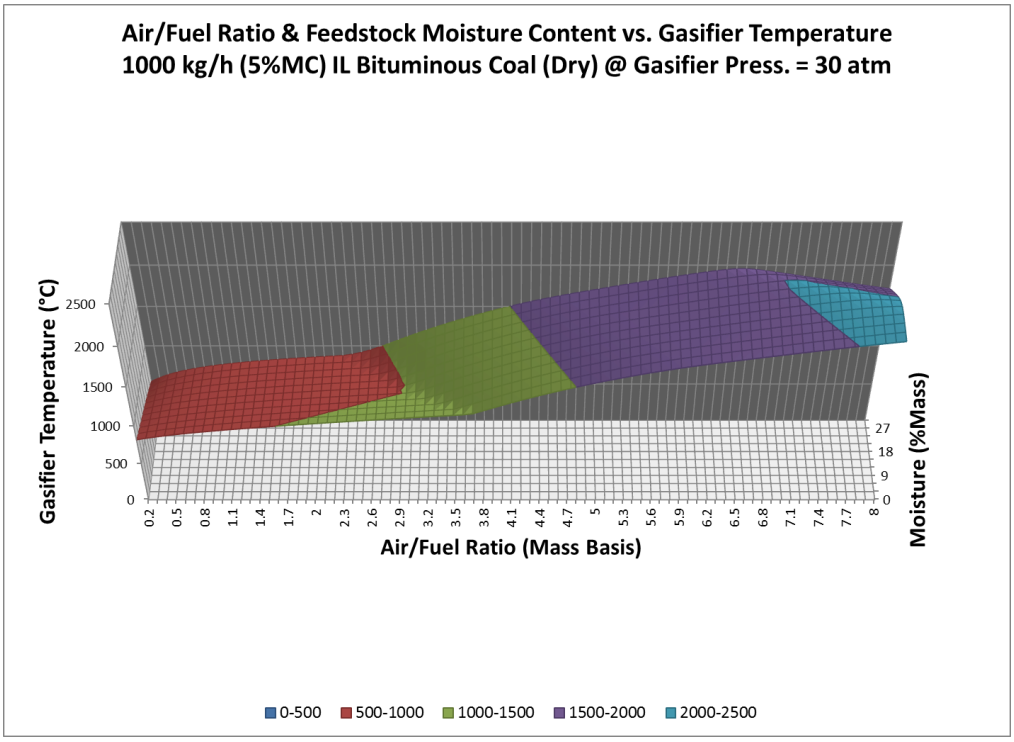

Figure 6.46 – ILC: AFR & feedstock moisture vs gasifier temperature (dry-feed)

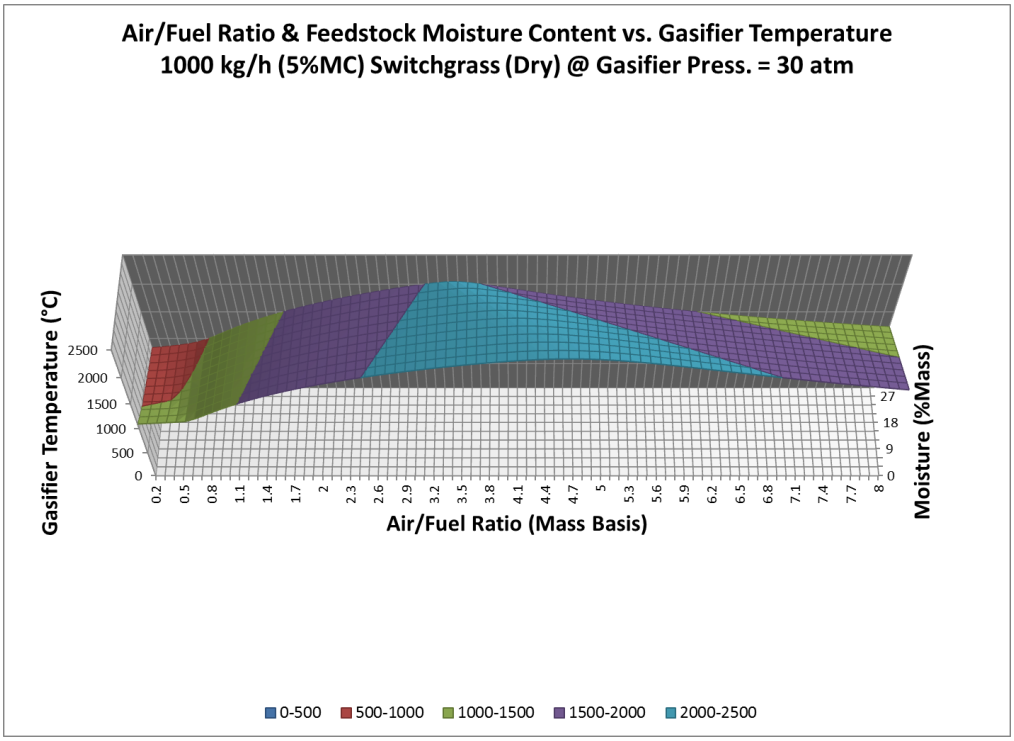

Figure 6.47 – SWG: AFR & feedstock moisture vs gasifier temperature (dry-feed)

6.5.1.8 Varying AFR & Feedstock Moisture Content – Dry-Feed – Effect on DECOMP Heat

For all of the feedstocks, increasing the moisture content decreases the energy required for decomposition in RYIELD. For all of the feedstocks at the same moisture content, the fraction of energy required to decompose the feedstock relative to the energy required to decompose the feedstock when completely dry is roughly the same.

Feedstock Moisture Content vs. Decomposition Energy								
1000 kg/h Feedstock (Dry) @ Gasifier Press. = 30 atm								
%Moisture	MT Sub-Bitum. Coal		IL Bituminous Coal		So. Pine Wood		Switchgrass	
	Q_{DECOMP} (Gcal/h)	Compared to 0% Moisture	Q_{DECOMP} (Gcal/h)	Compared to 0% Moisture	Q_{DECOMP} (Gcal/h)	Compared to 0% Moisture	Q_{DECOMP} (Gcal/h)	Compared to 0% Moisture
30	1.091	69.9%	0.053	67.9%	0.459	69.8%	0.273	70.5%
27	1.139	73.0%	0.056	72.0%	0.479	72.9%	0.286	73.8%
24	1.186	76.1%	0.060	76.1%	0.500	76.0%	0.298	77.1%
21	1.234	79.1%	0.063	80.1%	0.520	79.1%	0.311	80.4%
18	1.282	82.2%	0.066	84.2%	0.541	82.3%	0.324	83.6%
15	1.329	85.2%	0.069	88.2%	0.561	85.4%	0.336	86.9%
12	1.377	88.3%	0.072	91.7%	0.582	88.4%	0.349	90.2%
9	1.425	91.3%	0.075	95.4%	0.602	91.5%	0.362	93.5%
6	1.472	94.4%	0.077	98.7%	0.622	94.6%	0.374	96.7%
3	1.518	97.3%	0.079	100.9%	0.641	97.5%	0.387	100.0%
0	1.560	100.0%	0.078	100.0%	0.658	100.0%	0.387	100.0%

Table 6.4 – Feedstock moisture vs. decomposition energy (dry-feed)

6.5.2 Varying AFR & Feedstock Moisture Content – Analysis

Some of the results from increasing moisture content are surprising. Increasing feedstock moisture causes increasing gasifier temperature in certain regions of AFRs for both of the coals. This phenomenon seems problematic from an intuitive standpoint. It would be expected that increasing feedstock moisture content would always decrease gasifier temperature as energy is used to vaporize the water rather than to raise the

temperature of the gasifier; that is, more energy is used to provide latent heat as opposed to sensible heat. Additionally, increasing the moisture fraction accordingly decreases the fraction of combustibles in the feedstock, which are the sources of heat in the system. Upon examination, it is observed that increasing feedstock moisture dramatically decreases the energy required to decompose the feedstock in the first reactor (DECOMP) within the simulation. Thus, as the moisture content increases, the energy available to the second reactor (GASIFIER) also increases. This is the dominating effect in these sensitivity analyses.

From a qualitative standpoint, checking this phenomenon against the behavior of the slurry-feed configuration with increasing makeup water would seem to be a valid comparison. Upon comparison, the behavior of the dry-feed configuration with increasing moisture does not correlate with the results of the slurry-feed configuration with increasing makeup water, which is configured to allow the addition of water between the DECOMP and GASIFIER units. In those sensitivity analyses, the flow of water was varied to evaluate the effect that the solids content would have on the process. Increasing makeup water decreases the temperature in each case.

Further investigation into Aspen Plus® explains this behavior. Because nonconventional components must be converted into known chemical compounds to take part in the simulation, the enthalpy of the nonconventional component must be accounted for to accurately reflect the total system energy balance. In the presented configuration, the stream COALFEED must have an enthalpy assigned to it to allow material and energy balances to take place in the DECOMP reactor. The enthalpy of the nonconventional material stream (COALFEED), is comprised of two parts: 1) the heat of

formation and 2) the sensible heat component. If stream temperature and pressure are at or near standard temperature and pressure (which they are in the presented simulations), then the sensible heat component of the enthalpy is none or negligible. Thus, the key part of the enthalpy is the heat of formation. Since heterogeneous solids do not have standard heats of formation like known pure substances (e.g. methane), Aspen Plus® gives the user two options for estimating the heat of formation of the solids (i.e. feedstocks). The first option, labeled in the software as "Heat of Combustion-Based Correlation", estimates the heat of formation utilizing the higher heating value and the ultimate analysis of the feedstock according to the following equation (Aspen Plus® v8.4):

$$\Delta_f h_i^d = \Delta_c h_i^d - (1.418\times10^6 w_{H,i}^d + 3.278\times10^5 w_{C,i}^d + 9.264\times10^4 w_{S,i}^d \ldots \\ \ldots - 2.418\times10^4 w_{N,i}^d - 1.426\times10^4 w_{Cl,i}^d)10^2 \quad (20)$$

$\Delta_f h_i^d$ - heat of formation of substance *i* (dry-basis)

$\Delta_c h_i^d$ - heat of combustion of substance *i* (dry-basis)

$w_{X,i}^d$ - weight fraction of component *x* in substance *i* (dry-basis)

An evaluation of this equation by hand confirms that, over the range of selected moisture contents, increasing the moisture fraction does decrease the magnitude of the heat of formation.

The second option for estimating the heat of formation of the feedstocks, labeled in the software as "Direct Correlation", uses empirically fitted parameters along with the ultimate analysis weight fractions to estimate the heat of formation. It was desired to rerun the cases for increasing moisture content using this method as a check against the first method, but the "Direct Correlation" method requires the user to input the reflectance of the feedstock, which was not available.

Among the surveyed literature, no other reports of increasing feedstock moisture content causing increased temperature were found. Two separate groups that studied the impact of feedstock moisture on gasifier temperature reported that increasing moisture decreases gasifier temperature (Roy *et al.*, 2009; Ramanan *et al*., 2008).

6.5.3 Varying AFR & Feedstock Moisture Content – Implications

With the techniques and commercial modeling programs currently available, modeling coal and/or biomass gasification requires some method of assessing the enthalpy of the feedstock to perform material and energy balances. In Aspen Plus®, there are two methods available to account for the heat of formation of the nonconventional components (i.e. feedstocks), which is essential to determining the enthalpy of the gasifier feed stream. The results from this portion of the work, varying feedstock moisture content, have introduced some question into the ability of one of these correlations. Further investigation into estimating the heat of formation of nonconventional components is needed.

6.6 Varying AFR & Air Temperature

The air-to-fuel ratio and the temperature of the air were varied for both feed configurations at 30 atm.

6.6.1 Varying AFR & Air Temperature – Dry-Feed – Results

6.6.1.1 Varying AFR & Air Temperature – Dry-Feed – Effect on Carbon in Syngas

Increasing air temperature causes decreased carbon in the syngas for all four feedstocks. The results for Illinois bituminous coal are shown in the following figure.

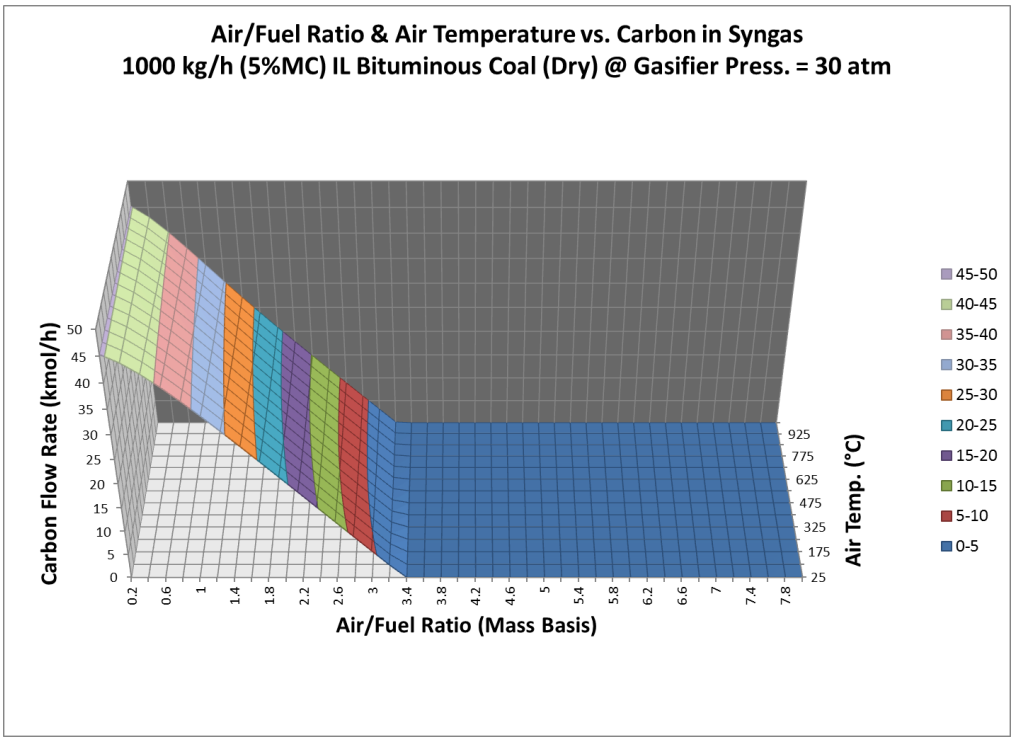

Figure 6.48 – ILC: AFR & air temperature vs. carbon in syngas (dry-feed)

6.6.1.2 Varying AFR & Air Temperature – Dry-Feed – Effect on H_2 in Syngas

For all of the feedstocks, increasing the air temperature causes increased hydrogen in the syngas at AFRs less than AFR_{CC} and decreases hydrogen in the syngas at AFRs greater than AFR_{CC}. The following figure shows the effect in the Montana sub-bituminous coal.

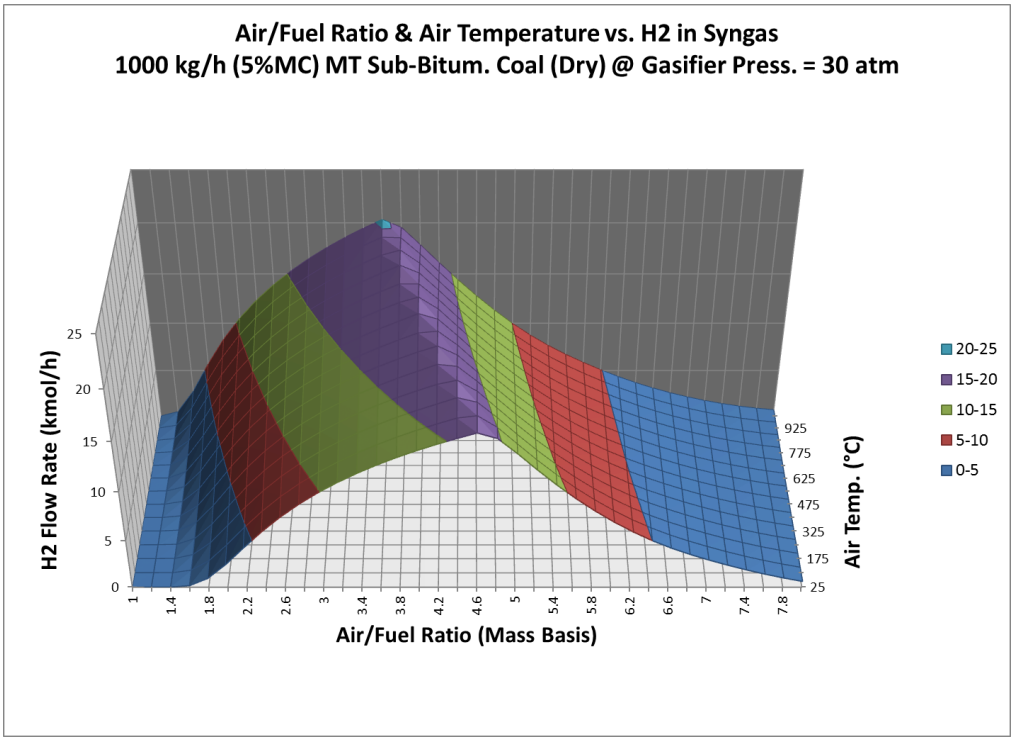

Figure 6.49 – MTC: AFR & air temperature vs. H_2 in syngas (dry-feed)

6.6.1.3 Varying AFR & Air Temperature – Dry-Feed – Effect on CO in Syngas

Increasing air temperature increases CO in the syngas for each of the four feedstocks. The following figure shows the results for Montana coal.

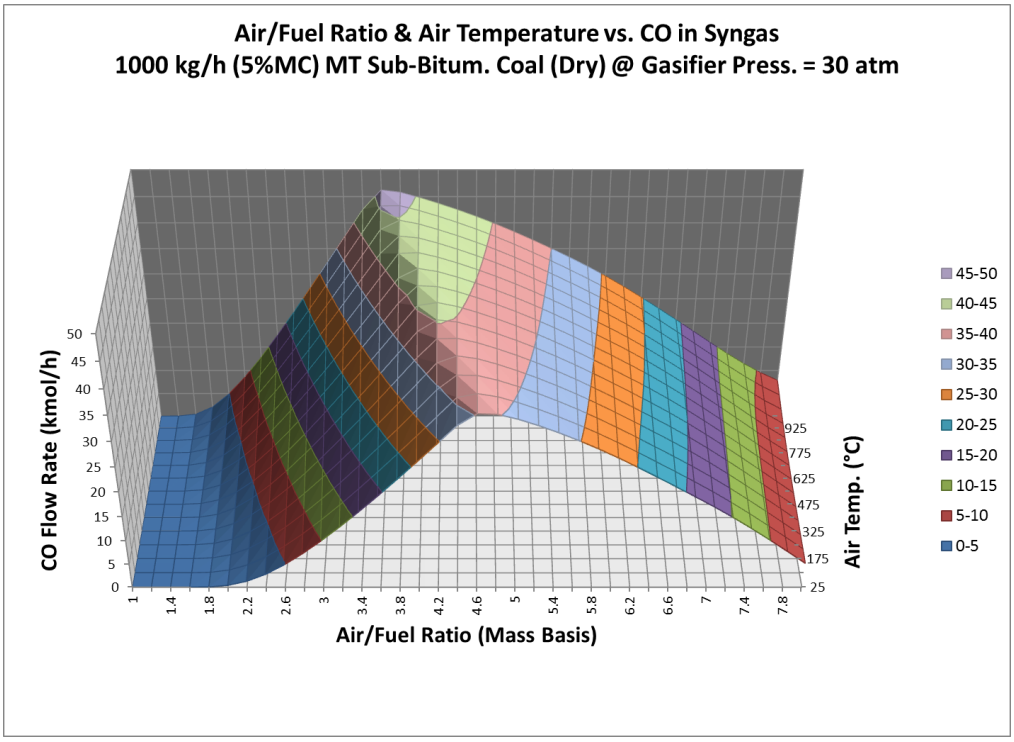

Figure 6.50 – MTC: AFR & air temperature vs. CO in syngas (dry-feed)

6.6.1.4 Varying AFR & Air Temperature – Dry-Feed – Effect on CO_2 in Syngas

For AFRs of 1.0-1.8, increasing air temperature causes increased CO_2 for Montana sub-bituminous coal. For the other three feedstocks, and for Montana coal at AFRs of 2.0-8.0, increasing air temperature decreases CO_2 in the syngas. The following figures depict the results for the Montana coal and Southern pine wood.

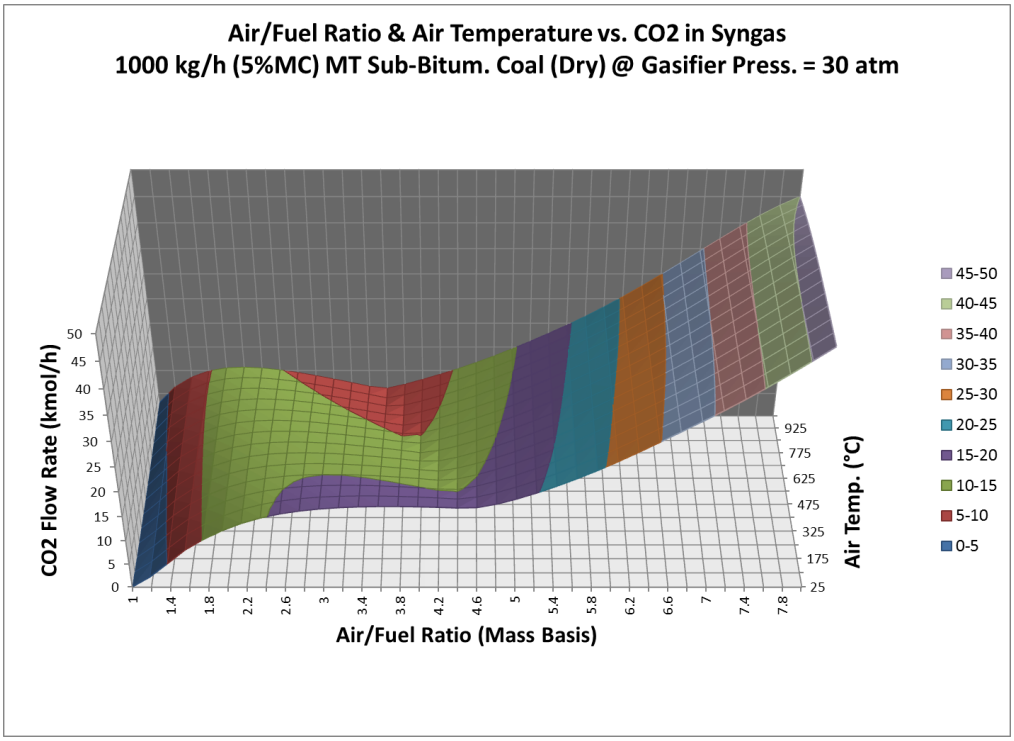

Figure 6.51 – MTC: AFR & air temperature vs. CO_2 in syngas (dry-feed)

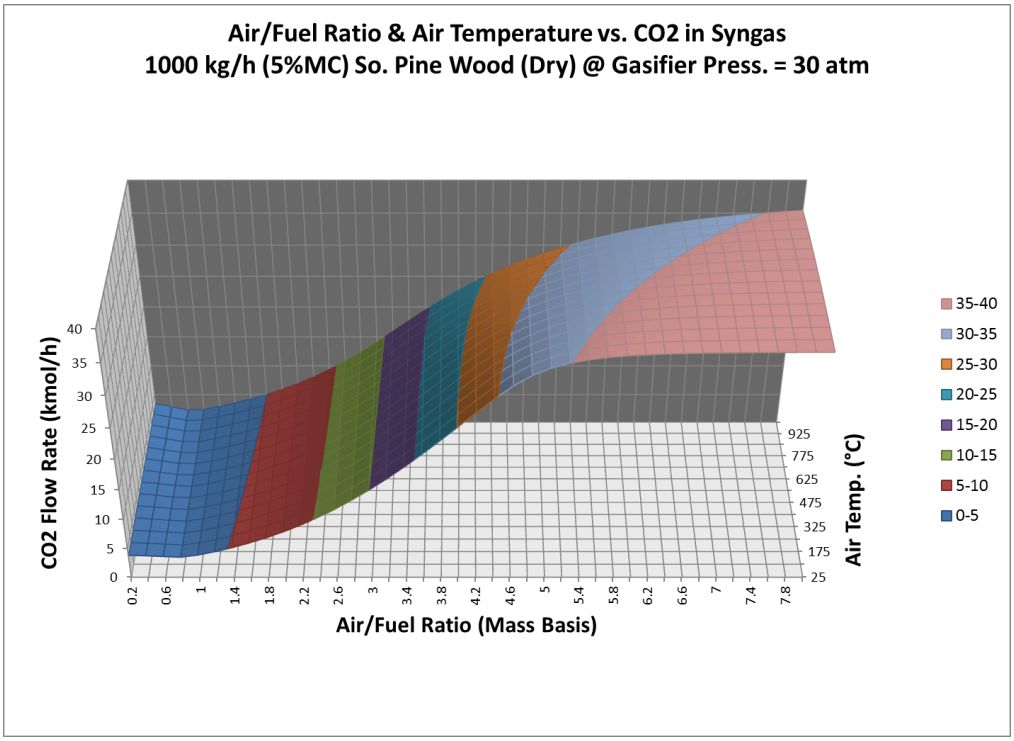

Figure 6.52 – SPW: AFR & air temperature vs. CO_2 in syngas (dry-feed)

6.6.1.5 Varying AFR & Air Temperature – Dry-Feed – Effect on CH_4 in Syngas

In the Montana sub-bituminous coal, increasing air temperature causes increasing methane at AFRs that are less than the AFR that generates the maximum amount of methane. At AFRs greater than the AFR that generates the maximum amount of methane, increasing air temperature causes the amount of methane in the syngas to decrease. For Illinois bituminous coal, Southern pine wood, and switchgrass, increasing air temperature causes decreased CH_4 regardless of the AFR. The results for the coal feedstocks are shown in the following figures.

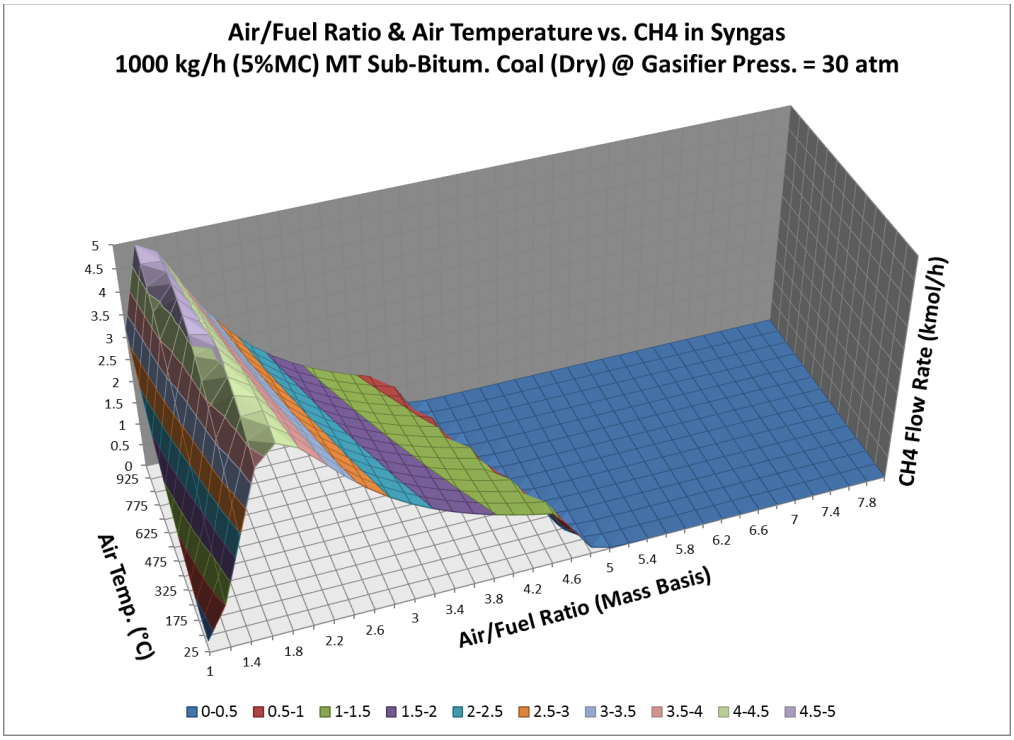

Figure 6.53 – MTC: AFR & air temperature vs. CH_4 in syngas (dry-feed)

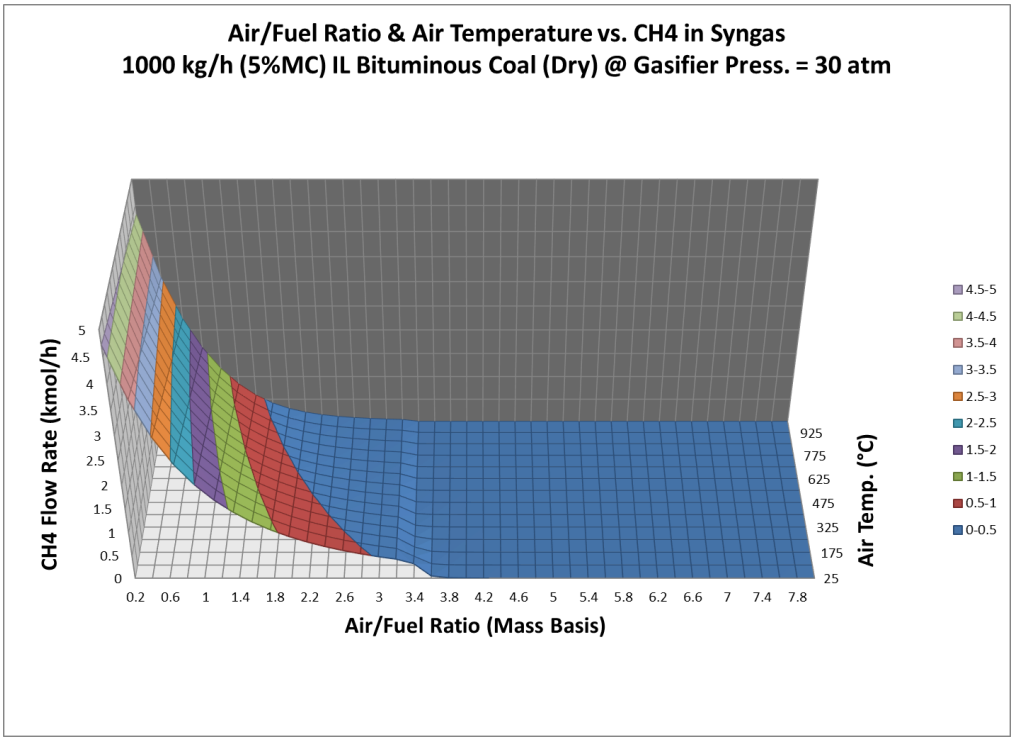

Figure 6.54 – ILC: AFR & air temperature vs. CH_4 in syngas (dry-feed)

6.6.1.6 Varying AFR & Air Temperature – Dry-Feed – Effect on H_2O in Syngas

For all of the feedstocks, increasing air temperature causes decreased water in the syngas at values less than AFR_{CC} and increases water in the syngas at AFRs greater than AFR_{CC}. The following chart depicts the results for the Montana sub-bituminous coal.

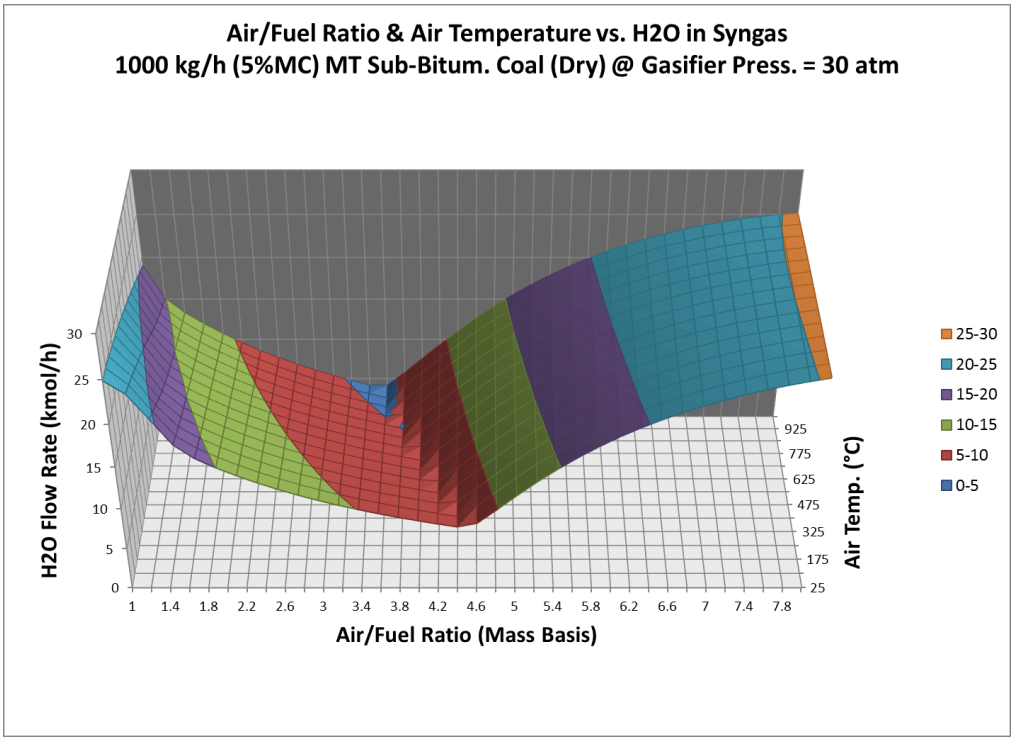

Figure 6.55 – MTC: AFR & air temperature vs. H_2O in syngas (dry-feed)

6.6.1.7 Varying AFR & Air Temperature – Dry-Feed – Effect on Gasifier Temperature

For all of the feedstocks, increasing the air temperature causes the temperature of the gasifier to rise. The following figure shows the effect for switchgrass.

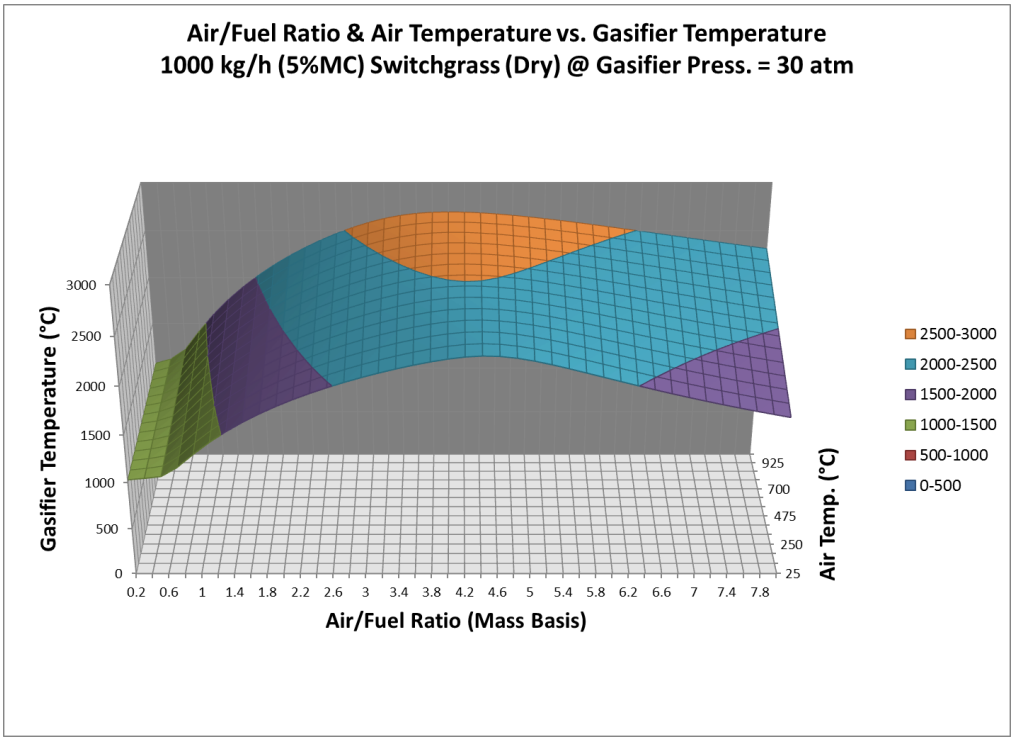

Figure 6.56 – SWG: AFR & air temperature vs. gasifier temperature (dry-feed)

6.6.2 Varying AFR & Air Temperature – Slurry-Feed – Results

With the exception of the effect on CO_2 in the syngas for Illinois bituminous coal, increasing air temperature has the same qualitative effects on the slurry-feed configuration as it did on the dry-feed configuration. At low AFRs (0.2-0.6), increasing air temperature causes increased CO_2 in the syngas for the Illinois coal. The following graph shows the results.

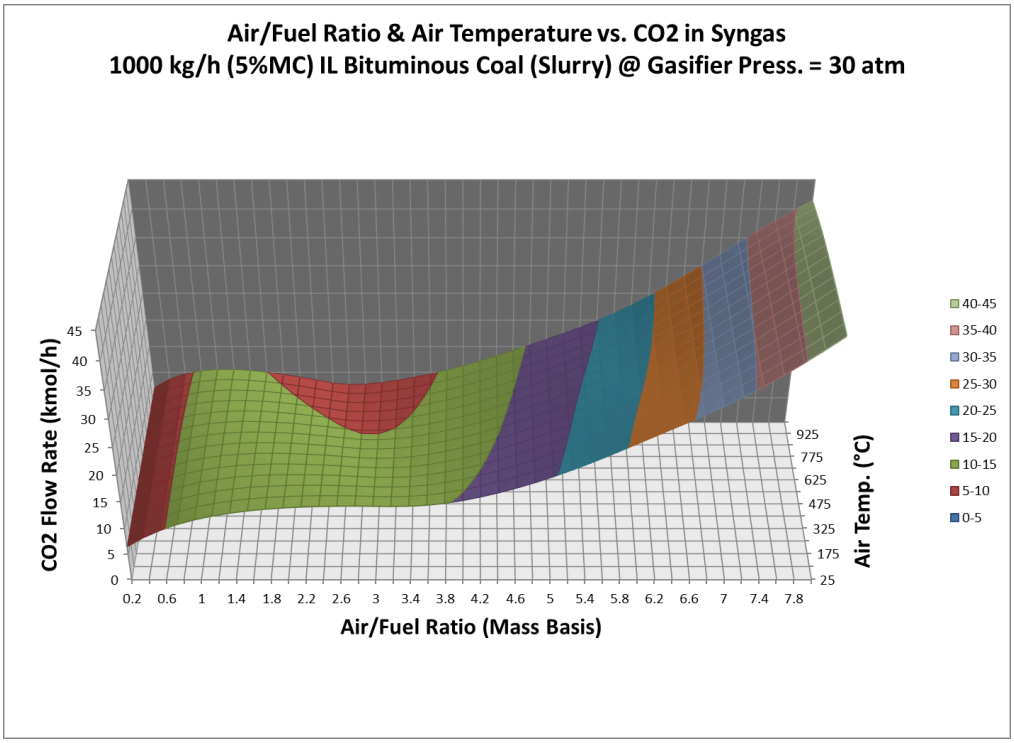

Figure 6.57 – ILC: AFR & air temperature vs. CO_2 in syngas (slurry-feed)

6.6.3 Varying AFR & Air Temperature – Analysis

The results of varying oxidation air temperature follow what would be expected from gasification theory. Recall the water-gas and Boudouard reactions:

$$C + H_2O \leftrightarrow CO + H_2 \qquad (\Delta H = +131 \text{ kJ/mol}) \qquad (5)$$

$$C + CO_2 \leftrightarrow 2\ CO \qquad (\Delta H = +172 \text{ kJ/mol}) \qquad (6)$$

With the water-gas reaction and the Boudouard reaction both being endothermic reactions and being two of the primary reactions in gasification systems, it follows that increasing the energy of the system would increase both hydrogen and carbon monoxide in the syngas. The explanation of the differing responses of hydrogen and carbon monoxide to increasing air temperature at air-to-fuel ratios greater than AFR_{CC} could be attributed to the water-gas shift reaction:

$$CO + H_2O \leftrightarrow CO_2 + H_2 \qquad (\Delta H = -41 \text{ kJ/mol}) \qquad (10)$$

With no carbon remaining for reactions, the water-gas shift reaction dominates the system. Increasing temperature favors the reversal of the reaction towards the production of carbon monoxide and water. Thus, at AFRs greater than AFR_{CC}, increasing air temperature decreases H_2 and CO_2 in the syngas but increases CO and H_2O.

6.6.4 Varying AFR & Air Temperature – Implications

There are no significant equilibrium modeling implications of note from the observations.

6.7 Carrier Gas Addition

Examining the current literature on equilibrium-based gasification models, it is apparent that dry-feed models often neglect to include the carrier gas. This sensitivity study examines the inclusion of either N_2 or CO_2 as a carrier gas at 5 atm, 30 atm, and 60 atm. For each feedstock, the AFR used was the value that resulted in 90% molar conversion when the simulation was executed with no carrier gas included.

The results are presented in a format to show how including a carrier gas changed the results from the case where no carrier gas was included ("base case").

6.7.1 Carrier Gas Addition – Results

6.7.1.1 Carrier Gas Addition – Effect on Carbon in Syngas

Nitrogen carrier gas causes more carbon to be present in the syngas, and the effect increases with increasing pressure. Using carbon dioxide as a carrier gas causes increased carbon in the syngas for Montana coal and Southern pine wood, and the effect increases with pressure for both. Carbon dioxide causes decreased carbon in the syngas of the Illinois coal, but there is no direct correlation with pressure. CO_2 also decreases carbon in the syngas from switchgrass at the low and middle pressures, but increases carbon in the syngas at the high pressure.

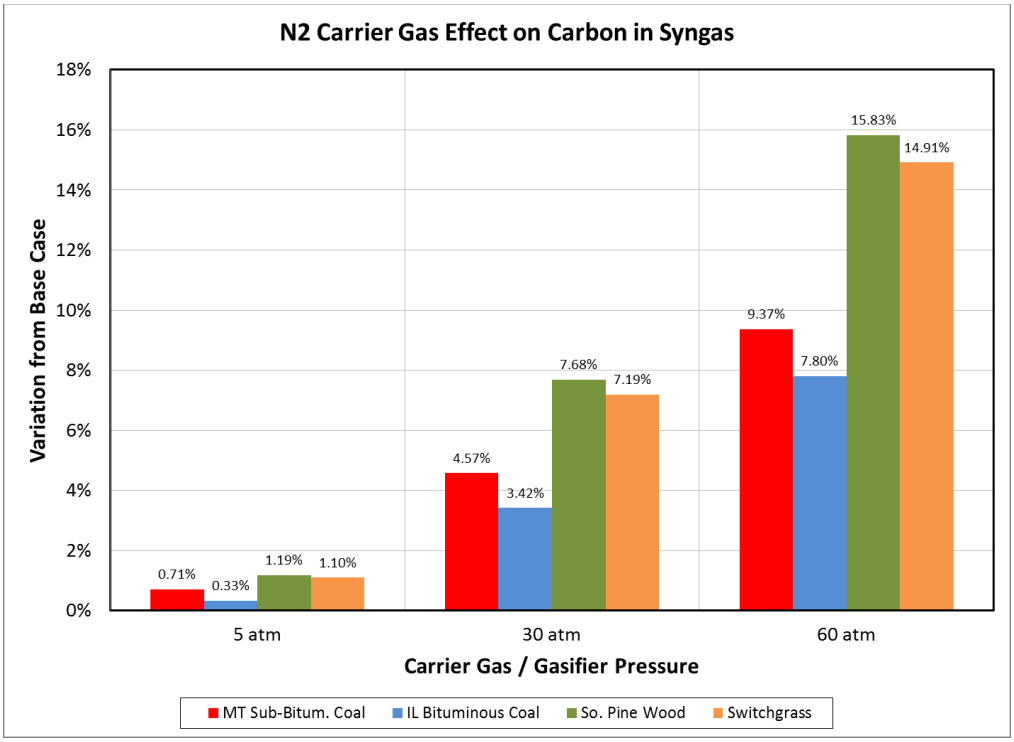

Figure 6.58 – N_2 carrier gas: pressure vs. carbon in syngas

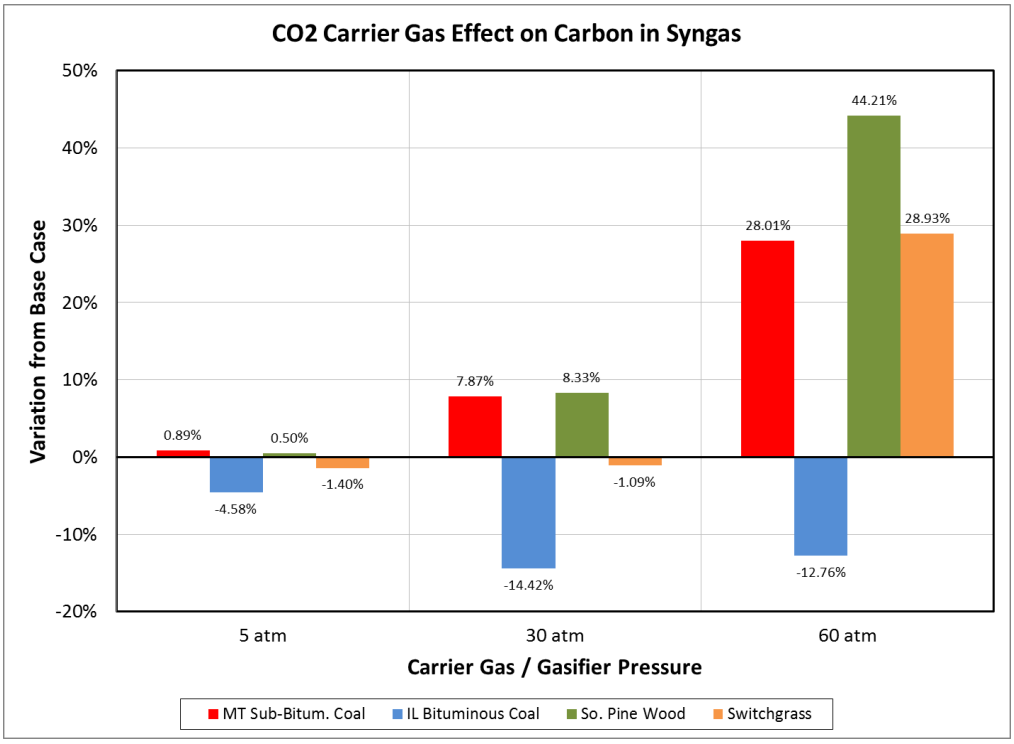

Figure 6.59 – CO_2 carrier gas: pressure vs. carbon in syngas

6.7.1.2 Carrier Gas Addition – Effect on H_2 in Syngas

Both nitrogen and carbon dioxide as a carrier gas decreases the flow of hydrogen in the syngas. Increasing pressure increases the effect for both gases. Overall, the effect of carbon dioxide is much greater than that of nitrogen.

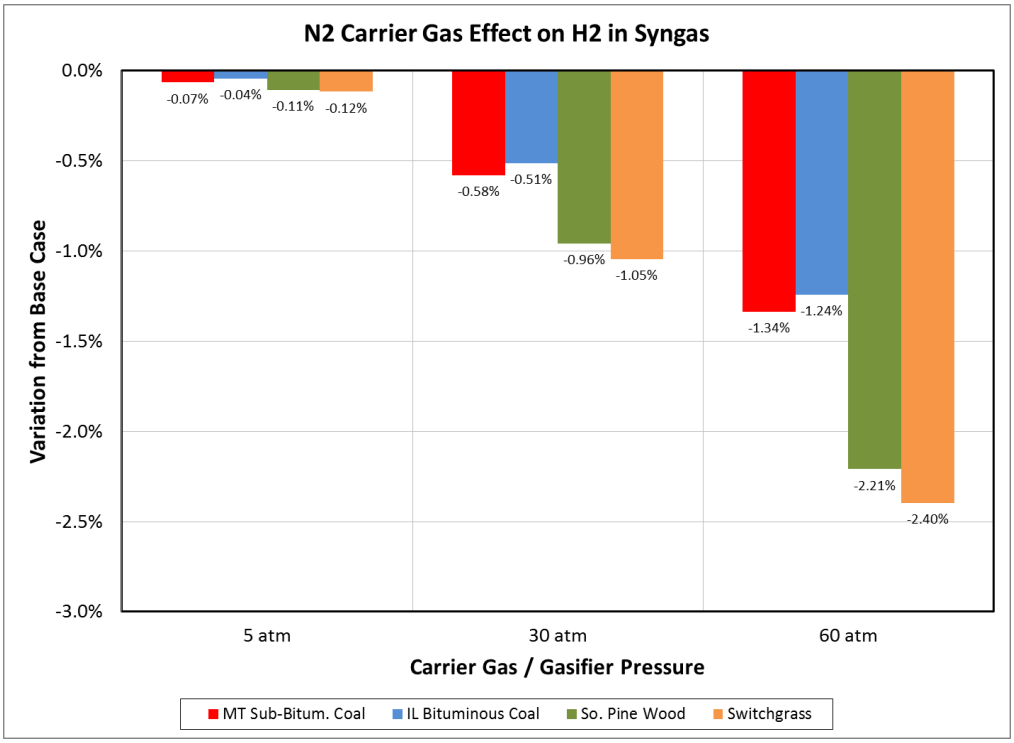

Figure 6.60 – N_2 carrier gas: pressure vs. H_2 in syngas

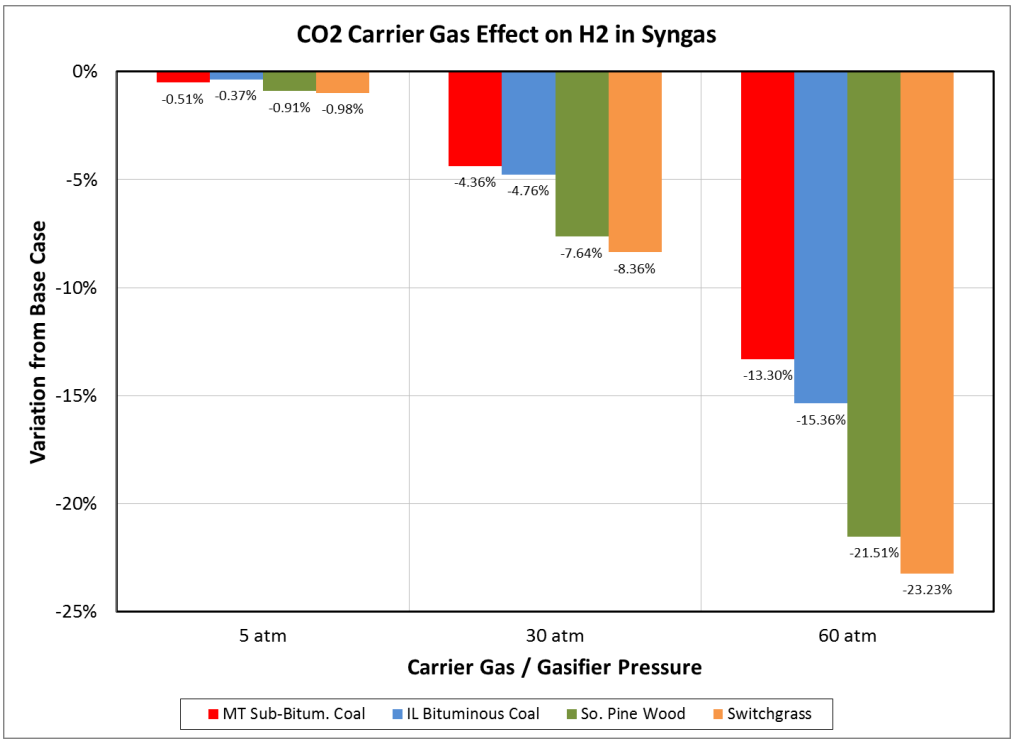

Figure 6.61 – CO_2 carrier gas: pressure vs. H_2 in syngas

6.7.1.3 Carrier Gas Addition – Effect on CO in Syngas

Nitrogen carrier gas causes less carbon monoxide to be present in the syngas, and the effect increases with increasing pressure. Using carbon dioxide as the carrier gas causes decreased COforthe Montana coal, with greater system pressures resulting in increasingly less CO in the syngas. Conversely, CO_2 carrier gas increases CO for the Illinois coal and both biomass feedstocks, with the magnitude of the effect showing a direct relationship to pressure for the Illinois coal and the switchgrass, but not for the Southern pine wood.

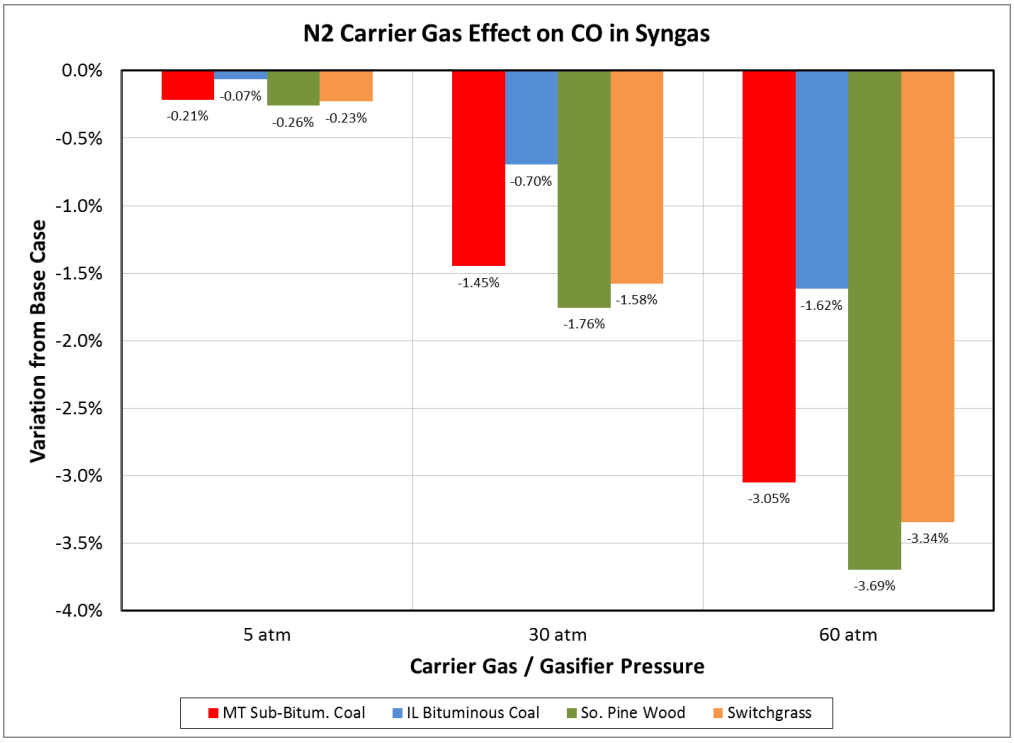

Figure 6.62 – N_2 carrier gas: pressure vs. CO in syngas

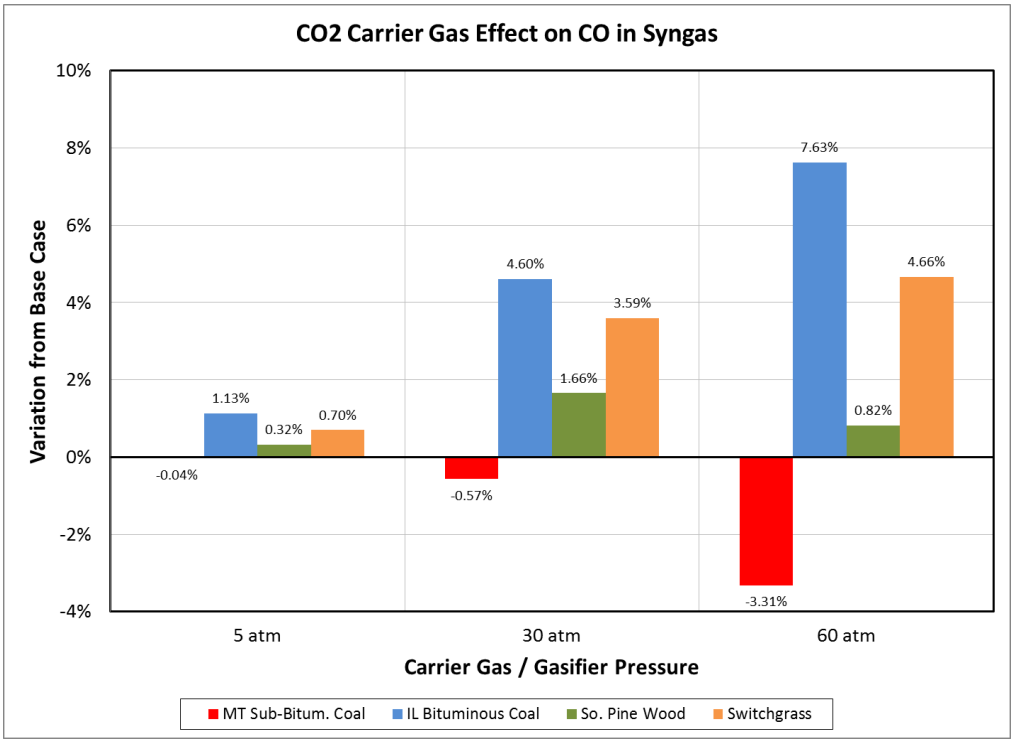

Figure 6.63 – CO_2 carrier gas: pressure vs. CO in syngas

6.7.1.4 Carrier Gas Addition – Effect on CO_2 in Syngas

Both nitrogen and carbon dioxide as a carrier gas increase the flow of carbon dioxide in the syngas. Increasing pressure increases the effect for both gases. Overall, the effect of carbon dioxide is much greater than that of nitrogen.

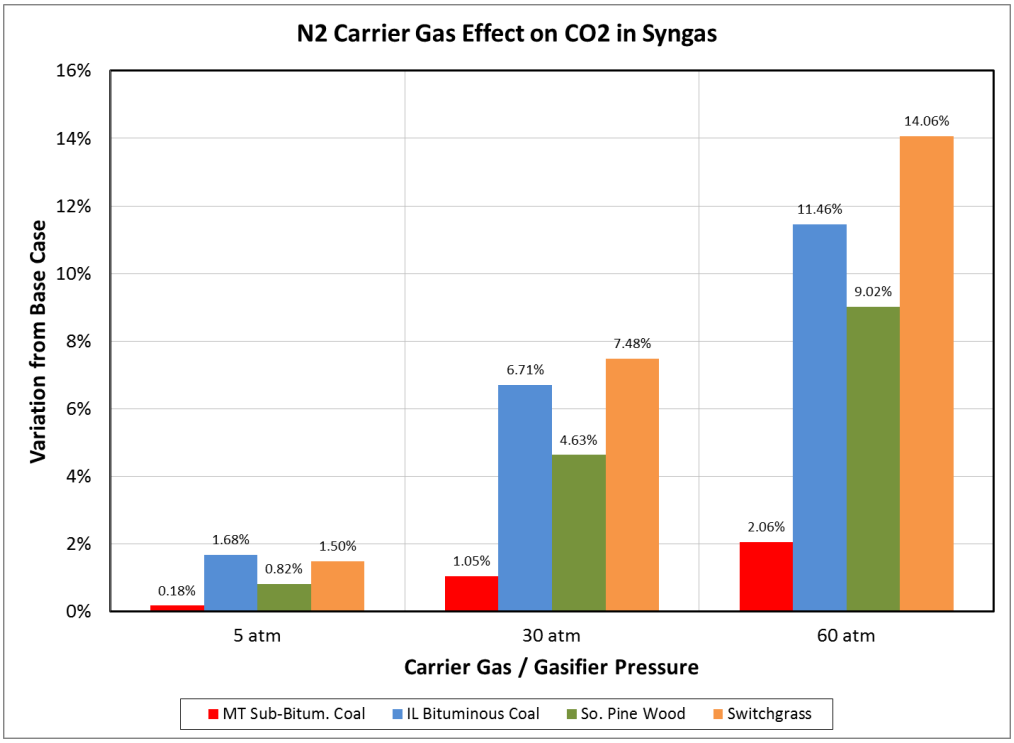

Figure 6.64 – N_2 carrier gas: pressure vs. CO_2 in syngas

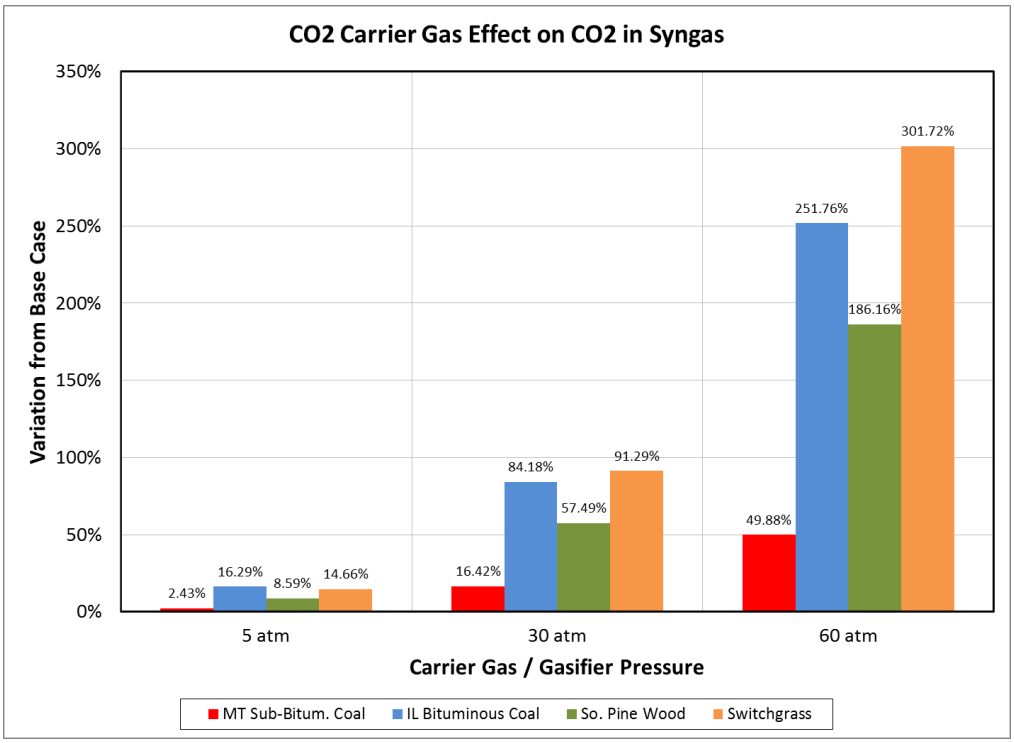

Figure 6.65 – CO_2 carrier gas: pressure vs. CO_2 in syngas

6.7.1.5 Carrier Gas Addition – Effect on CH_4 in Syngas

N_2 carrier gas increases the amount of methane in the syngas for all four feedstocks, with increasing pressure resulting in increased methane in the syngas. The same effect is seen for Illinois bituminous coal, Southern pine wood, and switchgrass when using CO_2 as the carrier gas. Using CO_2 causes a slight increase in methane in the syngas from Montana sub-bituminous coal at the low pressure, but causes increasingly lower flows of methane in the syngas at the middle and high pressures.

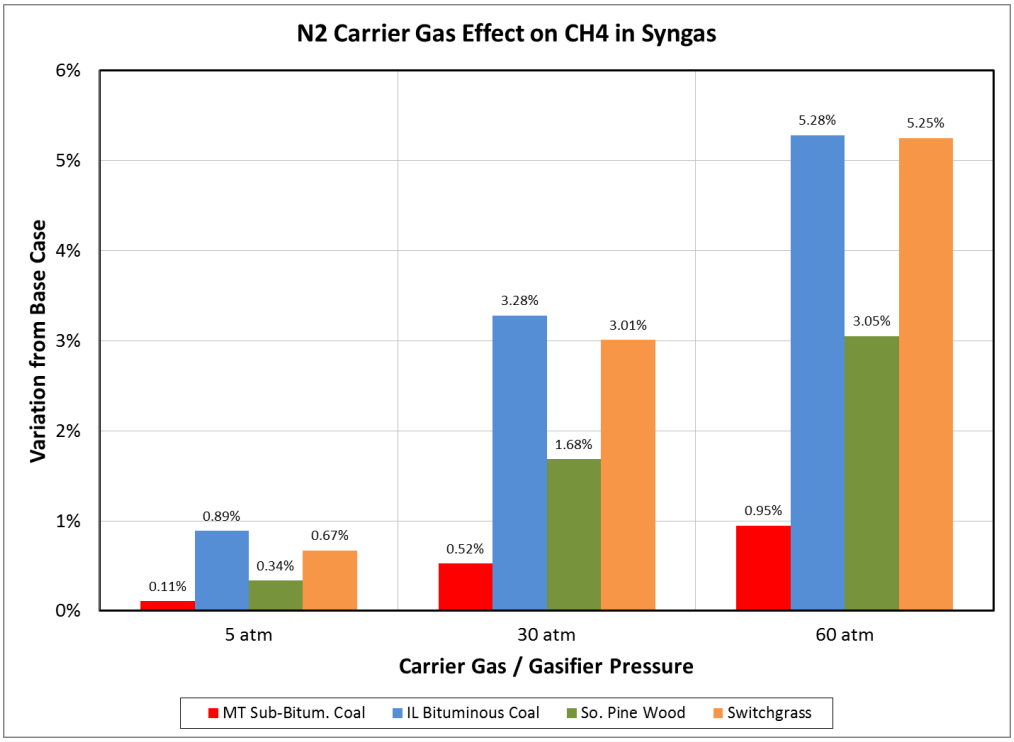

Figure 6.66 – N_2 carrier gas: pressure vs. CH_4 in syngas

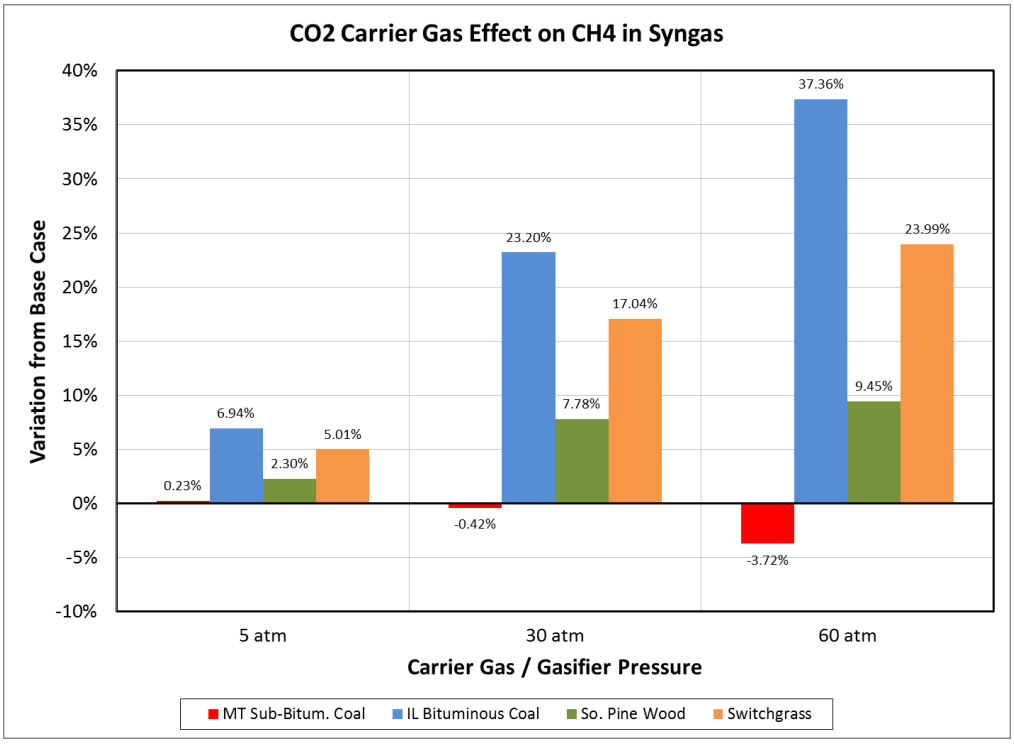

Figure 6.67 – CO_2 carrier gas: pressure vs. CH_4 in syngas

6.7.1.6 Carrier Gas Addition – Effect on H_2O in Syngas

Both nitrogen and carbon dioxide as a carrier gas increases the flow of water in the syngas. Increasing pressure increases the effect for both gases. Overall, the effect of carbon dioxide is much greater than that of nitrogen.

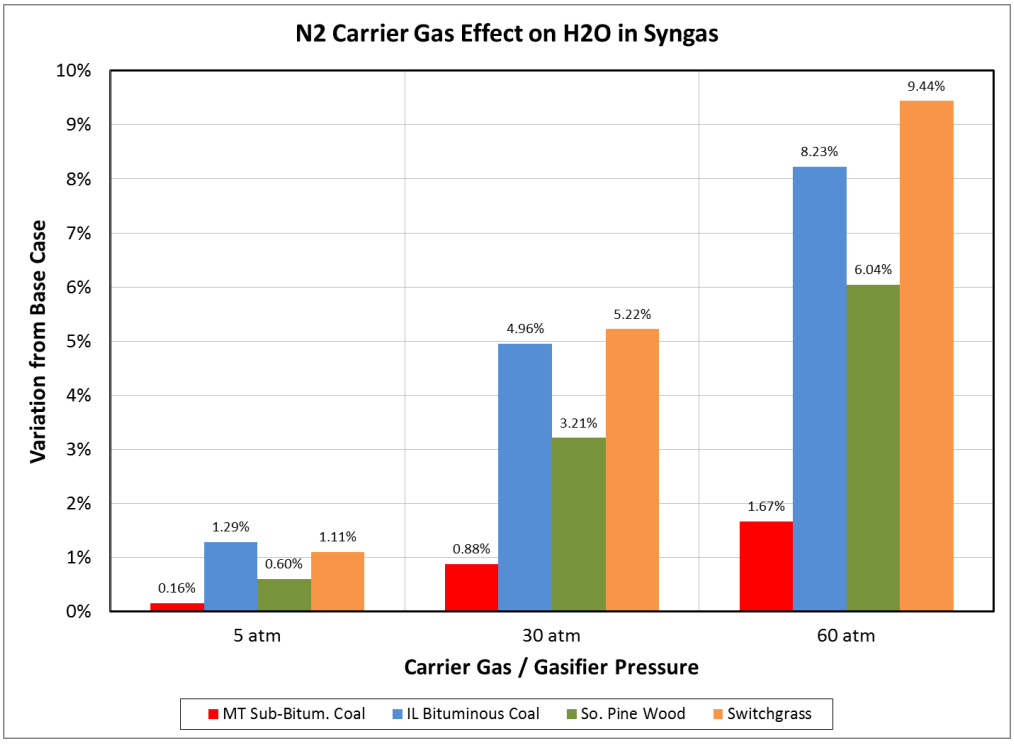

Figure 6.68 – N_2 carrier gas: pressure vs. H_2O in syngas

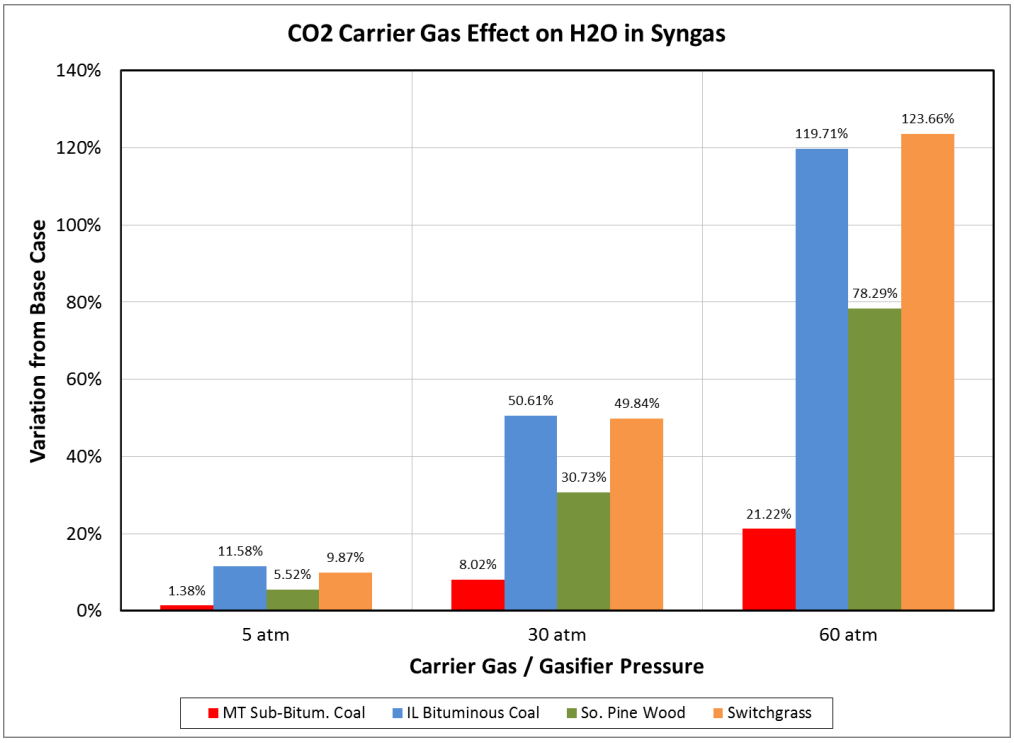

Figure 6.69 – CO_2 carrier gas: pressure vs. H_2O in syngas

6.7.1.7 Carrier Gas Addition – Effect on Gasifier Temperature

Both nitrogen and carbon dioxide as a carrier gas decreases the temperature of the gasifier. Increasing pressure increases the effect for both gases. Overall, the effect of carbon dioxide is much greater than that of nitrogen.

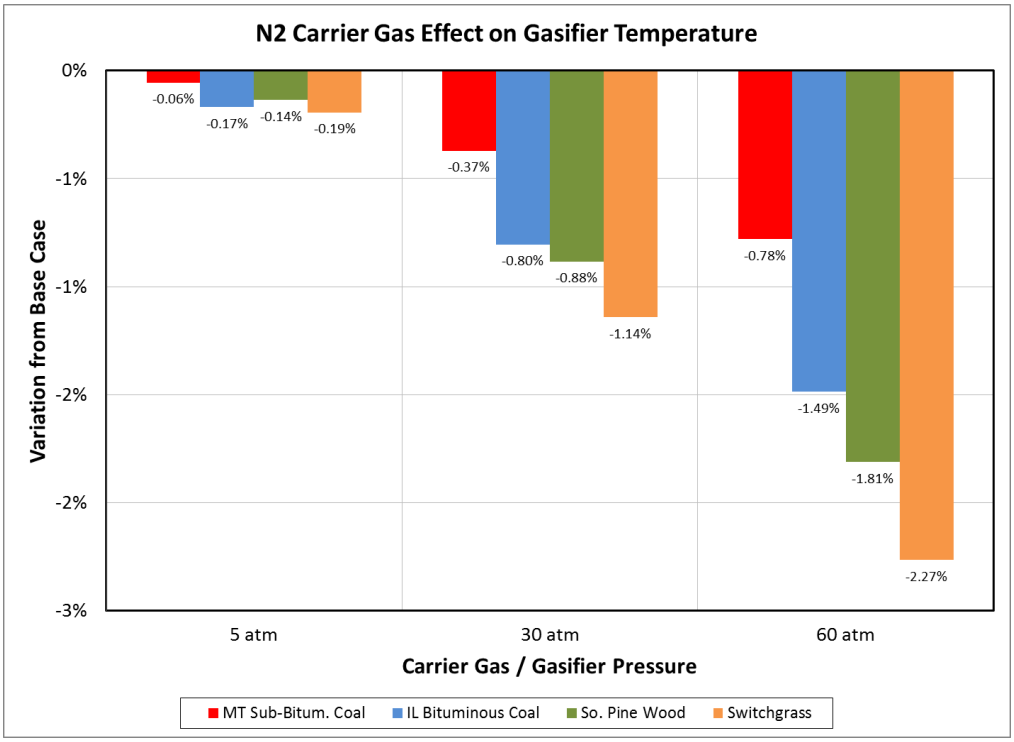

Figure 6.70 – N_2 carrier gas: pressure vs. gasifier temperature

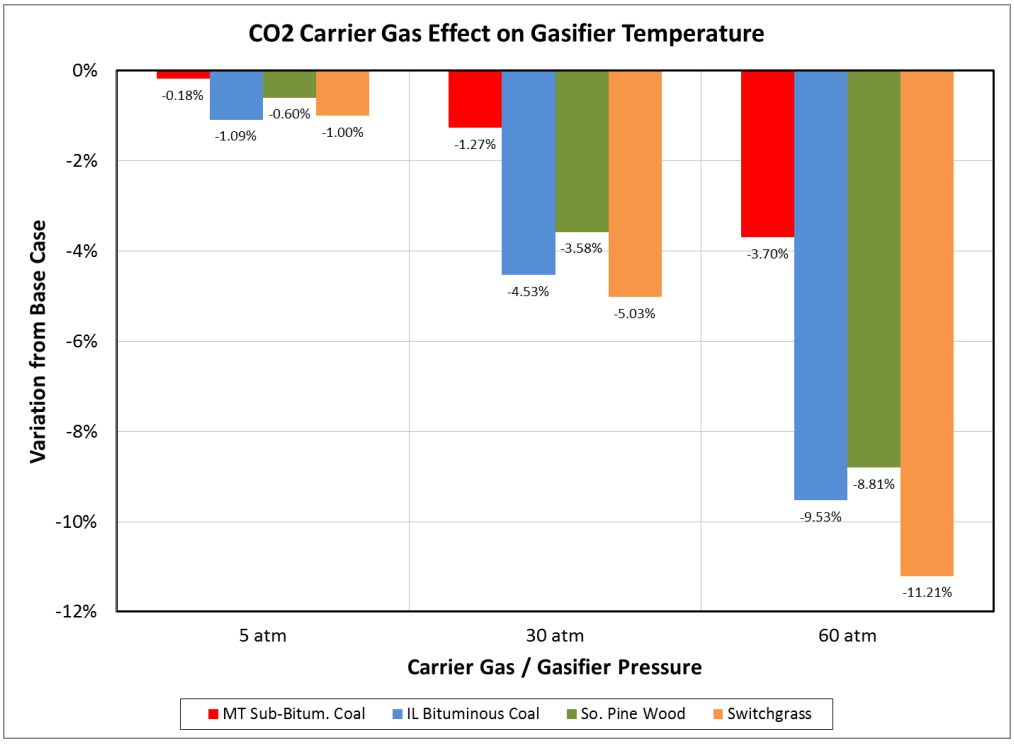

Figure 6.71 – CO_2 carrier gas: pressure vs. gasifier temperature

6.7.2 Carrier Gas Addition – Analysis

As seen in the results, the magnitude of the impact of including a carrier gas in the simulation of the dry-feed systems varies widely. Generally, nitrogen carrier gas has a much smaller impact than carbon dioxide carrier gas, and the impact of either gas on the system increases with increasing pressure. As an inert, the impact of nitrogen on the equilibrium compositions of the syngas product is limited to being a diluent, particularly in reducing gasifier temperature. Carbon dioxide, however, being a key reactant/product of the gasification system impacts the equilibrium of the various components directly.

Examining the two key desired products in the syngas, hydrogen and carbon monoxide, it follows that increasing carbon dioxide in the system would decrease the hydrogen in the product gas. Recall two previously listed reactions:

$$CO + H_2O \leftrightarrow CO_2 + H_2 \qquad (\Delta H = -41 \text{ kJ/mol}) \qquad (10)$$

$$C + 2\ H_2O \leftrightarrow CO_2 + 2\ H_2 \qquad (\Delta H = +90.1 \text{ kJ/mol}) \qquad (11)$$

These are the only two reactions that include both hydrogen and carbon dioxide. With both compounds being on the same side in both reactions, it follows that increasing carbon dioxide in the system would shift the reactions away from H_2 and CO_2.

Considering the impact of additional CO_2 on the CO in the syngas, recall the following reactions:

$$C + CO_2 \leftrightarrow 2\ CO \qquad (\Delta H = +172 \text{ kJ/mol}) \qquad (6)$$

$$CO + H_2O \leftrightarrow CO_2 + H_2 \qquad (\Delta H = -41 \text{ kJ/mol}) \qquad (10)$$

Again, these are the only two reversible reactions that include both carbon monoxide and carbon dioxide. As was previously stated when evaluating the impact of increasing CO_2 on H_2, the water-gas shift reaction (Eq. 10) shifts away from CO_2 and H_2 and thus toward CO and H_2O. Additionally, the Boudouard reaction (Eq. 6) also shifts toward CO with increasing CO_2. Therefore, the effect of increasing carbon dioxide as a carrier gas generally follows what would be expected, with the one exception of the impact on CO in the Montana sub-bituminous coal.

For both of the carrier gases, the increasing effect with increasing pressure is attributable to the larger mass of gas that is required to pressurize the feed to the higher gasifier pressures. No other studies of carrier gas effects were found in the literature to compare with the results.

6.7.3 Carrier Gas Addition – Implications

At first glance, omitting the carrier gas stream from the simulation of a dry-feed gasifier might seem to be a reasonable simplification, and indeed, when using nitrogen at lower pressures, such a simplification may be acceptable, but when using nitrogen at higher pressures or when using CO_2 at any pressure, the carrier gas stream should be included. Because this analysis was conducted later on in the research that is presented in this thesis, this approach is not reflected in the other results that are presented, but any future work on gasification modeling would do well to include the carrier gas due to its potentially significant effect on the material and energy balance of a gasification system.

6.8 Varying Sulfur Analysis Values

To evaluate the impact of the form of the sulfur in the sulfur-bearing feedstocks, a sensitivity analysis was conducted to vary the allocation of the sulfur between the potential types. Because only the coal feedstocks contain sulfur, the biomass feedstocks were not included in the sensitivity study. The coal feedstocks were evaluated at 30 atm in both dry-feed and slurry-feed configurations. For each feedstock, the AFR used was the value that resulted in 90% molar conversion with the original sulfur analysis values.

6.8.1 Varying Sulfur Analysis Values – Dry-Feed – Results

Qualitatively, the results from varying the sulfur analysis of the coal feedstocks in a dry-feed configuration are the same. Three different allocations of the sulfur in the feedstocks (1. Pyritic = 100%, Sulfates = 0%, Organic = 0%; 2. Pyritic = 0%, Sulfates = 0%, Organic = 100%; 3. Pyritic = 50%, Sulfates = 0%, Organic = 50%) result in

maximum values for H_2 and CO in the syngas and the maximum temperature of the gasifier. The same three allocations also result in minimum values for H_2O, CO_2, CH_4, and C in the syngas and the lowest value for decomposition energy. The allocation of 100% of the sulfur to the sulfate form causes the highest values of H_2O, CO_2, CH_4, and C in the syngas and the highest gasifier temperature while also causing the lowest values for H_2, CO, and gasifier temperature. The other combinations of the three forms of sulfur give mid-range values for each of the measured variables. The following tables show the results from the sensitivity analyses.

Montana Sub-Bituminous Coal (Dry-Feed @ Gasifier Pressure 5 atm)											
Case	Sulfur Fractions			Product Flow Rate						Decomp Energy	Gasifier Temp.
	Pyritic	Sulfate	Organic	H2	H2O	CO	CO2	CH4	C		
				(kmol/h)	(kmol/h)	(kmol/h)	(kmol/h)	(kmol/h)	(kmol/h)	(Gcal/h)	(°C)
1	100%	0%	0%	17.665	6.263	30.904	15.861	0.767	5.336	-1.490	727.76
2	0%	100%	0%	17.852	6.111	31.775	15.501	0.750	4.842	-1.465	731.51
3	0%	0%	100%	17.665	6.263	30.904	15.861	0.767	5.336	-1.490	727.76
4	50%	50%	0%	17.758	6.187	31.339	15.681	0.758	5.089	-1.477	729.64
5	50%	0%	50%	17.665	6.263	30.904	15.861	0.767	5.336	-1.490	727.76
6	0%	50%	50%	17.758	6.187	31.339	15.681	0.758	5.089	-1.477	729.64
7	33.3%	33.3%	33.3%	17.727	6.212	31.194	15.741	0.761	5.172	-1.482	729.01
Base	45.0%	10.0%	45.0%	17.683	6.248	30.991	15.825	0.765	5.287	-1.488	728.14

Table 6.5 – MTC: sulfur fractions vs. syngas component flows (dry-feed, 5 atm)

Montana Sub-Bituminous Coal (Dry-Feed @ Gasifier Pressure 30 atm)											
Case	Sulfur Fractions			Product Flow Rate						Decomp Energy	Gasifier Temp.
	Pyritic	Sulfate	Organic	H2	H2O	CO	CO2	CH4	C		
				(kmol/h)	(kmol/h)	(kmol/h)	(kmol/h)	(kmol/h)	(kmol/h)	(Gcal/h)	(°C)
1	100%	0%	0%	14.688	8.163	29.315	16.931	1.289	5.333	-1.490	814.65
2	0%	100%	0%	14.885	8.008	30.131	16.600	1.269	4.868	-1.465	818.91
3	0%	0%	100%	14.688	8.163	29.315	16.931	1.289	5.333	-1.490	814.65
4	50%	50%	0%	14.786	8.085	29.722	16.766	1.279	5.101	-1.477	816.78
5	50%	0%	50%	14.688	8.163	29.315	16.931	1.289	5.333	-1.490	814.65
6	0%	50%	50%	14.786	8.085	29.722	16.766	1.279	5.101	-1.477	816.78
7	33.3%	33.3%	33.3%	14.754	8.111	29.586	16.821	1.283	5.178	-1.482	816.07
Base	45.0%	10.0%	45.0%	14.707	8.148	29.396	16.898	1.287	5.287	-1.488	815.08

Table 6.6 – MTC: sulfur fractions vs. syngas component flows (dry-feed, 30 atm)

Montana Sub-Bituminous Coal (Dry-Feed @ Gasifier Pressure 60 atm)											
Case	Sulfur Fractions			Product Flow Rate						Decomp Energy	Gasifier Temp.
	Pyritic	Sulfate	Organic	H2	H2O	CO	CO2	CH4	C		
				(kmol/h)	(kmol/h)	(kmol/h)	(kmol/h)	(kmol/h)	(kmol/h)	(Gcal/h)	(°C)
1	100%	0%	0%	13.390	8.977	28.468	17.547	1.520	5.332	-1.490	851.17
2	0%	100%	0%	13.585	8.824	29.262	17.227	1.500	4.880	-1.465	855.67
3	0%	0%	100%	13.390	8.977	28.468	17.547	1.520	5.332	-1.490	851.17
4	50%	50%	0%	13.487	8.901	28.865	17.388	1.510	5.106	-1.477	853.42
5	50%	0%	50%	13.390	8.977	28.468	17.547	1.520	5.332	-1.490	851.17
6	0%	50%	50%	13.487	8.901	28.865	17.388	1.510	5.106	-1.477	853.42
7	33.3%	33.3%	33.3%	13.455	8.926	28.732	17.441	1.513	5.181	-1.482	852.67
Base	45.0%	10.0%	45.0%	13.409	8.962	28.548	17.516	1.518	5.287	-1.488	851.62

Table 6.7 – MTC: sulfur fractions vs. syngas component flows (dry-feed, 60 atm)

Illinois Bituminous Coal (Dry-Feed @ Gasifier Pressure 5 atm)											
Case	Sulfur Fractions			Product Flow Rate						Decomp Energy	Gasifier Temp.
	Pyritic	Sulfate	Organic	H2	H2O	CO	CO2	CH4	C		
				(kmol/h)	(kmol/h)	(kmol/h)	(kmol/h)	(kmol/h)	(kmol/h)	(Gcal/h)	(°C)
1	100%	0%	0%	22.921	0.583	47.946	0.772	0.153	5.501	-0.087	984.92
2	0%	100%	0%	23.228	0.366	48.842	0.432	0.109	4.990	0.003	1036.92
3	0%	0%	100%	22.921	0.583	47.946	0.772	0.153	5.501	-0.087	984.92
4	50%	50%	0%	23.088	0.464	48.448	0.581	0.130	5.215	-0.042	1010.05
5	50%	0%	50%	22.921	0.583	47.946	0.772	0.153	5.501	-0.087	984.92
6	0%	50%	50%	23.088	0.464	48.448	0.581	0.130	5.215	-0.042	1010.05
7	33.3%	33.3%	33.3%	23.036	0.501	48.293	0.639	0.137	5.303	-0.057	1001.47
Base	45.0%	10.0%	45.0%	22.957	0.557	48.056	0.730	0.148	5.438	-0.078	989.79

Table 6.8 – ILC: sulfur fractions vs. syngas component flows (dry-feed, 5 atm)

Illinois Bituminous Coal (Dry-Feed @ Gasifier Pressure 30 atm)											
Case	Sulfur Fractions			Product Flow Rate						Decomp Energy	Gasifier Temp.
	Pyritic	Sulfate	Organic	H2	H2O	CO	CO2	CH4	C		
				(kmol/h)	(kmol/h)	(kmol/h)	(kmol/h)	(kmol/h)	(kmol/h)	(Gcal/h)	(°C)
1	100%	0%	0%	21.226	1.612	46.461	1.901	0.476	5.534	-0.087	1055.13
2	0%	100%	0%	21.803	1.217	47.998	1.330	0.386	4.658	0.003	1094.38
3	0%	0%	100%	21.226	1.612	46.461	1.901	0.476	5.534	-0.087	1055.13
4	50%	50%	0%	21.523	1.407	47.271	1.599	0.430	5.073	-0.042	1074.09
5	50%	0%	50%	21.226	1.612	46.461	1.901	0.476	5.534	-0.087	1055.13
6	0%	50%	50%	21.523	1.407	47.271	1.599	0.430	5.073	-0.042	1074.09
7	33.3%	33.3%	33.3%	21.426	1.474	47.010	1.696	0.445	5.221	-0.057	1067.63
Base	45.0%	10.0%	45.0%	21.287	1.570	46.630	1.838	0.466	5.438	-0.078	1058.82

Table 6.9 – ILC: sulfur fractions vs. syngas component flows (dry-feed, 30 atm)

Illinois Bituminous Coal (Dry-Feed @ Gasifier Pressure 60 atm)											
Case	Sulfur Fractions			Product Flow Rate						Decomp Energy	Gasifier Temp.
	Pyritic	Sulfate	Organic	H2	H2O	CO	CO2	CH4	C		
				(kmol/h)	(kmol/h)	(kmol/h)	(kmol/h)	(kmol/h)	(kmol/h)	(Gcal/h)	(°C)
1	100%	0%	0%	20.189	2.225	45.635	2.516	0.678	5.543	-0.087	1090.35
2	0%	100%	0%	20.848	1.777	47.350	1.883	0.575	4.565	0.003	1125.91
3	0%	0%	100%	20.189	2.225	45.635	2.516	0.678	5.543	-0.087	1090.35
4	50%	50%	0%	20.525	1.995	46.526	2.186	0.626	5.035	-0.042	1107.61
5	50%	0%	50%	20.189	2.225	45.635	2.516	0.678	5.543	-0.087	1090.35
6	0%	50%	50%	20.525	1.995	46.526	2.186	0.626	5.035	-0.042	1107.61
7	33.3%	33.3%	33.3%	20.414	2.070	46.236	2.293	0.644	5.200	-0.057	1101.74
Base	45.0%	10.0%	45.0%	20.257	2.178	45.818	2.448	0.668	5.438	-0.078	1093.72

Table 6.10 – ILC: sulfur fractions vs. syngas component flows (dry-feed, 60 atm)

6.8.2 Varying Sulfur Analysis Values – Slurry-Feed – Results

Qualitatively, the results from varying the sulfur analysis of the coal feedstocks in a slurry-feed configuration are the same as the dry-feed configuration. Three different allocations of the sulfur in the feedstocks (1. Pyritic = 100%, Sulfates = 0%, Organic = 0%; 2. Pyritic = 0%, Sulfates = 0%, Organic = 100%; 3. Pyritic = 50%, Sulfates = 0%, Organic = 50%) cause maximum values for H_2 and CO in the syngas and the maximum

temperature of the gasifier. The same three allocations also result in minimum values for H_2O, CO_2, CH_4, and C in the syngas and the lowest value for decomposition energy. The allocation of 100% of the sulfur to the sulfate form results in the highest values of H_2O, CO_2, CH_4, and C in the syngas and the highest gasifier temperature while also causing the lowest values for H_2, CO, and gasifier temperature. The other combinations of the three forms of sulfur result in mid-range values for each of the measured variables. The following tables show the results from the sensitivity analyses.

Montana Sub-Bituminous Coal (Slurry-Feed @ Gasifier Pressure 5 atm)											
Case	Sulfur Fractions			Product Flow Rate						Decomp Energy	Gasifier Temp.
	Pyritic	Sulfate	Organic	H2	H2O	CO	CO2	CH4	C		
				(kmol/h)	(kmol/h)	(kmol/h)	(kmol/h)	(kmol/h)	(kmol/h)	(Gcal/h)	(°C)
1	100%	0%	0%	22.985	19.141	15.633	28.952	3.547	4.736	-1.490	635.62
2	0%	100%	0%	23.385	18.862	16.336	28.740	3.487	4.305	-1.465	639.38
3	0%	0%	100%	22.985	19.141	15.633	28.952	3.547	4.736	-1.490	635.62
4	50%	50%	0%	23.186	19.001	15.983	28.847	3.517	4.521	-1.477	637.51
5	50%	0%	50%	22.985	19.141	15.633	28.952	3.547	4.736	-1.490	635.62
6	0%	50%	50%	23.186	19.001	15.983	28.847	3.517	4.521	-1.477	637.51
7	33.3%	33.3%	33.3%	23.119	19.048	15.866	28.882	3.527	4.593	-1.482	636.88
Base	45.0%	10.0%	45.0%	23.025	19.113	15.703	28.931	3.541	4.693	-1.488	636

Table 6.11 – MTC: sulfur fractions vs. syngas component flows (slurry-feed, 5 atm)

Montana Sub-Bituminous Coal (Slurry-Feed @ Gasifier Pressure 30 atm)											
Case	Sulfur Fractions			Product Flow Rate						Decomp Energy	Gasifier Temp.
	Pyritic	Sulfate	Organic	H2	H2O	CO	CO2	CH4	C		
				(kmol/h)	(kmol/h)	(kmol/h)	(kmol/h)	(kmol/h)	(kmol/h)	(Gcal/h)	(°C)
1	100%	0%	0%	17.732	21.660	15.469	29.000	4.882	3.517	-1.490	713.14
2	0%	100%	0%	18.087	21.414	16.137	28.789	4.827	3.115	-1.465	717.44
3	0%	0%	100%	17.732	21.660	15.469	29.000	4.882	3.517	-1.490	713.14
4	50%	50%	0%	17.910	21.537	15.802	28.895	4.854	3.317	-1.477	715.3
5	50%	0%	50%	17.732	21.660	15.469	29.000	4.882	3.517	-1.490	713.14
6	0%	50%	50%	17.910	21.537	15.802	28.895	4.854	3.317	-1.477	715.3
7	33.3%	33.3%	33.3%	17.851	21.577	15.691	28.930	4.863	3.384	-1.482	714.58
Base	45.0%	10.0%	45.0%	17.768	21.635	15.536	28.979	4.876	3.477	-1.488	713.57

Table 6.12 – MTC: sulfur fractions vs. syngas component flows (slurry-feed, 30 atm)

Montana Sub-Bituminous Coal (Slurry-Feed @ Gasifier Pressure 60 atm)											
Case	Sulfur Fractions			Product Flow Rate						Decomp Energy	Gasifier Temp.
	Pyritic	Sulfate	Organic	H2	H2O	CO	CO2	CH4	C		
				(kmol/h)	(kmol/h)	(kmol/h)	(kmol/h)	(kmol/h)	(kmol/h)	(Gcal/h)	(°C)
1	100%	0%	0%	15.734	22.641	15.191	29.249	5.369	3.059	-1.490	745.35
2	0%	100%	0%	16.064	22.410	15.841	29.040	5.320	2.668	-1.465	749.91
3	0%	0%	100%	15.734	22.641	15.191	29.249	5.369	3.059	-1.490	745.35
4	50%	50%	0%	15.899	22.525	15.515	29.145	5.344	2.864	-1.477	747.64
5	50%	0%	50%	15.734	22.641	15.191	29.249	5.369	3.059	-1.490	745.35
6	0%	50%	50%	15.899	22.525	15.515	29.145	5.344	2.864	-1.477	747.64
7	33.3%	33.3%	33.3%	15.844	22.564	15.407	29.180	5.353	2.929	-1.482	746.88
Base	45.0%	10.0%	45.0%	15.767	22.618	15.256	29.228	5.364	3.020	-1.488	745.81

Table 6.13 – MTC: sulfur fractions vs. syngas component flows (slurry-feed, 60 atm)

Illinois Bituminous Coal (Slurry-Feed @ Gasifier Pressure 5 atm)											
Case	Sulfur Fractions			Product Flow Rate						Decomp Energy	Gasifier Temp.
	Pyritic	Sulfate	Organic	H2	H2O	CO	CO2	CH4	C		
				(kmol/h)	(kmol/h)	(kmol/h)	(kmol/h)	(kmol/h)	(kmol/h)	(Gcal/h)	(°C)
1	100%	0%	0%	33.398	9.807	36.178	13.939	2.183	2.073	-0.087	751.89
2	0%	100%	0%	34.478	9.034	39.145	12.842	2.030	0.356	0.003	763.91
3	0%	0%	100%	33.398	9.807	36.178	13.939	2.183	2.073	-0.087	751.89
4	50%	50%	0%	33.942	9.418	37.660	13.392	2.106	1.215	-0.042	757.89
5	50%	0%	50%	33.398	9.807	36.178	13.939	2.183	2.073	-0.087	751.89
6	0%	50%	50%	33.942	9.418	37.660	13.392	2.106	1.215	-0.042	757.89
7	33.3%	33.3%	33.3%	33.761	9.547	37.166	13.575	2.131	1.501	-0.057	755.89
Base	45.0%	10.0%	45.0%	33.507	9.729	36.474	13.830	2.167	1.901	-0.078	753.09

Table 6.14 – ILC: sulfur fractions vs. syngas component flows (slurry-feed, 5 atm)

Illinois Bituminous Coal (Slurry-Feed @ Gasifier Pressure 30 atm)											
Case	Sulfur Fractions			Product Flow Rate						Decomp Energy	Gasifier Temp.
	Pyritic	Sulfate	Organic	H2	H2O	CO	CO2	CH4	C		
				(kmol/h)	(kmol/h)	(kmol/h)	(kmol/h)	(kmol/h)	(kmol/h)	(Gcal/h)	(°C)
1	100%	0%	0%	27.887	12.435	34.553	14.339	3.593	1.888	-0.087	847.67
2	0%	100%	0%	29.042	11.648	37.333	13.342	3.410	0.287	0.003	861.43
3	0%	0%	100%	27.887	12.435	34.553	14.339	3.593	1.888	-0.087	847.67
4	50%	50%	0%	28.466	12.041	35.941	13.842	3.501	1.088	-0.042	854.55
5	50%	0%	50%	27.887	12.435	34.553	14.339	3.593	1.888	-0.087	847.67
6	0%	50%	50%	28.466	12.041	35.941	13.842	3.501	1.088	-0.042	854.55
7	33.3%	33.3%	33.3%	28.274	12.172	35.478	14.008	3.532	1.355	-0.057	852.26
Base	45.0%	10.0%	45.0%	28.004	12.356	34.830	14.240	3.575	1.729	-0.078	849.05

Table 6.15 – ILC: sulfur fractions vs. syngas component flows (slurry-feed, 30 atm)

Illinois Bituminous Coal (Slurry-Feed @ Gasifier Pressure 60 atm)											
Case	Sulfur Fractions			Product Flow Rate						Decomp Energy	Gasifier Temp.
	Pyritic	Sulfate	Organic	H2	H2O	CO	CO2	CH4	C		
				(kmol/h)	(kmol/h)	(kmol/h)	(kmol/h)	(kmol/h)	(kmol/h)	(Gcal/h)	(°C)
1	100%	0%	0%	25.546	13.530	33.834	14.658	4.195	1.685	-0.087	889.04
2	0%	100%	0%	26.691	12.753	36.544	13.692	4.012	0.124	0.003	903.62
3	0%	0%	100%	25.546	13.530	33.834	14.658	4.195	1.685	-0.087	889.04
4	50%	50%	0%	26.119	13.141	35.188	14.176	4.104	0.905	-0.042	896.33
5	50%	0%	50%	25.546	13.530	33.834	14.658	4.195	1.685	-0.087	889.04
6	0%	50%	50%	26.119	13.141	35.188	14.176	4.104	0.905	-0.042	896.33
7	33.3%	33.3%	33.3%	25.928	13.270	34.736	14.337	4.134	1.165	-0.057	893.9
Base	45.0%	10.0%	45.0%	25.660	13.452	34.105	14.562	4.177	1.529	-0.078	890.5

Table 6.16 – ILC: sulfur fractions vs. syngas component flows (slurry-feed, 60 atm)

6.8.3 Varying Sulfur Analysis Values – Dry-Feed & Slurry-Feed – Results

The following table shows how the maximum increase and maximum decrease of the various variables from the sensitivity analysis of the form of sulfur in the feedstock relate to the base case. The Illinois bituminous coal shows a much greater response to varying the form of the sulfur than does the Montana sub-bituminous coal.

Feedstock	Gasifier Pressure (atm)	Feed Config.	Max/Min	Product Flow Rates						Gasifier Temp.
				H2	H2O	CO	CO2	CH4	CARBON	
MT Sub-Bitum. Coal	5	Dry	Max	0.95%	0.24%	2.53%	0.23%	0.23%	0.93%	0.46%
MT Sub-Bitum. Coal	5	Dry	Min	-0.11%	-2.19%	-0.28%	-2.04%	-2.04%	-8.41%	-0.05%
MT Sub-Bitum. Coal	5	Slurry	Max	1.56%	0.15%	4.03%	0.07%	0.17%	0.91%	0.53%
MT Sub-Bitum. Coal	5	Slurry	Min	-0.17%	-1.31%	-0.45%	-0.66%	-1.53%	-8.27%	-0.06%
MT Sub-Bitum. Coal	30	Dry	Max	1.21%	0.19%	2.50%	0.20%	0.16%	0.88%	0.47%
MT Sub-Bitum. Coal	30	Dry	Min	-0.13%	-1.72%	-0.28%	-1.76%	-1.45%	-7.92%	-0.05%
MT Sub-Bitum. Coal	30	Slurry	Max	1.79%	0.11%	3.87%	0.07%	0.11%	1.15%	0.54%
MT Sub-Bitum. Coal	30	Slurry	Min	-0.20%	-1.02%	-0.43%	-0.66%	-1.00%	-10.41%	-0.06%
MT Sub-Bitum. Coal	60	Dry	Max	1.31%	0.17%	2.50%	0.18%	0.14%	0.85%	0.48%
MT Sub-Bitum. Coal	60	Dry	Min	-0.15%	-1.54%	-0.28%	-1.64%	-1.23%	-7.70%	-0.05%
MT Sub-Bitum. Coal	60	Slurry	Max	1.88%	0.10%	3.84%	0.07%	0.09%	1.29%	0.55%
MT Sub-Bitum. Coal	60	Slurry	Min	-0.21%	-0.92%	-0.42%	-0.64%	-0.83%	-11.66%	-0.06%
IL Bitum. Coal	5	Dry	Max	1.18%	4.57%	1.64%	5.74%	3.36%	1.15%	4.76%
IL Bitum. Coal	5	Dry	Min	-0.15%	-34.23%	-0.23%	-40.81%	-26.82%	-8.25%	-0.49%
IL Bitum. Coal	5	Slurry	Max	2.90%	0.80%	7.32%	0.79%	0.72%	9.02%	1.44%
IL Bitum. Coal	5	Slurry	Min	-0.33%	-7.14%	-0.81%	-7.15%	-6.35%	-81.27%	-0.16%
IL Bitum. Coal	30	Dry	Max	2.42%	2.69%	2.93%	3.43%	1.98%	1.77%	3.36%
IL Bitum. Coal	30	Dry	Min	-0.29%	-22.46%	-0.36%	-27.62%	-17.22%	-14.34%	-0.35%
IL Bitum. Coal	30	Slurry	Max	3.71%	0.64%	7.19%	0.70%	0.51%	9.25%	1.46%
IL Bitum. Coal	30	Slurry	Min	-0.41%	-5.73%	-0.80%	-6.30%	-4.59%	-83.40%	-0.16%
IL Bitum. Coal	60	Dry	Max	2.91%	2.15%	3.34%	2.78%	1.57%	1.92%	2.94%
IL Bitum. Coal	60	Dry	Min	-0.34%	-18.42%	-0.40%	-23.08%	-13.91%	-16.06%	-0.31%
IL Bitum. Coal	60	Slurry	Max	4.01%	0.58%	7.15%	0.66%	0.44%	10.19%	1.47%
IL Bitum. Coal	60	Slurry	Min	-0.45%	-5.20%	-0.79%	-5.98%	-3.94%	-91.90%	-0.16%

Table 6.17 – MTC & ILC: summary of effects from varying sulfur fractions

6.8.4 Varying Sulfur Analysis Values – Analysis

Because sulfur components play a very minimal role in the overall system material balance, the main impact of varying the sulfur is on the required decomposition energy. Because of the energy stream connecting the DECOMP and GASIFIER blocks in the simulations (see Section 4.7), any energy not used in decomposing the feedstock to its constituent components is used to raise the temperature of the gasifier; thus, any impacts to the composition of the syngas product are related to the temperature change the occurs in the gasifier as the type of sulfur is varied.

6.8.5 Varying Sulfur Analysis Values – Implications

As seen in the results, adjusting the distribution of the sulfur in a feedstock between the pyritic, organic, and sulfate forms can dramatically impact the composition of the syngas product; thus, for accurately evaluating potential feedstocks using equilibrium modeling, the sulfur analysis should be performed. This can pose challenges when attempting to use feedstock characterizations from literature, which often do not contain an analysis of the sulfur content. Thus, for future work in gasification modeling, it is important to obtain a sulfur analysis for any potential feedstock and incorporate it into the modeling effort.

6.9 Additional Simulations

Only a portion of the sensitivity analyses that were conducted are presented in this thesis. In addition to the results that were presented for the carrier gas study (Section 6.7), additional data showing the effects of different blends of carrier gas (N_2/CO_2) is available. Two additional studies were also carried out for both dry-feed and slurry-feed configurations. Studies evaluating the effects of increasing oxygen content of the combustion air and the effects of recycling carbon dioxide back to the gasifier were conducted. Additionally, for every sensitivity study that was performed, the study was conducted at low, medium, and high pressure (5 atm, 30 atm, and 60 atm), although only the medium pressure results are presented in this thesis when pressure itself was not a variable. In all, over 150 sensitivity analyses were performed. To aid any future researchers who might wish to review the data, it will be kept on file with Auburn University's Department of Chemical Engineering.

7. Conclusions & Future Work

From the results and analyses that have been presented in this thesis, several key points can be concluded regarding the nature of equilibrium modeling of gasification:

1) Any attempt to perform a parametric analysis using a gasification model should account for the impact of the air-to-fuel ratio (sometimes referred to as "equivalence ratio" in other sources). In non-air systems (e.g. oxygen-enriched), the concept still holds. The evaluation of any of the gasification system parameters should also include varying the rate at which the oxidant is introduced to this system. This will aid in determining whether any observed impacts from the other variable are localized to a particular region of the air-to-fuel relationship, or if they generally hold across the entire range of the gasification region.

2) Additional work is needed in the area of developing simple modifications to equilibrium models to account for the actual approach to equilibrium of various configurations (e.g. fluidized bed) for use in feasibility studies. This will make commercial modeling of gasification more accurate without resorting to kinetic models, which are significantly less accessible.

3) Additional work is needed in accounting for the heat of formation of the feedstocks in gasification models.

4) For dry-feed systems, the carrier gas should not be neglected when creating a model, particularly at higher pressures. Further work in the area of selecting a carrier gas for various dry-feed gasifier configurations, including the possibility of blended carrier gases (e.g. N_2/CO_2), is also recommended.

5) For sulfur-bearing feedstocks, the impact of the form of the sulfur is not insignificant. Proximate and ultimate analysis data, along with the higher heating value, are readily available for many potential feedstocks from published literature. What is often lacking, however, is the sulfur analysis that accompanies these analyses. Thus, it would benefit the gasification research community in general to conduct a sulfur analysis on any feedstock in consideration and present this data along with the other standard three pieces of data. This will allow for greater ease of use by others.

Additionally, considering gasification research as a whole, when publishing the analysis data for a potential feedstock, the dry-basis values should always be presented with the as-received values. This will allow future researchers to more readily compare various feedstocks. Lastly, though not directly related to the work presented in this thesis, the development of "package" gasifiers might allow for power generation and/or fuel production in remote areas where traditional fuels may be scarce but biomass is abundant.

References

Adhikari, S. *Biomass Gasification*. January 26, 2010.

Ariyapadi, S., Shires, P., Bhargava, M., & Ebbern, D. KBR's Transport Gasifier (TRIG™) – An Advanced Gasification Technology for SNG Production from Low-Rank Coals. Presented at: Twenty-fifth Annual International Pittsburgh Coal Conference. September 29-October 2, 2008, Pittsburgh, Pennsylvania.

Aspen Technology, Inc. *Aspen Plus® v8.4*.

Azzone, E., Morini, M., & Pinelli, M. (2012) Development of an equilibrium model for the simulation of thermochemical gasification and application to agricultural residues. *Renewable Energy.* 46, pp.248-254. DOI:10.1016/j.renene.2012.03.017

Barman, N. S., Ghosh, S., & De, S. (2012). Gasification of biomass in a fixed bed downdraft gasifier – A realistic model including tar. *Bioresource Technology.* 107, pp.505-511. DOI:10.1016/j.biortech.2011.12.124

Clayton, S. J., Stiegel, G. J., & Wimer, J. G. U.S. DOE's Perspective on Long-Term Market Trends and R&D Needs in Gasification. Presented at: 5th European Gasification Conference. April 8-10, 2002, Noordwijk, The Netherlands.

Damiani, L. & Trucco, A. (2010) An Experimental Data Based Correction Method of Biomass Gasification Equilibrium Modeling. *Journal of Solar Energy Engineering.* 132 (8), pp.031011-1-031011-11. DOI:10.1115/1.4001463

Doherty, W., Reynolds, A., & Kennedy, D. (2009) The effect of air preheating in a biomass CFB gasifier using ASPEN Plus simulation. *Biomass & Bioenergy.* 33, pp.1158-1167. DOI:10.1016/j.biombioe.2009.05.004

Eastman. *Eastman Gasification Overview*. March 22, 2005. Available from: http://www.eastman.com/PublicDocs/Gasification/Eastman_Gasification_Overview.pdf

Eden, M. R. *Design of Acetic Acid Production Process from Coal and/or Biomass Resources*. Lecture notes distributed in CHEN-4470 at Auburn University. Spring 2010.

Elvers, B., Hawkins, S., Ravenscroft, M., Rounsaville, J. F., & Schulz, G. (eds). (1989) *Ullmann's Encyclopedia of Industrial Chemistry*, 5th edition, vol. A12. New York: VCH Publishers.

Foster Wheeler. Gasification/IGCC. http://www.fwc.com/What-We-Do/Refining/Refinery-Power-Integration-%281%29/Gasification-IGCC.aspx

Gaur, S. & Reed, T. B. (1998) *Thermal Data for Natural and Synthetic Fuels.* New York: Marcel Dekker, Inc.

Grol, E. & Yang, W. (2009) Evaluation of Alternate Water Gas Shift Configurations for IGCC Systems. U. S. Department of Energy – National Energy Technology Laboratory (NETL). Available from: http://www.netl.doe.gov/File%20Library/Research/Energy%20Analysis/Publications/DOE-NETL-401-080509-EvalAltWaterGasShiftConfigIGCCSystems.pdf

Gungor, A., Ozbayoglu, M., Kasnakoglu, C., Biyikoglu, A., & Uysal, B. Z. (2012) A parametric study on coal gasification for the production of syngas. *Chemical Papers.* 66 (7), pp.677-683. DOI:10.2478/s11696-012-0164-0

Hannula, I., & Kurkela, E. (2010) A semi-empirical model for pressurised air-blown fluidised-bed gasification of biomass. *Bioresource Technology.* 101 pp.4608-4615. DOI:10.1016/j.biortech.2010.01.072

Higman, C. & van der Burgt, M. (2003) *Gasification*. Boston: Elsevier.

Irankhah, A., Haghtalab, A., Farahani, E. V., & Sadaghianizadeh, K. (2007) Fischer-Tropsch Reaction Kinetics of Cobalt Catalyst in Supercritical Phase. *Journal of Natural Gas Chemistry.* 16, pp.115-120. DOI:10.1016/S1003-9953(07)60036-X

Knoef, H. A. M. (ed.). (2005) *Handbook Biomass Gasification.* The Netherlands: Biomass Technology Group.

Lee, H., Choi, S., & Paek, M. (2010) Interpretation of coal gasification modeling in commercial process analysis simulation codes. *Journal of Mechanical Science and Technology.* 24 (7), pp.1515-1521. DOI:10.1007/s12206-010-0411-7

Lee, S., Speight, J. G., & Loyalka, S. K. (2007) *Handbook of Alternative Fuel Technologies.* Boca Raton: CRC Press.

Li, X., Grace, J. R., Watkinson, A. P., Lim, C. J., & Ergüdenler, A. (2001) Equilibrium modeling of gasfication: a free energy minimization approach and its application to a circulating fluidized bed coal gasifier. *Fuel.* 80, pp.195-207. DOI:10.1016/S0016-2361(00)00074-0

Nikoo, M. B. & Mahinpey, N. (2008) Simulation of biomass gasification in fluidized bed reactor using ASPEN PLUS. *Biomass & Bioenergy.* 32, pp.1245-1254. DOI:10.1016/j.biombioe.2008.02.020

Perry, R. H. & Green, D. W. (eds). (1997) *Perry's Chemical Engineers' Handbook*, 7th edition. New York: McGraw-Hill.

Phillips, J. Different Types of Gasifiers and Their Integration with Gas Turbines. EPRI / Advanced Coal Generation. Available from: https://netl.doe.gov/File%20Library/Research/Coal/energy%20systems/turbines/handbook/1-2-1.pdf

Probstein, R. F. & Hicks, R. E. (1990) *Synthetic Fuels*. Cambridge: pH Press.

Puig-Arnavat, M., Bruno, J. C., & Coronas, A. (2012) Modified Thermodynamic Equilibrium Model for Biomass Gasification: A Study of the Influence of Operating Conditions. *Energy & Fuels.* 26, pp.1385-1394. DOI:10.1021/ef2019462

Radmanesh, R., Chaouki, J., & Guy, C. (2006) Biomass Gasification in a Bubbling Fluidized Bed Reactor: Experiments and Modeling. *AIChE Journal*. 52 (12), pp.4258-4272. DOI:10.1002/aic.11020

Ramanan, M. V., Lakshmanan, E., Sethumadhavan, R., & Renganarayanan, S. (2008) Modeling and Experimental Validation of Cashew Nut Shell Char Gasification Adopting Chemical Equilibrium Approach. *Energy & Fuels.* 22 (3), pp.2070-2078. DOI:10.1021/ef700467x

Roy, P. C., Datta, A., & Chakraborty, N. (2009) Modelling of a downdraft biomass gasifier with finite rate kinetics in the reduction zone. *International Journal of Energy Research.* 33, pp.833-851. DOI:10.1002/er.1517

Shadle, L. J., Berry, D. A., & Syamlal, M. (2002). Coal Conversion Processes, Gasification. *Kirk-Othmer Encyclopedia of Chemical Technology*. John Wiley & Sons, Inc. DOI:10.1002/0471238961.0701190913010801.a01.pub2

Schuster, G., Löffler, G., Weigl, K., & Hofbauer, H. (2001) Biomass steam gasification – an extensive parametric modeling study. *Bioresource Technology.* 77, pp.71-79. DOI:10.1016/S0960-8524(00)00115-2

Shell. Cleaner Coal. http://www.shell.com/global/future-energy/innovation/inspiring-stories/cleaner-coal.html.

Shen, C., Chen, W., Hsu, H., Sheu, J., & Hsieh, T. (2012) Co-gasification performance of coal and petroleum coke blends in a pilot-scale pressurized entrained-flow gasifier. *International Journal of Energy Research.* 36, pp.499-508. DOI:10.1002/er.1821

Shen, L., Gao, Y., & Xiao, J. (2008) Simulation of hydrogen production from biomass gasification in interconnected fluidized beds. *Biomass & Bioenergy.* 32 pp.120-127. DOI:10.1016/j.biombioe.2007.08.002

U. S. Department of Energy – National Energy Technology Laboratory (NETL). Coal Gasification Systems. http://www.netl.doe.gov/research/coal/energy-systems/gasification

U. S. Department of Energy – National Energy Technology Laboratory (NETL). Gasifipedia. http://www.netl.doe.gov/gasifipedia/index.html

Vaezi, M., Passandideh-Fard, M., Moghiman, M., & Charmchi, M. (2011). Gasification of heavy fuel oils: A thermochemical equilibrium approach. *Fuel.* 90, pp.878-885. DOI:10.1016/j.fuel.2010.10.011

Valin, S., Ravel, S., Guillaudeau, J., & Thiery, S. (2010) Comprehensive study of the influence of total pressure on products yields in fluidized bed gasification of wood sawdust. *Fuel Processing Technology.* 91, pp.1222-1228. DOI:10.1016/j.fuproc.2010.04.001

Warnecke, R. (2000) Gasification of biomass: comparison of fixed bed and fluidized bed gasifier. *Biomass & Bioenergy.* 18, pp.489-497. DOI:10.1016/S0961-9534(00)00009-X

World Coal Association. (2014) Coal the most abundant fossil fuel. http://www.worldcoal.org/extract/coal-the-most-abundant-fossil-fuel-3223/